International Agreement Report

TRAC-PF1 MOD1 Post Test Calculations of the OECD LOFT Experiment LP-SB-1

Prepared by
E. J. Allen

United Kingdom Atomic Energy Authority
Winfrith, Dorchester
Dorset, England

**International
Agreement Report**

TRAC-PF1 MOD1 Post Test Calculations of the OECD LOFT Experiment LP-SB-1

Prepared by
E. J. Allen

United Kingdom Atomic Energy Authority
Winfrith, Dorchester
Dorset, England

SUMMARY

Analysis of the small, hot leg break, OECD LOFT Experiment
LP-SB-1 using the "best-estimate" computer code TRAC-PF1/MOD1 is
presented.

Descriptions of the LOFT facility and the LP-SB-1 experiment are
given and development of the TRAC-PF1/MOD1 input model is
detailed. The calculations performed in achieving the
steady state conditions, from which the experiment was initiated,
and the specification of experimental boundary conditions are
outlined.

Results of a "Base Case" transient calculation are found to be
generally consistent with those reported by other members of the
OECD LOFT Program Review Group. The experimental trends with
respect to pressure histories and minimum system mass inventory
are reasonably well reproduced by the TRAC-PF1/MOD1 calculation.
However, the inability of TRAC-PF1/MOD1 to account for main-pipe
stratification in determining fluid conditions in a side branch
leads to significant discrepancies between the measured and
predicted break line and hot leg densities and is identified as
the main reason for the poorly predicted break mass flow rate.

Implementation, via the TRAC-PF1/MOD1 control system, of
correlations for determining side branch quality as a function of
main-pipe stratified liquid level are shown to be effective in
improving the predicted hot leg and break line densities and
break mass flow rate. The remaining differences between measured
and predicted data are considered to be due to deficiencies in
the TRAC-PF1/MOD1 critical flow model and the sensitivity of the
break flow to the hot leg liquid level behaviour.

It is recommended that some means of accounting for the effect of
main-pipe stratified liquid level, in determining fluid
conditions in a side branch, be implemented in the TRAC-PF1/MOD1
code.

It is also suggested that a closer examination of the factors
influencing the draining of the steam generator tubes is required
to resolve the observed discrepancies in hot leg liquid level
behaviour.

CONTENTS

CONTENTS (Cont'd)

CONTENTS (Cont'd)

TABLES

FIGURES

1. INTRODUCTION

This paper describes post-test calculations of the OECD LOFT small, hot leg break experiment LP-SB-1 using the "best-estimate" computer code TRAC-PF1/MOD1. Sections 2, 3 and 4 describe the LOFT facility, the LP-SB-1 experiment and the versions of TRAC-PF1/MOD1 used, respectively. Development of the input model is detailed in Section 5 and the calculations performed in achieving the steady state conditions, from which the experiment was initiated, are outlined in Section 6. The experimental boundary conditions, and the way in which they are specified to the code, are defined in Section 7. Section 8 describes the "Base Case" transient calculation. The effects of implementing correlations for predicting branch line quality as a function of main branch stratified liquid level are examined in Sections 9 and 10. The effect of varying the choked flow multiplier is also discussed in Section 10. The main conclusions and recommendations from the analysis are summarised in Sections 11 and 12.

2. THE LOSS OF FLUID TEST (LOFT) FACILITY

The Loss of Fluid Test (LOFT) facility, at the Idaho National Engineering Laboratory (INEL), is a 50 MW(t) Pressurised Water Reactor (PWR) system designed to simulate the major components and system responses of a commercial PWR during Loss-of-Coolant Accidents (LOCAs) or operational transient accidents. The experimental assembly is instrumented in order that system variables can be measured and recorded during transients. The facility is comprised of five major subsystems - the reactor vessel, the operating (intact) loop, the "broken" loop, the blowdown suppression system and the Emergency Core Cooling System (ECCS). The configuration of the major LOFT components, for experiment LP-SB-1, is shown in Figure 1.

The operating (intact) loop simulates three loops of a commercial four-loop PWR and contains a steam generator (of vertical, U-tube design), two primary coolant pumps (in parallel), a pressurizer, a venturi flowmeter and connecting piping. The break location for experiment LP-SB-1 was in the hot leg of the intact loop between the steam generator and the reactor vessel.

The broken loop consists of a hot leg and a cold leg connected to the reactor vessel and the blowdown suppression tank header. Each leg contains a Quick-Opening Blowdown Valve (QOBV), a recirculation line, an isolation valve and connecting piping. The recirculation lines provide a small flow from the broken loop to the intact loop and are used to maintain the broken loop fluid temperature at approximately the core inlet temperature prior to experiment initiation. During experiment LP-SB-1, the QOBVs and the isolation valves remained closed (because the break was in the operating loop). The broken loop spool pieces, with orifices to simulate the steam generator and pump hydraulic resistances, were not installed for experiment LP-SB-1. These were replaced by a straight piping spool piece.

The LOFT reactor vessel has an annular downcomer, a lower plenum, lower core support plates, a nuclear core (containing 1300 fuel rods) and an upper plenum. The downcomer is connected to the cold legs of the operating and broken loops, and the upper plenum is connected to the hot legs of the operating and broken loops.

The LOFT ECCS consists of two accumulators, a High Pressure Injection System (HPIS) and a Low Pressure Injection System (LPIS). Each system is designed to inject scaled flows of emergency core coolant directly into the primary coolant system. The accumulators and LPIS were not used during experiment LP-SB-1 and scaled HPIS flow was directed into the Intact Loop Cold Leg (ILCL). Volume scaling of the HPIS flow was based on the assumption that only one of the three charging pumps and one of the three HPIS pumps, in the reference plant, were available.

3. EXPERIMENT LP-SB-1

Experiment LP-SB-1 was conducted on 23 June 1983 in the LOFT facility at the Idaho National Engineering Laboratory. LP-SB-1 was the second in a series of experiments, sponsored by a consortium of countries under the auspices of the Organisation for Economic Cooperation and Development (OECD), designed to address small break issues raised as a result of the accident at Three Mile Island in 1979.

The LP-SB-1 experiment simulated a 7.6 cm (3 inch) equivalent diameter break in a hot leg pipe of a commercial PWR. LP-SB-1 was one of a pair of experiments aimed at addressing the effects of early and delayed pump trip on system behaviour. The primary coolant pumps were tripped early in experiment LP-SB-1 and pump trip was delayed in experiment LP-SB-2. The following objectives were defined for the two small break experiments (1):

i)   Determine system transient response characteristics for hot leg small break LOCAs with early and delayed pump trip and break size of 7.62 cm (3 inch) equivalent diameter.

ii) Determine the system mass inventory, mass distribution, and core heat transfer characteristics when pumps are shut off under high system void conditions (LP-SB-2).

iii) Provide integral nuclear system data for assessing the ability of computer codes to predict system response during a small break LOCA.

iv) Obtain data which can be used to investigate emergency core coolant distribution, thermal mixing and effect on core coolant mass inventory.

v)   Provide data for evaluating the usefulness of accident diagnosis techniques in identifying small hot leg break LOCA characteristics.

Experiment LP-SB-1 was initiated, from operating conditions representative of those in a commercial PWR, by opening a valve in the Intact Loop Hot Leg (ILHL) break line. The primary side pressure history and the timings of significant events during the experiment are shown on Figure 2. The primary coolant system pressure decreased to the reactor scram and feedwater trip setpoint (14.57 MPa) in 1.4 seconds. The Main Steam Control Valve (MSCV) was closed manually upon verification of reactor scram. The main feedwater was isolated at 3.8 seconds and the MSCV was fully closed at 15.4 seconds. The primary coolant system pressure decreased rapidly to the primary coolant pump trip setpoint (11.12 MPa) at 24.6 seconds and the pressurizer indicated zero liquid level at 34.6 seconds. The HPIS setpoint signal of 8.24 MPa was reached at 41.4 seconds and the system pressure had declined to fluid saturation in the break line at 57.5 seconds. Auxiliary feedwater was manually initiated at 1.1 minutes and turned off at 31.1 minutes. Following break uncovery at 11.9 minutes, the high quality steam flow out of the break caused a further acceleration in the primary coolant system depressurisation rate. The primary system pressure fell below the steam generator secondary pressure at approximately 18 minutes. The minimum primary coolant system mass inventory was reached after 37 minutes at which time the HPIS flow rate exceeded the break flow rate and primary coolant system refill began. The experiment was terminated, after one hour, when the primary coolant system pressure had fallen to 2.5 MPa. The liquid inventory in the reactor vessel remained at least 1.5 m above the top of the core during the transient and sufficient cooling was present to keep the fuel cladding temperatures close to the saturation temperature of the fluid in the reactor vessel.

4. TRAC-PF1/MOD1

TRAC (Transient Reactor Analysis Code) is an advanced "best-estimate" computer code, developed at the Los Alamos National Laboratory, for analysing transients in thermal hydraulic systems. Specifically, TRAC-PF1/MOD1 was developed for analysing postulated accidents in PWRs. The versions of the code used for the calculations described in this paper were Version BØ2A and Version BØ2C which contain the LANL updates to TRAC-PF1/MOD1 Version 12.7.

5. TRAC-PF1/MOD1 INPUT MODEL FOR LP-SB-1

The development of a TRAC-PF1/MOD1 input model for analysis of the LOFT small break experiment LP-SB-1 was based on a TRAC-PF1/MOD1 large break deck for LP-FP-1. The FP-1 deck, developed at AEEW, originated from the LANL input deck for experiment L2-3. Additional published data on the LOFT facility (2,3,4) were employed, where necessary, in producing the small break deck.

The required modifications to the large break deck are described in References 5 and 6 and include:

i) Replacement of the three-dimensional vessel with a one-dimensional representation.

ii) Removal of the accumulator and the LPIS.

iii) Removal of the broken loop steam generator and pump simulators.

iv) Inclusion of the ILHL break.

v) Inclusion of the steam generator secondary side auxiliary feedwater.

vi) Inclusion of the primary pump injection.

Additional modifications by Neill (7) - to the position of the ECCS injection in the ILCL - and Pelayo (8) - to the steam generator recirculation ratio and nodalisation - were also incorporated in the LP-SB-1 input deck.

Figures 3, 4 and 5 show the nodalisation diagrams for the primary system, the reactor vessel and the steam generator secondary side, respectively. A total of 36 components, 42 junctions and 147 cells were used in the model.

A microfiche listing of the TRAC-PF1/MOD1 input deck for LP-SB-1 (used for the steady state calculation) is contained in Appendix I.

6. STEADY STATE CALCULATION

Version BØ2A of the TRAC-PF1/MOD1 code - which incorporates the updates contained in LANL Version 12.7 - was used for the steady state calculations. Steady state mode calculations were run for 550 seconds and, in order to determine system conditions during transient mode code operation, a short period (50 seconds) of transient mode "steady state" (ie with no BREAK in the circuit) was also run. In running the steady state calculation, a total of 680 seconds of CPU time were used with an average time step size of 0.12 seconds (see Figures 6 and 7). It was found that the calculation converged to a steady state more readily when the maximum allowable time step was reduced from 1.0 seconds to 0.1 seconds.

The calculations were performed with control systems governing the behaviour of the steam generator secondary side steam and feedwater mass flow rates and the speed of the primary coolant pumps.

The initial conditions predicted by TRAC-PF1/MOD1 for experiment LP-SB-1 are compared with the measured data in Table 1. The calculations produced stable initial conditions, within the quoted experimental uncertainties (see Figures 8-23*), for all

* The steady decline in primary system pressure and pressurizer temperature, pressure and liquid level, at 550 seconds (as indicated in Figures 9, 20, 21 and 22 respectively) is due to the differing treatment, by TRAC-PF1/MOD1, of the PRESSURIZER component when in the transient mode, as opposed to the steady state mode, of code operation.

significant parameters with the exception of the steam volume and the liquid level in the pressurizer. The figures predicted for these quantities were outside the uncertainties of the experimental data due, it is thought, to differences between the experiment and the TRAC-PF1/MOD1 input deck in the interpretation of the pressurizer geometry. The pressurizer volume implied by the LP-SB-1 Experiment Analysis and Summary Report (EASR) (9), the TRAC-PF1/MOD1 large break input decks and the LOFT specification (2) differ as shown in Table 2. Efforts to resolve the discrepancies were unsuccessful. The approach adopted, in performing the steady state calculations, was to specify the initial pressurizer liquid volume as quoted for the experiment, but to allow the initial steam volume to be outside the uncertainties of the experimental data.

The magnitudes of the steady state pressure drops around the primary circuit, the environmental heat losses from the system and the core bypass flow rates, obtained from the TRAC-PF1/MOD1 calculations, were in reasonable agreement with the available LOFT data as shown in Tables 3, 4 and 5, respectively. Achievement of these initial system conditions is discussed in detail in References 5 and 6.

7.   BOUNDARY CONDITIONS FOR TRANSIENT CALCULATIONS

7.1 Decay Heat Data

Following reactor scram, decay heat data were specified to the TRAC-PF1/MOD1 transient calculation by means of a "power versus time" table. In deriving the table, the approach adopted by Hall and Brown (14) was followed and two sources of information were used. During the first 250 seconds of the transient, when both neutron and fission power were expected to be present, data were taken from the RELAP5/MOD1 input deck used for the pre-test prediction of LP-SB-1 (15). When fission power only was present, the data contained in Reference 16 were appropriate and these data were used from 250 seconds until the end of the transient. The power table used in the TRAC-PF1/MOD1 calculation of LP-SB-1 is reproduced as Table 6.

7.2 Primary Pump Injection

During experiment LP-SB-1, the primary coolant pump injection system was set up to deliver a total flow of 0.095 ls^{-1} to the primary coolant pumps (9, 17). This was simulated in the TRAC-PF1/MOD1 model by using "FILL" components to supply the primary pump injection system with liquid at a constant rate of 1.2974×10^{-3} ms^{-1}. The flow areas of the pump injection pipes were 3.6613×10^{-2} m^2 which implied an injection rate of 4.75×10^{-5} m^3s^{-1}, or 0.0475 ls^{-1}, to each pump.

7.3 Steam Generator Secondary Side Auxiliary Feedwater Flow

In experiment LP-SB-1, the steam generator secondary side auxiliary feedwater flow, of 0.5 ls^{-1} (17), was manually initiated at 63.4 seconds and turned off at 1864.8 seconds (9). This was simulated, in the TRAC-PF1/MOD1 calculation, by using a "FILL" component to provide feedwater to the secondary side of the steam generator at a flow rate of 0.061673 ms^{-1} during the required period. The flow area of the auxiliary feedwater system pipework was 0.0081073 m^2 implying a flow rate of 5×10^{-4} m^3s^{-1} or 0.5 ls^{-1}. The "time versus velocity" table used is given in Table 7.

7.4 High Pressure Injection System

The HPIS was initiated in experiment LP-SB-1 when the ILHL pressure had fallen to 8.24 MPa (9). The table of HPIS flow rate against Primary Coolant System (PCS) pressure, used in the TRAC-PF1/MOD1 calculation, was derived from that given in the Experiment Specification Document (17) and is reproduced in Table 8.

7.5 Operational Setpoints

The operational setpoints (for reactor scram, main feedwater shut off, MSCV closure, primary pump trip, HPIS initiation and auxiliary feedwater initiation) measured during the experiment, and the way in which the setpoints were specified in the TRAC-PF1/MOD1 calculation, are given in Table 9.

8. BASE CASE CALCULATION

8.1 Introduction

The initial transient calculation, termed the "Base Case Calculation", was restarted from the end of the transient-mode "steady state" calculation. The FILL component, originally attached to the break line, was replaced by a BREAK component in order to initiate the transient. As for the steady state calculations, Version BØ2A of TRAC-PF1/MOD1 – which incorporates the code updates contained in LANL Version 12.7 – was used for the Base Case Calculation.

In this Section, the TRAC-PF1/MOD1 predictions are compared with the experimental data and with the results presented – by members of the OECD LOFT Program Review Group – in the LP-SB-1 "Comparison Report" (18).

8.2 CPU Usage and Time Step Behaviour

Four thousand seconds of elapsed transient were calculated, requiring 11,332 seconds of CRAY X-MP CPU time (see Figure 24). This corresponds to a CPU/real time ratio of 2.8. The user-specified minimum allowable time step throughout the calculation was 10^{-5} seconds. The maximum time step was limited to 0.5 seconds for the first 1500 seconds of the transient.

Shortly after this time, the code attempted to reduce the time step below the minimum allowable value. It was necessary to reduce the maximum permitted time step to 0.1 seconds, for the remainder of the transient, to enable the calculation to proceed (see Figure 25). The average time step for the calculation (problem time/total number of time steps) was 0.08 seconds. The very small cell (7.238×10^{-6} m^3) representing the leakage path between the reactor vessel and the core barrel nozzles (bypass path 4 - component number 83) was the dominant component responsible for limiting the time step size throughout the transient.

8.3 Chronology of Events

A comparison of the measured and predicted timings of significant events during the LP-SB-1 transient is given in Table 10.

The experiment was initiated by opening the valve in the ILHL break line. The primary coolant system pressure decreased rapidly to the reactor scram and main feedwater trip set point of 14.57 MPa and, following a 2 second delay, closure of the main steam control valve was initiated. Isolation of the main feedwater took 2.4 seconds. The timings of these initial events were predicted, by the TRAC-PF1/MOD1 calculation, to within ~ 1 second.

In the experiment, the main steam control valve was fully closed at 15.4 seconds. Although not documented in the experiment specification, the steam flow bypass valve was opened once during the experiment, at ~ 30 seconds, when the secondary side pressure exceeded ~ 6.7 MPa. This was simulated, in the TRAC-PF1/MOD1 calculation, by allowing the main steam control valve to reopen.

The primary coolant system pressure continued to decrease rapidly and reached the primary coolant pump trip set point (11.12 MPa) after 24.6 seconds and the HPIS initiation set point (8.24 MPa) after 41.4 seconds. The timings of both these trips were very well predicted by the TRAC calculation.

After 43 seconds, the primary coolant pumps had coasted down to their flywheel uncoupling frequency (12.5 Hz). TRAC predicted this to occur some 3 seconds later than in the experiment.

Fluid saturation in the break line, signalling the end of subcooled blowdown, occurred at 57.5 seconds in the experiment. This was predicted to occur some 7 seconds later in the calculation.

The auxiliary feedwater was initiated at 63.4 seconds and turned off at 1864.8 seconds. Identical timings were used for the TRAC calculation.

A further acceleration in the experimental primary coolant system depressurisation rate occurred when the break started to uncover at 715 seconds. Prior to this time, and following the end of subcooled blowdown, the break mass flow rate was under-predicted

by TRAC and the start of break uncovery was not calculated until
~ 1200 seconds.

The time at which the primary coolant system pressure fell below
the secondary system pressure (1077 seconds in the experiment)
was over-predicted by some 300 seconds.

Minimum primary system coolant mass inventory is estimated to
have occurred at between 1800 seconds and 2200 seconds in the
experiment. The predicted time of minimum primary system mass
inventory was ~ 1680 seconds (defined as the time at which the
HPIS plus pump injection mass flow rates exceeded the break mass
flow rate).

The experiment was terminated at 3668 seconds when the primary
coolant system pressure had fallen to the termination criterion
of 2.487 MPa. This was predicted to occur over 400 seconds
earlier, at 3227 seconds, in the TRAC calculation.

8.4 General Observations

8.4.1   Break Mass Flow Rate and Break Line Density

The measured and predicted break mass flow rates and break
upstream densities are shown in Figures 26 and 27, respectively.
(Subcooled and two-phase choked flow multipliers of 1.0 were used
throughout the calculation). It can be seen that, prior to the
time of measured break uncovery (~ 700 seconds), TRAC-PF1/MOD1
under-predicted the break line density and the break mass flow
rate. The time at which the break was predicted to uncover
occurred some 500 seconds later than in the experiment. Figure
28 indicates that, with the exception of the GRS
(W Germany - DRUFAN 02) results, all participants of the OECD
LOFT Program Review Group (18) also under-predicted the break
mass flow rate during the first ~ 700 seconds of the transient
and over-predicted the time of break uncovery.

8.4.2   Primary System Densities

A comparison of the measured and predicted ILHL densities is
shown in Figure 29. In contrast to the experimental behaviour,
the TRAC-PF1/MOD1 calculation predicted that the ILHL emptied
completely at ~ 1500 seconds. A similar trend was observed by
participants of the OECD LOFT Program Review Group (18), as shown
in Figure 30.

A comparison of the measured and predicted ILCL densities is
shown in Figure 31. In common with the results from the OECD
LOFT Program Review Group (18) (see Figure 32), the TRAC-PF1/MOD1
calculation predicted that the ILCL started to empty several
hundred seconds later than in the experiment. The predicted rate
at which the ILCL emptied was more rapid than that observed
experimentally.

8.4.3   Primary System Mass Inventory

TRAC-PF1/MOD1 predictions of the primary system mass inventory*
are compared with those of the OECD LOFT Program Review Group and
with the measured data in Figure 33. The predicted rate of
primary system mass depletion, prior to the time of experimental
break uncovery (~ 700 seconds), was lower than that measured.
Although not accurately known from the experimental data, minimum
primary system mass inventory was estimated to have occurred at
between 1800 and 2200 seconds (9). The time of minimum primary
system mass inventory (defined as the time at which the HPIS plus
pump injection mass flow rates exceeded the break mass flow rate)
was predicted by TRAC-PF1/MOD1 to have occurred earlier, at
~ 1700 seconds. The calculated minimum primary system mass
inventory appeared to be in reasonable agreement with the
measured data. The core void fractions, calculated by
TRAC-PF1/MOD1, and shown in Figure 34, indicate that, as observed
in the experiment, no core uncovery was predicted.

8.4.4   System Pressure

A comparison of the measured and predicted primary system
pressure histories is shown in Figure 35. As indicated by the
correctly predicted timings of the primary coolant pump trip and
the HPIS initiation, the initial rapid subcooled depressurisation
was well represented. Following the end of subcooled blowdown,
and prior to the measured time of break uncovery, the slow rate
of depressurisation was reasonably well reproduced. The increase
in the rate of depressurisation, due to uncovery of the break,
was predicted to occur later (at ~ 1200 seconds) than in the
experiment. This led to a slight over-prediction of primary side
pressure, for a while, following the measured time of break
uncovery. As shown in Figure 36, the calculations performed by
the participants of the OECD LOFT Program Review Group also
predicted the rate of subcooled depressurisation well. Following
the end of subcooled blowdown, and prior to the time of measured
break uncovery, all calculations predicted a lower than measured
pressure plateau. Consistent with their late predictions of the
time of break uncovery, all calculations, with the exception of
GRS, over-predicted the timing of the increased rate of
depressurisation.

The overall secondary side pressure history is reasonably well-
predicted as shown in Figure 37 and compares favourably with the
calculations performed by participants of the OECD LOFT Program
Review Group (see Figure 38). Following "closure" of the MSCV,

---

* In calculating the predicted primary system mass inventory, all
  flows into/out of the primary circuit during the transient were
  added to/subtracted from the initial primary system mass. The
  initial primary system mass included all system components
  except the secondary side of the steam generator component
  (component numbers 20, 21, 22 and 27) and the steam line valve
  (component number 23).

its minimum flow area was restricted to 0.35% of its fully-opened value to account for the steam leakage which occurred during the experiment.

8.5 Detailed Discussion

8.5.1 Break Mass Flow Rate and Break Line Density

The ILHL void fraction calculated by TRAC-PF1/MOD1 is shown in Figure 39; the time at which stratification in the hot leg is predicted to occur is also indicated. Figure 39 shows that when single phase conditions were predicted in the hot leg, ie subcooled liquid (< 60 seconds) or high quality steam (> 1400 seconds), the mass flow rate in the break line was well predicted. However, during stratified flow conditions, TRAC-PF1/MOD1 takes no account of the hot leg liquid level in determining the density of the fluid in the break line. The density assumed, at the entrance to a branchline, is the volume weighted density of the steam and liquid phases in the main pipe. The break line density is therefore under-predicted when the stratified level is above the break and over-predicted when the level is below the break.

In order to gain an indication of the effects of TRAC-PF1/MOD1's inability to account for hot leg flow stratification on break line density, relative to any deficiency in its critical flow model, a TRAC-PF1/MOD1 calculation was performed on a "stand-alone" model of the LP-SB-1 break line. The calculation, in which the density of the fluid being fed to the break line was altered, indicated that, in order for the TRAC critical flow model to predict the measured break mass flow rate, the calculated break line density would need to be similar to that measured (see Table 11) ie at ~ 500 seconds, the reported break flow was calculated by TRAC-PF1/MOD1 using a break line density ~ 4% greater than that measured experimentally. The break line density and break mass flow rate predicted by the Base Case Calculation, at 500 seconds, were ~ 20% less than those measured. The tentative conclusion from this calculation was that the poorly predicted break mass flow rate, observed in the Base Case Calculation, was mainly due to TRAC-PF1/MOD1's inability to account for the effects of hot leg flow stratification on break line density, rather than deficiencies in its critical flow model. (The RELAP5/MOD2 analysis of LP-SB-1 (14), in which the difficulty in accounting for the effects of hot leg flow stratification had been overcome, found the critical flow model to be inadequate for low quality conditions).

In order to comprehensively assess the effects of TRAC-PF1/MOD1's inability to account for hot leg flow stratification in determining fluid conditions in the break line, correlations for predicting branchline flow quality as a function of mainline stratified liquid level were implemented in the LP-SB-1 input deck and the Base Case Calculation was re-run as described in Sections 9 and 10.

8.5.2   Running Speed

The dominant component responsible for limiting the time step size throughout the Base Case Calculation was the very small cell (7.238×10^{-6} m^3) used to represent the leakage path between the reactor vessel and the core barrel nozzles (Bypass Pach 4 - Component Number 83). This component was responsible for the code "crashing" at ~ 1500 seconds (see Section 8.2). On increasing the volume of this component, and decreasing that of its neighbouring PLENUM component, by ~ 3.5×10^{-3} m^3, significant improvements in the running speed of the code were realised and it was no longer necessary to reduce the maximum allowable time step in order for the code to continue running. Increasing the volume of Bypass Path 4 reduced the CPU to problem time ratio from 2.15 to 1.32 between 500 and 1500 seconds (see Figure 40).

8.6   Summary

1)   The following points summarise the general observations made on the TRAC-PF1/MOD1 Base Case Calculation of LP-SB-1. The findings tended to be consistent with those of the OECD LOFT Program Review Group (18).

   i)   Prior to the time of measured break uncovery, the break line density, break mass flow rate and rate of primary side mass depletion were under-predicted.

   ii)   The time at which the break uncovered was over-predicted.

   iii)   In contrast to the experimental behaviour, the ILHL was predicted to empty.

   iv)   The time at which the ILCL started to empty was predicted to occur later than in the experiment. The predicted rate at which the cold leg emptied was more rapid than that measured.

   v)   The minimum primary system mass inventory was in reasonable agreement with the measured data - as observed in the experiment, no core uncovery was predicted.

   vi)   The overall trends in primary and secondary system pressure histories were reasonably well reproduced.

2)   The tentative conclusion from a TRAC-PF1/MOD1 calculation using a "stand-alone" model of the LP-SB-1 break line was that the poorly predicted break mass flow rate was mainly a consequence of TRAC-PF1/MOD1's inability to account for the effects of hot leg flow stratification on break line density (rather than deficiencies in its critical flow model).

3)   The dominant factor responsible for limiting the time step size throughout the Base Case Calculation was the very small volume (7.238×10^{-6} m^3) of the cell representing the

leakage path between the reactor vessel and the core barrel nozzles. Increasing the size of this cell by $\sim 3.5 \times 10^{-3}$ m^3 led to an improvement in the CPU to problem time ratio of $\sim 40\%$ over a 1000 second period.

9. BASE CASE CALCULATION WITH EPRI CORRELATION

9.1 Introduction

In order to take account of the hot leg stratified liquid level in determining the fluid conditions in the break line, EPRI (Electric Power Research Institute, USA) correlations (19) for predicting the liquid levels at which the onset of vapour pull through and liquid entrainment occur and the resulting branchline flow quality were implemented in the LP-SB-1 input deck. The correlations are described in Appendix II. The transient was re-run using Version BØ2C of the TRAC-PF1/MOD1 code which employs a branch offtake quality model for stratified flow.

9.2 General Observations

9.2.1 Break Mass Flow Rate and Break Line Density

As shown in Figure 41, implementation of the EPRI correlation greatly improved the predicted break line density for the initial 500 seconds of the transient. Although this led to an improved break mass flow rate over this period, the break flow still tended to be under-predicted, as shown in Figure 42. Break uncovery occurred earlier than in the Base Case Calculation but still significantly (~ 300 seconds) later than in the experiment. The discrepancies between the measured and predicted break line densities prior to ~ 150 seconds are a consequence of the offtake model only operating when fluid conditions in the main pipe are fully stratified. The divergence of the measured and predicted break line density and break mass flow rate at ~ 500 seconds is discussed in Section 9.3.

9.2.2 Primary System Densities

As shown in Figure 43, implementation of the EPRI correlation greatly improved the predicted ILHL density behaviour. Contrary to the Base Case Calculation, and in line with the experimental measurements, no emptying of the ILHL was predicted by the revised calculation.

Figure 44 indicates that although some improvement to the time at which the ILCL started to empty was achieved by the revised calculation, the rate at which the cold leg emptied was still more rapid than that observed experimentally.

9.2.3 Primary System Mass Inventory

As shown in Figure 45, the improvement (over the first 500 seconds) in the predicted break mass flow rate (on implementing the EPRI correlation) caused the primary system mass to deplete slightly more rapidly than in the Base Case

Calculation. However, because the ILHL did not empty in the revised calculation, the minimum primary system mass inventory remained ~ 200 kg higher than that predicted by the Base Case Calculation.

9.2.4   System Pressure

The differences in the break mass flow rate predicted by the Base Case and the EPRI Correlation Calculations are manifested in slightly different primary and secondary pressure history trends, as shown in Figures 46 and 47, respectively.

9.3   Detailed Discussion

9.3.1   ILHL Liquid Level Behaviour

The ILHL liquid level and the level at which the EPRI correlation predicts the onset of vapour pull through to occur (h_p) are shown in Figure 48. When the ILHL liquid level falls below h_p (ie after ~ 500 seconds), vapour pull-through is invoked in the EPRI correlation and the quality in the break line increases. As was seen in Figures 41 and 42, there follows a consequent decline in break line density and break mass flow rate which clearly represents a departure from the experimental behaviour.

The predicted ILHL liquid level is compared with that measured during the experiment in Figure 49. Although well predicted during the initial part of the transient, the calculated level fell by ~ 2 cm at ~ 500 seconds. The experimental data show the liquid level to have remained constant (at ~ 7 cm above the centre line) from ~ 200 seconds until the decline to break uncovery started at ~ 700 seconds. This difference in ILHL liquid level behaviour is significant because the EPRI correlation predicts vapour pull-through to commence when the liquid level is ~ 6 cm above the centre line. The difference, between the calculation and the experiment, in the behaviour of the ILHL liquid levels is thus responsible for the observed discrepancies in break line density and for the predicted decline in break mass flow rate at ~ 500 seconds.

9.3.2   Time of Break Uncovery

The likely effect, on the break line density (and the time at which the break uncovers), of the ILHL liquid level (or the level at which vapour pull through is predicted to occur) is shown in Figure 50a. The effect of the amount of system mass required to be discharged, prior to break uncovery, is shown in Figure 50b. For the current calculation, it seems likely that, had the liquid level been correctly predicted (or the level at which vapour pull-through is assumed to occur had been lower), the time at which the break uncovered would still have been over-predicted by ~ 200 seconds - see Figure 51 which shows the TRAC-PF1/MOD1 predicted break line density when the EPRI correlation is modified to reduce h_p.

Three factors have been identified which would contribute to the time of break uncovery being over-predicted:

i)   prior to the time at which vapour pull through is predicted to occur, the break mass flow rate is under-predicted (by the TRAC-PF1/MOD1 critical flow model) by ~ 0.5 kgs^{-1}. After 700 seconds (the time at which the break started to uncover in the experiment), this would result in a system mass excess in the calculation of ~ 350 kg and could account for the time of break uncovery being over-predicted by ~ 120 seconds;

ii) the volume of the Reflood Assist Bypass Line, implied by the TRAC-PF1/MOD1 input deck, was found, after reference to the LOFT specification document (2), to be too large by ~ 0.21 m^3. This could account for the time of break uncovery being over-predicted by ~ 60 seconds;

iii) the TRAC-PF1/MOD1 interphase drag model causes the density in the core to be underestimated by ~ 10% (20). This could cause the time of break uncovery to be over-predicted by ~ 20 seconds (see Appendix III).

9.4 Summary

Accounting for the hot leg stratified liquid level in determining the fluid conditions in the break line, by implementing the EPRI correlation for branchline flow quality, resulted in the following:

i)   the predicted break line density was greatly improved for the first 500 seconds of the transient;

ii) although the predicted break mass flow rate was improved during the first 500 seconds of the transient, it still tended to be under-predicted;

iii) although break uncovery was predicted to occur earlier than for the Base Case Calculation, it was still significantly (~ 300 seconds) later than in the experiment;

iv) a difference, between the calculation and the experiment, in the behaviour of the ILHL liquid levels was responsible for discrepancies in the break line density and for a decline in the predicted break mass flow rate at ~ 500 seconds;

v)   had the ILHL liquid level been correctly predicted and no such decline in break mass flow rate occurred at ~ 500 seconds, the time at which the break uncovered would still have been over-predicted by ~ 200 seconds. The earlier under-prediction of break mass flow rate, the volume of the Reflood Assist Bypass Line being too

large and the core density being under-predicted by the
TRAC-PF1/MOD1 interphase drag model were identified as
factors contributing to the late prediction of break
uncovery;

vi) in line with the experimental measurements, and
     contrary to the Base Case Calculation, no emptying of
     the ILHL was predicted to occur;

vii) although there was some improvement to the time at
     which the ILCL started to empty, the rate at which it
     emptied was still more rapid than that observed
     experimentally.

10. BASE CASE CALCULATION WITH EPRI CORRELATION AND INPUT MODEL MODIFICATIONS

10.1 Introduction

In Section 9, the difference in behaviour of the ILHL liquid
level, between the experiment and the TRAC-PF1/MOD1 calculation
employing the EPRI correlation, was identified as being
responsible for the observed discrepancies in the break line
density and for the decline in break mass flow rate at ~ 500
seconds. Had the liquid level been correctly predicted, however,
it was thought that the time at which the break uncovered would
still have been over-predicted by some 200 seconds. One of the
factors identified as contributing to this was the volume of the
Reflood Assist Bypass Line specified in the TRAC-PF1/MOD1 input
deck. This was found to be ~ 0.2 m^3 too large and thought to
account for the time of break uncovery being over-predicted by ~
60 seconds.

Prior to investigating the behaviour of the ILHL liquid level in
more detail, it was decided to re-run the calculation with the
volume of the Reflood Assist Bypass Line corrected. Two minor
errors, identified in the Base Case input model, were also
corrected at this stage, ie:

i)   correction of GRAV terms in Lower Plenum;

ii) correction of effective cell lengths (and associated
     FRICs) for PLENUM components.

Also, the volume of Bypass Path 4 - responsible for limiting the
time step size in the Base Case Calculation - was increased (and
the volume of its neighbouring PLENUM component decreased). All
modifications made to the Base Case input deck are detailed in
Appendix IV.

In this Section, the calculation employing the modified input
deck is used to investigate the behaviour of the ILHL stratified
liquid level. The influence, on the ILHL level, of the choice of
correlation used for determining the level at which vapour pull
through occurs is discussed and the effect of varying the choked
flow multiplier at the end of the break line is also examined.

A series of pictures showing, at 200 second intervals, the predicted void fraction distribution, the liquid and vapour velocities and the occurrences of stratified flow conditions throughout the system is shown in Appendix V.

10.2 General Observations

10.2.1   Break Mass Flow Rate and Break Line Density

As expected, and as shown in Figure 52, decreasing the volume of the Reflood Assist Bypass Line reduced the time taken for the break to uncover. A similar "shift" - see Figure 53 - is observed in the predicted break line density.

10.2.2   Primary System Densities

The ILHL and ILCL densities, predicted using the modified input deck, follow the same trend as in the previous calculation. As expected, however, the reduction in the size of the Reflood Assist Bypass Line causes events to occur slightly earlier - see Figures 54 and 55.

10.2.3   Primary System Mass Inventory

The primary system mass inventory, predicted using the modified input deck, follows a similar trend to the previous calculation. The effect of reducing the size of the Reflood Assist Bypass Line is observed as a constant deviation prior to the time of break uncovery. The system empties to the same level in both calculations, however, and the size of the Reflood Assist Bypass Line does not therefore influence the minimum primary system mass inventory - see Figure 56.

10.2.4   System Pressure

As shown in Figures 57 and 58, altering the size of the Reflood Assist Bypass Line has very little effect on the primary and secondary system pressure histories.

10.3 Detailed Discussion

10.3.1   ILHL Liquid Level Behaviour

Figure 59 indicates that the predicted decrease in ILHL liquid level (which now occurs just after 400 seconds) coincides with the time at which natural circulation in the ILHL is calculated to have ceased. In the experiment, natural circulation ended at ~ 500 seconds (9); however, the experimental hot leg liquid level (calculated from the density measured by the middle beam of the hot leg densitometer) showed no decline at this time (see Figure 49). In line with the TRAC-PF1/MOD1 calculations, the predictions of the OECD LOFT Program Review Group (18) show the ILHL density and liquid level to be lower than that measured between ~ 400 and ~ 700 seconds (see Figures 30 and 60). Figure 61 indicates that between 550 seconds and 950 seconds, liquid is predicted to flow back from the steam generator towards the

break. Experimental measurements suggest (9) that there was some flow from the steam generator to the break after ~ 400 seconds and this is considered responsible (9) for maintaining the hot leg level at ~ 7 cm above the centre line until ~ 700 seconds. The delay in the time at which liquid starts to drain back from the steam generator following the end of natural circulation, in the TRAC-PF1/MOD1 calculation, appears to be linked to the difference in behaviour of the ILHL liquid levels.

A mass flow balance on the ILHL, taken from the TRAC-PF1/MOD1 calculation is shown in Figure 62. It is clearly seen that the declines in the predicted ILHL liquid level (at ~ 400 seconds and at ~ 800 seconds - see Figure 59) correspond to the periods during which the break flow exceeded the sum of the flow from the vessel to the break and the flow from the steam generator to the break.

Factors governing the flow between the steam generator and the break have not been fully investigated. The magnitude and direction of this flow, however, are clearly significant in determining the ILHL liquid level behaviour (and hence the break flow).

10.3.2   Choice of Correlation

Although the experiments performed in the Two-Phase Flow Loop (TPFL) at INEL confirmed the forms of previously proposed correlations for predicting the mainline liquid levels at which vapour pull-through and liquid entrainment occur, different values for the constants used in the correlations were recommended (see Table 12). The TPFL experiments found the liquid level range, over which vapour pull through and liquid entrainment occurred, to be greater than previously reported.

It is found that implementation of the CATHARE correlation (C_p = 0.62), in the TRAC-PF1/MOD1 input deck, improves the agreement between the calculated and measured results, with respect to break line density and break mass flow rate, as shown in Figures 63 and 64. (Further improvement is realised when a correlation with no vapour pull-through (h_p = 0.142) is used). The CATHARE correlation predicts the onset of vapour pull through to occur when the ILHL liquid level is ~ 1 cm below that assumed by the EPRI correlation (see Figure 65). For experiment LP-SB-1, the discrepancies between the measured and predicted ILHL liquid levels become less significant, therefore, when the CATHARE, as opposed to the EPRI, correlation (for the level at which vapour pull-through commences) is used. Had the ILHL level been correctly predicted, however, it appears that the EPRI correlation would have performed satisfactorily.

The correlation for the level at which vapour pull-through occurs - implemented in a modified version of RELAP5/MOD2 (24) - is of the same form as the EPRI correlation, but a value of 0.75 is chosen for the coefficient C_p. Use of this coefficient would be expected to produce vapour pull-through at a main pipe liquid level between those predicted by the EPRI and CATHARE correlations.

The EPRI correlation for the branchline quality is found (19) to over-predict the branchline void fraction for main-pipe liquid levels just below the level at which vapour pull-through commences. This is considered (19) to be due partly to the fact that the correlation does not tend to zero as the vapour pull-through level is approached. The correlation for the branchline quality implemented in the modified version of RELAP5/MOD2 (24) is different from that proposed by EPRI. It has the advantage of tending to zero as the vapour pull-through level is approached and is found (19) to provide a better fit to experimental branchline void fraction data immediately after the onset of vapour pull-through.

The likely effect, therefore, on the current calculation, of implementing the correlations used in the modified version of RELAP5/MOD2, rather than the EPRI correlations, would be to delay the time at which vapour pull-through occurred and, for ILHL liquid levels just below the vapour pull-through level, to lessen the reduction in the break line density, ie to provide a slightly better fit to the experimental data.

10.3.3   Choice of Choked Flow Multiplier

Since it could be argued that, had the break mass flow rate been correctly predicted during the initial part of the transient, the observed discrepancy in ILHL liquid level behaviour may not have arisen, calculations were performed in which it was attempted to reproduce the experimental break mass flow rate more accurately. The break mass flow rates predicted by TRAC-PF1/MOD1 using 2-phase choked flow multipliers of 1.0 (Base Case with EPRI Correlation and Input Modifications) and 1.2 are shown in Figure 66. Although the initial experimental break mass flow rate is well reproduced using a choked flow multiplier of 1.2, the drop in predicted break flow at ~ 400 seconds (characteristic of previous calculations) is still noticeable, confirming that the ILHL liquid level behaviour is not correctly reproduced despite the initial break mass flow rate being well-represented.

10.4 Summary

1)   As expected, reducing the volume of the Reflood Assist Bypass Line improved the time at which the break uncovered.

2)   Natural circulation in the ILHL and the time at which liquid starts to drain back from the steam generator are important factors in determining the behaviour of the ILHL liquid level. The predicted delay between natural circulation ceasing and liquid starting to drain back from the steam generator (not observed in the experiment) is thought to account for the difference in behaviour, between the experiment and the calculation, of the ILHL liquid levels and hence the discrepancies in break mass flow rate.

3)   The discrepancies between the measured and predicted ILHL
        liquid levels become less significant when the CATHARE, as
        opposed to the EPRI, correlation for the level at which
        vapour pull-through commences is used. Use of the CATHARE
        correlation therefore improves the agreement between the
        measured and predicted break mass flow rates. Had the ILHL
        level been correctly predicted, however, it is thought that
        the EPRI correlation would have performed satisfactorily.

4)   Use of a 2-phase choked flow multiplier (at the end of the
        break line) of 1.2 indicated that the ILHL liquid level
        behaviour is not correctly predicted despite the initial
        break mass flow rate being well represented.

11. CONCLUSIONS

The main findings of the TRAC-PF1/MOD1 analysis of the OECD LOFT
experiment LP-SB-1 were as follows:

1)   Very small cells were identified as having a detrimental
        effect on the running speed of the calculation. It was
        demonstrated that increasing the volume of a particular cell
        reduced the CPU to problem time ratio by ~ 40%.

2)   The results of the TRAC-PF1/MOD1 Base Case Calculation of
        LP-SB-1 tended to be consistent with those reported by
        members of the OECD LOFT Program Review Group. The overall
        trends with respect to pressure histories and minimum system
        mass inventory were reasonably well represented by the
        TRAC-PF1/MOD1 calculation. The inability of TRAC-PF1/MOD1
        to account for the main branch stratified liquid level in
        determining fluid conditions in a side branch led to
        discrepancies between the measured and predicted break line
        and ILHL densities and was found to be the main reason for
        the observed differences in break mass flow rate.

3)   Implementation of an EPRI correlation, for determining side
        branch quality as a function of main-pipe stratified liquid
        level, was effective in improving the predicted break line
        density early in the transient. The break mass flow rate
        was also improved, although it remained slightly lower than
        that measured.

4)   A difference, between the TRAC-PF1/MOD1 calculation and the
        experiment, in the time at which liquid started to drain
        back from the steam generator was identified as a possible
        cause for small discrepancies in the ILHL liquid level
        behaviour. The effect of these discrepancies, on the
        break line density and break mass flow rate, became less
        significant when the CATHARE correlation (for predicting the
        level at which vapour pull through occurs) was implemented,
        rather than the EPRI correlation.

12. RECOMMENDATIONS

It is suggested that:

1) A means of accounting for the effect of main pipe stratified liquid level in determining fluid conditions in a side branch should be implemented in TRAC-PF1/MOD1.

2) A closer examination of the factors influencing the draining of the steam generator tubes is required to resolve the observed discrepancies in intact loop hot leg liquid level behaviour.

13. ACKNOWLEDGEMENTS

The guidance of Dr C G Richards (AEEW) and the support of Sr F Pelayo (CSN, Spain), during the course of this work, are gratefully acknowledged.

14. REFERENCES

1. PETERS M D, Quick Look Report On OECD LOFT Experiment LP-SB-1, July 1983 (OECD LOFT-T-3204)

2. REEDER D L, LOFT System and Test Description, July 1978 (TREE-1208, NUREG/CR-0247)

3. KEE E J, SCHALLY P J, WINTERS L, Base Input for LOFT RELAP5 Calculations, July 1980 (EGG-LOFT-5199)

4. GRUSH W H, TANAKA M, MARSILI P, Best-Estimate Prediction for the OECD LOFT Project Small Cold Leg Break Experiment LP-SB-3, November 1983 (OECD LOFT-T-3005)

5. ALLEN E J, Internal Document

6. ALLEN E J, Internal Document

7. NEILL A P, Internal Document

8. PELAYO F, TRAC-PF1-MOD1 Post-Test Calculations of the OECD LOFT Experiment LP-SB-2, March 1987, (AEEW - R 2202)

9. MODRO S M, FELDMAN E M, NEWMAN N and PETERS M D, Experiment Analysis and Summary Report on OECD LOFT Nuclear Experiments LP-SB-1 and LP-SB-2, May 1984 (OECD LOFT-T-3205)

10. BIRCHLEY J, Private Communication

11. JOUSE W C, Internal LOFT Reactor Vessel Core Bypass Flows, November 1981 (LO-17-81-044)

12. ALEMBERTI A, PROTO G, Experiment Analysis and Summary Report on OECD LOFT Nuclear Experiment LP-SB-3 (Draft), December 1985

13. BIRCHLEY J, Private Communication

14. HALL P C, BROWN G, RELAP5/MOD2, Calculations of OECD LOFT Test LP-SB-1, July 1986 (GD/PE-N/554 (REV)

15. CHEN T H, MODRO S M, Best Estimate Prediction for OECD LOFT Experiment LP-SB-1, May 1983 (OECD LOFT-T-3203)

16. McPHERSON G D, Decay Heat Data for OECD LOFT Experiments, October 1985 (Letter to OECD LOFT Programme Review Group Members)

17. MODRO S M, CHEN T H, OECD LOFT Project Experiment Specification Document, Hot Leg Small Break Experiments LP-SB-1 and LP-SB-2, April 1983 (OECD LOFT-T-3201)

18. ANODA Y, OECD LOFT Experiment LP-SB-1 and LP-SB-2 Calculation Comparison Report, July 1986 (Draft)

19. ANDERSON J L, BENEDETTI R L, Critical Flow Through Small Pipe Breaks, May 1986 (EPRI NP-4532)

20. ARDRON K, CLARE A, Interphase Drag Calculations in the RELAP5/MOD2 and TRAC-PF1/MOD1 Thermal Hydraulic Codes (GD/PE-N/557 (REVISED)

21. MEMPONTEIL A, Super Moby Dick - First Results of Phase Separation in Tees, Seminaire CATHARE, 5-6 Novembre 1985, Grenoble

22. Safety Code Development Group, Energy Division, LANL, TRAC-PF1/MOD1: An Advanced Best-Estimate Computer Program For Pressurised Water Reactor Thermal-Hydraulic Analysis, July 1986, (NUREG/CR-3858, LA-10157-MS)

23. BOYACK B E, STUMPF H, LIME J F, TRAC User's Guide (NUREG/CR-4442, LA-10590-M), November 1985

24. ARDRON K H, BRYCE W M, Internal Document

TABLE 1

INITIAL CONDITIONS FOR EXPERIMENT LP-SB-1

	MEASURED (2)	TRAC PREDICTED
PRIMARY COOLANT SYSTEM		
Core ΔT (K)	18.5 $\pm$ 1.7	18.9
Hot Leg Pressure (MPa)	15.00 $\pm$ 0.08	15.0
Cold Leg Temperature (K)	557.2 $\pm$ 1.5	557.7
Mass Flow Rate (kgs^{-1})	483.1 $\pm$ 3.2	483.1
REACTOR VESSEL		
Power Level (MW)	48.8 $\pm$ 1.2	48.8
STEAM GENERATOR SECONDARY SIDE		
Liquid Level (m)	3.12 $\pm$ 0.05	3.12
Water Temperature (K)	535.2 $\pm$ 3.6	536.6
Pressure (MPa)	5.53 $\pm$ 0.05	5.57
Mass Flow Rate (kgs^{-1})	25.79 $\pm$ 0.77	25.57
PRESSURIZER		
Liquid Volume (m^3)	0.625 $\pm$ 0.001	0.624
Steam Volume (m^3)	0.377 $\pm$ 0.001	0.308[a]
Water Temperature (K)	615.8 $\pm$ 8.2	615.2
Pressure (MPa)	15.06 $\pm$ 0.11	14.98
Liquid Level (m)	1.072 $\pm$ 0.002	1.384[a]
BROKEN LOOP		
Cold Leg Temperature (K)	555.7 $\pm$ 6.3	557.7

a These figures are not within the uncertainties of the experimental
  data possibly due to a difference, between the experiment and the
  TRAC input deck, in the interpretation of the pressurizer geometry.

TABLE 2

PRESSURIZER VOLUME

REFERENCE		PRESSURIZER VOLUME (m^3)
LP-SB-1 EASR (9)		1.002
TRAC-PF1/MOD1 INPUT DECK		0.932
LOFT SPECIFICATION (2)	TABLE XXI	0.96
	TABLE A-2	0.931

TABLE 3

STEADY STATE PRESSURE DROPS

PART OF REACTOR SYSTEM	COMPONENT/CELL		TRAC-PF1/MOD1 CALCULATED PRESSURE DROP		TRAC -hρg	AVAILABLE PRESSURE DROP DATA SCALED TO MASS FLOW RATE OF 483.1 kgs^{-1} (kPa)
	FROM	TO	(MPa)	(kPa)		
Cold Leg	6/2p	7/9	15.1742–15.1548	19.4		19.9(10)
Inlet Nozzle Filler Inlet Port Exit to Anulus Circum. Flow to Downcomer	7/9	86/1	15.1548–15.1191	35.7	42.1	48.4(11)
Downcomer	86/1	86/8	15.1191–15.1355	-16.4	6.9	7.8(11)
Turn and Mix Lower Core Support	86/8	89/1	15.1355–15.1059	29.6	29.6	30.8(11)
Lower End Boxes Fuel Pins Upper End Boxes	89/1	87/1	15.1059–15.0637	42.2	26.7	27.9(11)
Upper Stack Region Core Barrel and Reactor Vessel Nozzles Hot Leg	87/1	1/4	15.0637–14.9922	71.5	58.8	53.7(10,11)
Steam Generator	1/4	3/1s	14.9922–14.7650	227.0		224.7(10)

TABLE 4

STEADY STATE ENVIRONMENTAL HEAT LOSSES

	ENVIRONMENTAL HEAT LOSSES (kW)			
	ASSUMED FOR RELAP5 ANALYSES OF LOFT EXPERIMENTS (12)	ESTIMATED FROM LOFT EXPERIMENTS L9-1 AND L3-3 (13)	MEASURED WITH ALL FLUID IN PRIMARY COOLANT SYSTEM AT A TEMPERATURE OF 555K (13)	TRAC-PF1/MOD1 PREDICTIONS
Primary Coolant System	170			143
Reactor Pressure Vessel				89
Pressurizer	6			6
Steam Generator Secondary Side	20			19
TOTAL	196	200 ± 100	248	257

TABLE 5

STEADY STATE CORE BYPASS FLOW RATES

	Component/Cell No	TRAC-PF1/MOD1 Predictions		Available Data(11)
		Mass Flow Rate (kgs^{-1})	% Primary Mass Flow Rate	% Primary Mass Flow Rate
Paths 1, 2 and 3 Lower Core Support Structure, Lower End Box and Gauge Hole Bypasses	89/1s	16.93	3.5	3.5
Path 4 Outlet Nozzle Gap	83/1	13.23	2.7	1.28 - 3.54
Path 5 Core Barrel Alignment Key	79/1	0.20	0.04	0.04
Reflood Assist Bypass Valve (RABV)	31/3s	25.66	5.3	5.25

TABLE 6

TRANSIENT CALCULATION – DECAY HEAT POWER TABLE

Time After Scram (t, seconds)	$\dfrac{\text{Power at Time t}}{\text{Initial Power}}$ (15) (r)	Power (at time t) (48.8 r, MW)
0.0	1.0	48.8000
0.15	0.88	42.9440
0.3	0.76	37.0880
0.6	0.58	28.3040
0.85	0.176	8.5888
1.0	0.122605	5.9831
1.3	0.1	4.8800
2.0	0.087420	4.2661
4.0	0.075788	3.6985
7.0	0.064	3.1232
10.0	0.060012	2.9286
25.0	0.046738	2.2808
65.0	0.035	1.7080
100.0	0.031546	1.5394
250.0	0.025210	1.2302

a   Neutron and Fission Power

Time After Scram (Seconds)	Power (16) (MW)
650.0	0.93047
1000.0	0.82223
1500.0	0.71837
3000.0	0.54527
5000.0	0.43385
1.0 E5	0.07566

b   Fission Power

TABLE 7

TRANSIENT CALCULATION – STEAM GENERATOR
SECONDARY SIDE AUXILIARY FEEDWATER FLOW RATE TABLE

Transient Time (Seconds) (Time After Reactor Scram (1.4 Seconds) + 50 seconds)*	Liquid Velocity (ms^{-1})
0.0	0.0
111.9	0.0
112.0	0.061673
1913.4	0.061673
1913.5	0.0
4000.0	0.0

* Calculation was run in transient mode steady state for 50 seconds.

TABLE 8

TRANSIENT CALCULATION - HIGH PRESSURE INJECTION SYSTEM (HPIS) FLOW RATE TABLE

PCS Pressure (MPa)	HPIS Flow Rate (17) (ℓs^{-1})	HPIS Flow Rate for TRAC-PF1/MOD1 Calculation* (ms^{-1})
8.70	0.3155	0.0527
8.36	0.3155	0.0527
7.67	0.3918	0.0654
6.98	0.4883	0.0815
5.60	0.6031	0.1007
4.22	0.7022	0.1178
3.53	0.7583	0.1266
2.15	0.8505	0.1420
0.08	0.9564	0.1597

* flow area of HPIS piping = 5.9892×10^{-3} m^2

TABLE 9

OPERATIONAL SETPOINTS FOR EXPERIMENT LP-SB-1

Action	Measured During Experiment (9)		Specified to TRAC-PF1/MOD1 Calculation	
	Reference	Setpoint	Reference (Component/cell no)	Setpoint
Small-Break Valve Opened	Time	0 Seconds	Time	0 Seconds
Reactor Scrammed	ILHL Pressure	14.57±0.03 MPa	ILHL (99/1) Pressure	14.57 MPa
Main Feedwater Shut Off	ILHL Pressure	14.57±0.03 MPa	ILHL (99/1) Pressure	''
Main Steam Control Valve Started to Close	"Upon Verification of Reactor Scram"		2 seconds after Reactor Scram	14.57 MPa + 2 seconds
Primary Coolant Pumps Tripped	—	11.12 MPa	ILCL (7/5) Pressure	11.12 MPa
HPIS Flow Initiated	ILHL Pressure	8.24±0.03 MPa	ILHL (99/1) Pressure	8.24 MPa
Auxiliary Feed-water Initiated	Time After Reactor Scram	62±0.2 seconds	Time After Reactor Scram	62 seconds
Auxiliary Feed-water Terminated	Time After Initiation of Auxiliary Feed-water	1801.4±0.8 seconds	Time After Initiation of Auxiliary Feed-water	1801.4 seconds
Experiment Terminated	ILHL Pressure	2.487±0.001MPa	ILHL (99/1) Pressure	2.487 MPa

TABLE 10

LP-SB-1 BASE CASE TRANSIENT CALCULATION - CHRONOLOGY OF EVENTS

EVENT	TIME AFTER EXPERIMENT INITIATION(s)		
	MEASURED ([9])		TRAC PREDICTED
Small-break valve opened	0.0		0.0
Reactor scrammed	1.4	± 0.05	0.5
Main feedwater shut off	1.4	± 0.2	0.5
Main steam control valve started to close	3.4	± 0.2	2.5
Main feedwater isolated	3.8	± 0.05	2.6
Main steam control valve fully closed	15.4	± 0.2	54[a]
Primary coolant pumps tripped	24.6	± 0.2	25.7
Pressurizer liquid level below indicating range	34.6	± 0.4	53[b]
HPIS flow initiated	41.4	± 0.2	41.1
Primary coolant pump 1 coastdown completed	42.6	± 0.2	46.4
Primary coolant pump 2 coastdown completed	43.0	± 0.2	46.4
Subcooled blowdown ended	57.5	± 0.2	65[c]
Auxiliary feedwater initiated	63.4	± 0.2	63.4
Break started to uncover	715	± 3	~ 1200
Primary system pressure became less than secondary system pressure	1077	± 10	1380
Auxiliary feedwater shut off	1864.8	± 0.8	1864.8
HPIS flow rate exceeded break flow rate	1998.0	± 200	1820.0
HPIS + pump injection flow rate exceeded break flow rate	–		1680.0
Experiment termination criterion reached	3668	± 2.0	3227

a   The opening of the steam flow bypass valve during the transient was simulated using the main steam control valve.

b   Defined as the time when $\alpha = 1.0$ in bottom cell of pressuriser (level < 0.01 m after ~ 40 seconds).

c   Defined as the time when $T_{liq} = T_{sat}$ in the break line.

TABLE 11

RESULTS FROM STAND-ALONE BREAK LINE MODEL

	LF-SB-1 Experiment	'Stand-Alone' Break Line Model	Base Case Calculation
Break Mass Flow Rate (kgs^{-1})	4.0	4.0	3.3
Break Line Density (kgm^{-3})	~ 670	700	570

TABLE 12

COMPARISON OF COEFFICIENTS USED IN VAPOUR PULL
THROUGH AND LIQUID ENTRAINMENT CORRELATIONS

	EPRI (19)	SMOGLIE (19)	CATHARE (21)	ZUBER (19)
C_e	0.62	0.69	0.62	0.687
C_p	0.82	0.75	0.62	0.687

$$\frac{h_e}{D} = \frac{1}{2} - \frac{C_e}{D} \left[\frac{\dot{m}_g^2}{g\rho_g (\rho_f - \rho_g)} \right]^{0.2}$$

$$\frac{h_p}{D} = \frac{1}{2} + \frac{C_p}{D} \left[\frac{\dot{m}_f^2}{g\rho_f (\rho_f - \rho_g)} \right]^{0.2}$$

where

h_e = liquid level at which liquid entrainment begins (m)

h_p = liquid level at which vapour pull-through begins (m)

D = mainline internal diameter (m)

C_e = coefficient, as above

C_p = coefficient, as above

$\dot{m}_g$ = gas mass flow rate in branchline (kgs^{-1})

$\dot{m}_f$ = liquid mass flow rate in branchline (kgs^{-1})

g = acceleration due to gravity (ms^{-2})

ρ_g = gas density (kgm^{-3})

ρ_f = liquid density (kgm^{-3})

Intact loop

Broken loop

BL-1
experimental
measurement
station

Quick opening
valve (2)

PC-2
experimental
measurement
station

Steam
generator

Isolation
valve (2)

Pressurizer

BL-2
experimental
measurement
station

Gamma
densitometer

ECC cold leg
injection location

Pumps

PC-1
experimental
measurement
station

Drag disc
and turbine

Break plane

Reactor
vessel

Suppression
vessel

Downcomer

Core

CV-P139-57

Lower plenum

CV-P139-58

To BST

Reactor vessel
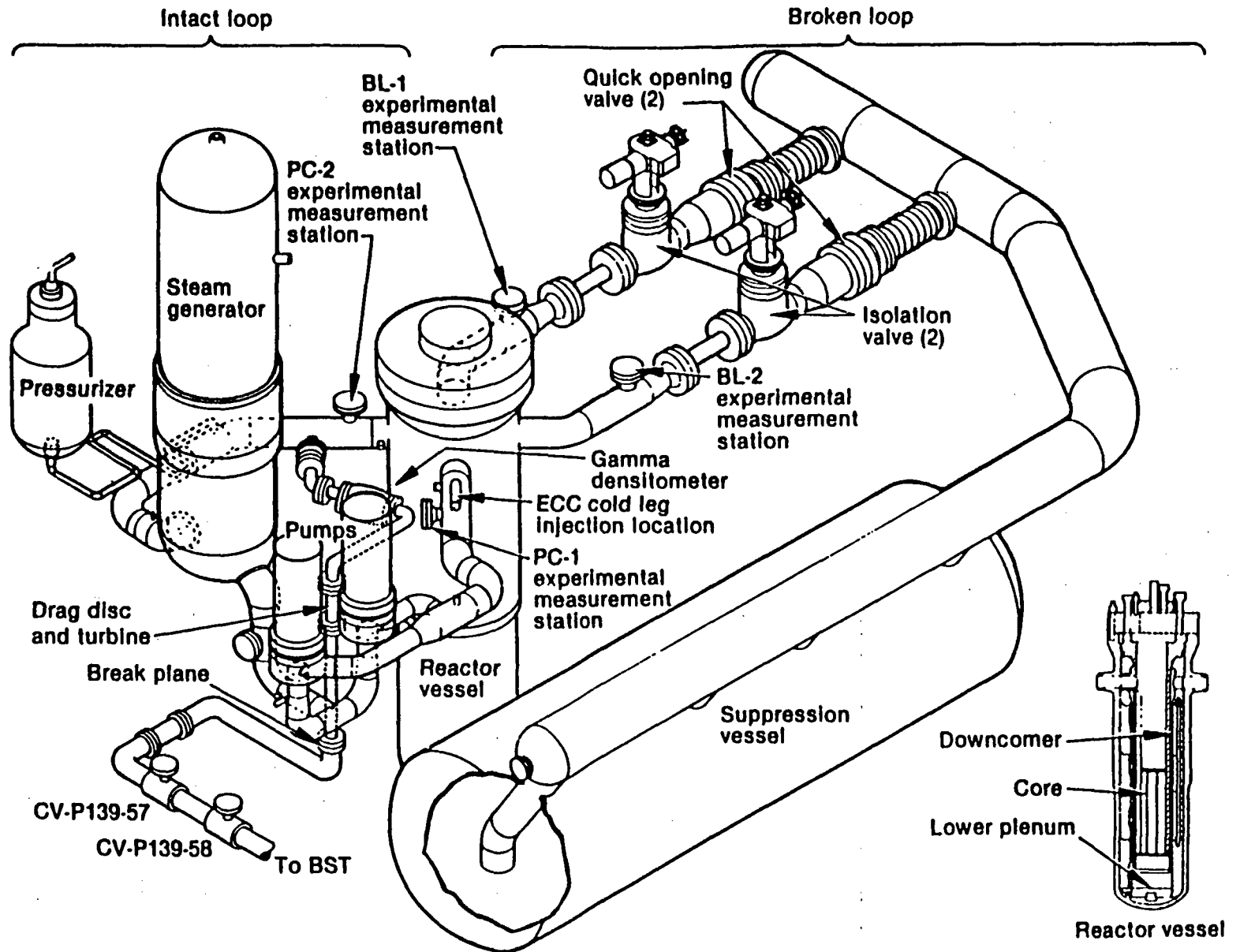
FIGURE 1

LOFT SYSTEM CONFIGURATION FOR LP-SB-1

EXPERIMENT LP-SB-1

Break initiated (0 s)
Reactor scram (1.4 s)

CL Press.(PE-PC-006)
Uncert = ± 0.088 MPa

Primary coolant pumps tripped (24.6 s)

Pressurizer emptied (34.6 s)

HPIS flow initiated (41.4 s)

Subcooled blowdown ended (57.5 s)
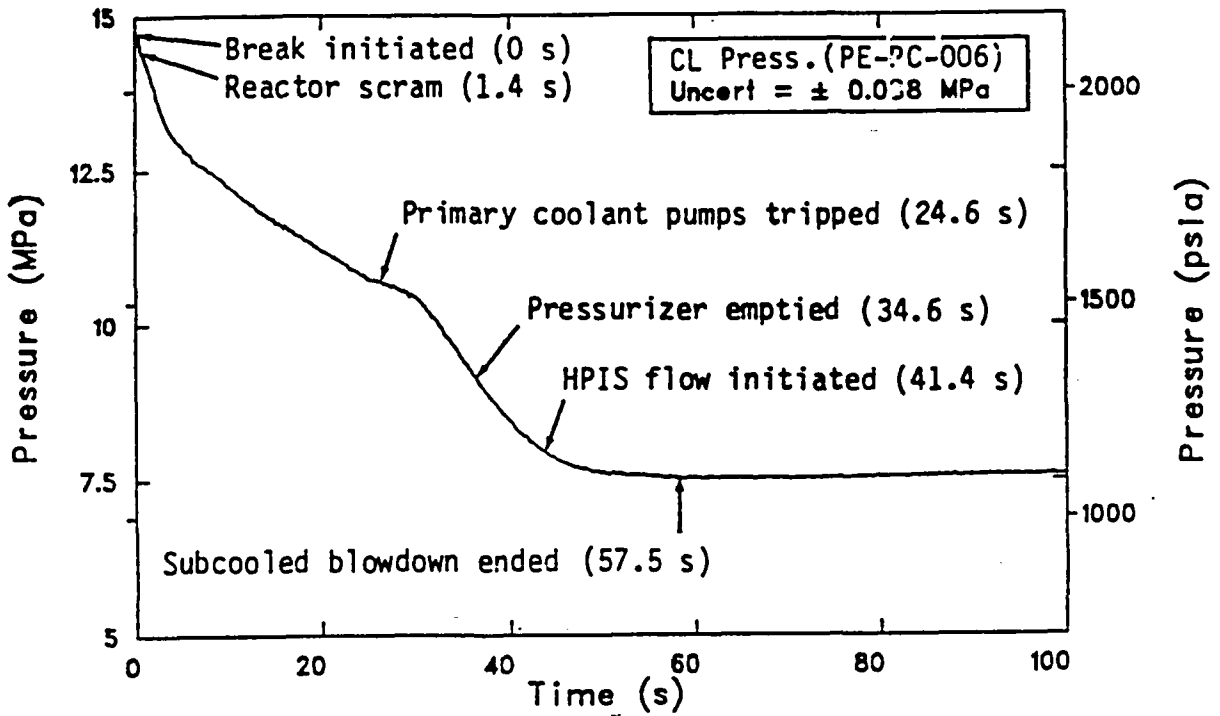
Primary system pressure (0 to 100 s).

EXPERIMENT LP-SB-1

CL Press.(PE-PC-006)
Uncert = ± 0.088 MPa

Break uncovered (715 s)

Primary pressure less than
secondary pressure (1077 s)

Experiment terminated (3668 s)
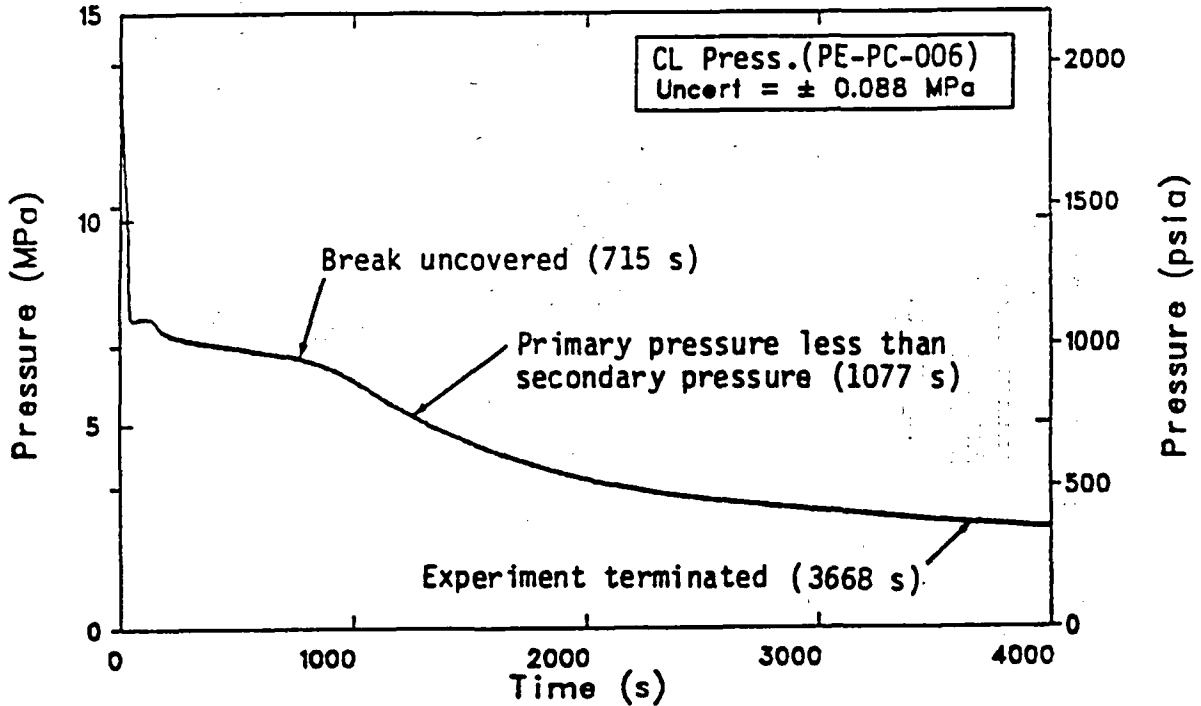
Primary system pressure (0 to 4000 s).

FIGURE 2

LP-SB-1 PRIMARY SYSTEM PRESSURE AND TIMINGS
OF SIGNIFICANT EVENTS

Component No	Component Name	Component No	Component Name
99	ILHL & Break Pipe	4	Pump No 2
1	Intact Loop Hot Leg	61	Pump No 2 Injection Tee
8	Pressurizer	5	Pump No 1
2	Steam Generator	63	Pump No 1 Injection Tee
3	Pump Suction	6	Pump Discharge
		7	Intact Loop Cold Leg
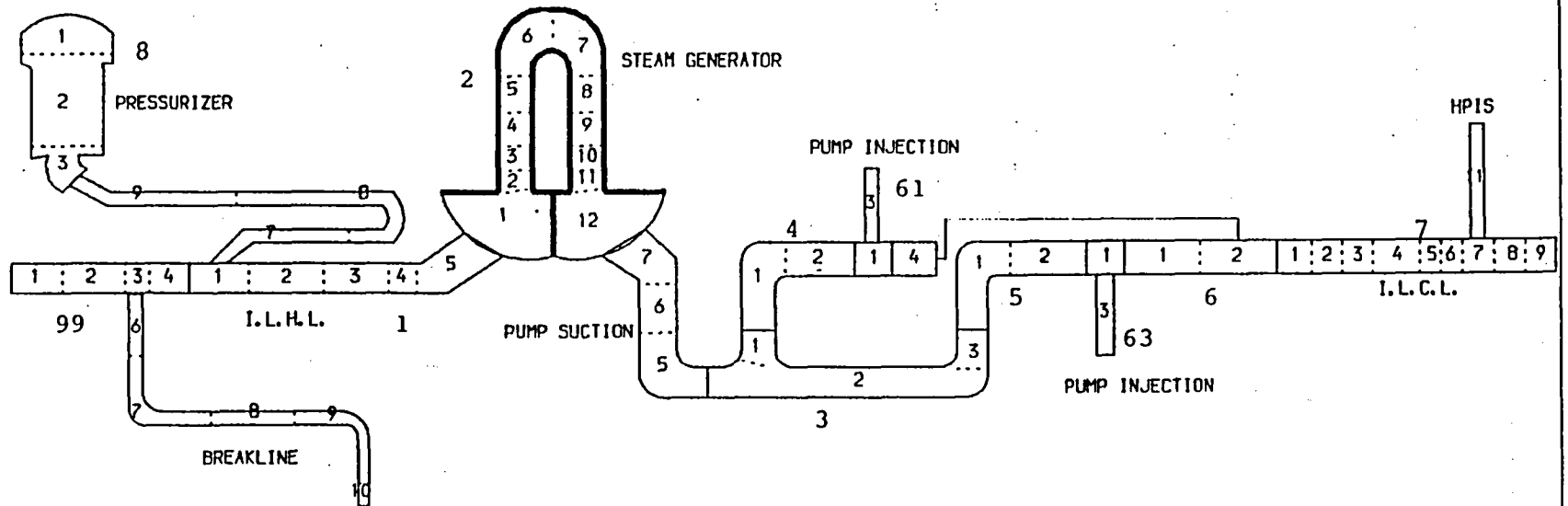
FIGURE 3a
PRIMARY SYSTEM NODALISATION DIAGRAM FOR LP-SB-1

(A) INTACT LOOP

Component No	Component Name
41	Broken Loop Cold Leg
31	Broken Loop Hot Leg
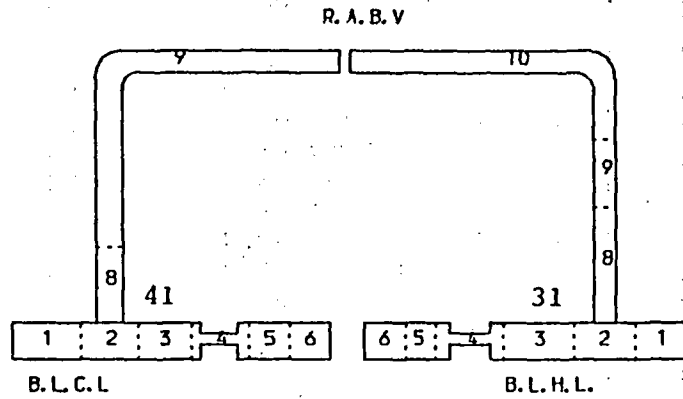
FIGURE 3b
PRIMARY SYSTEM NODALISATION DIAGRAM FOR LP-SB-1

(B) BROKEN LOOP

Vessel Representation for "System Mimic"
(See Appendix V)
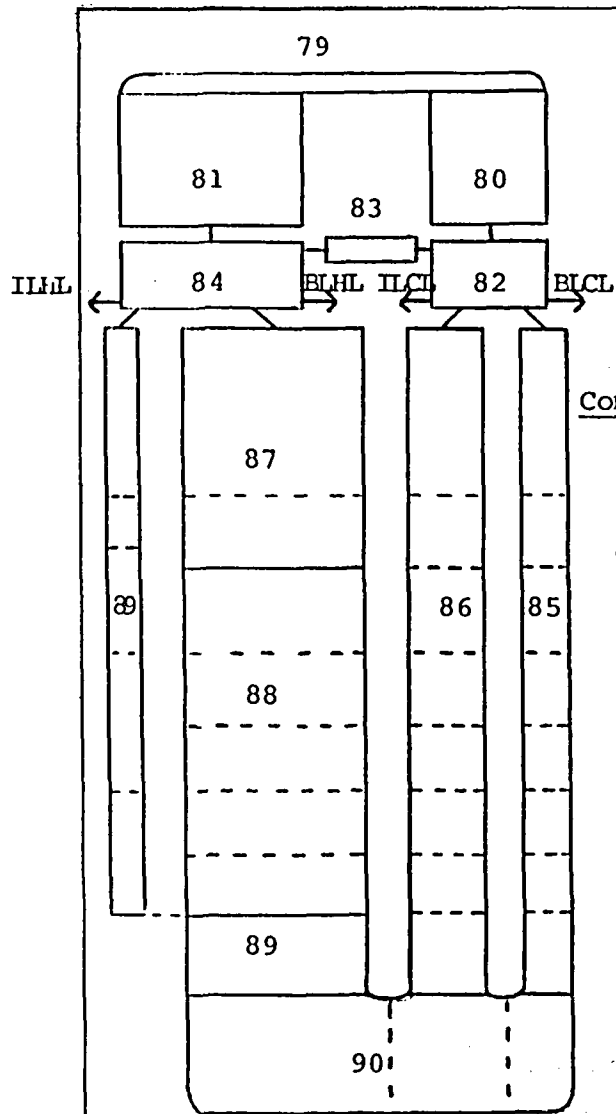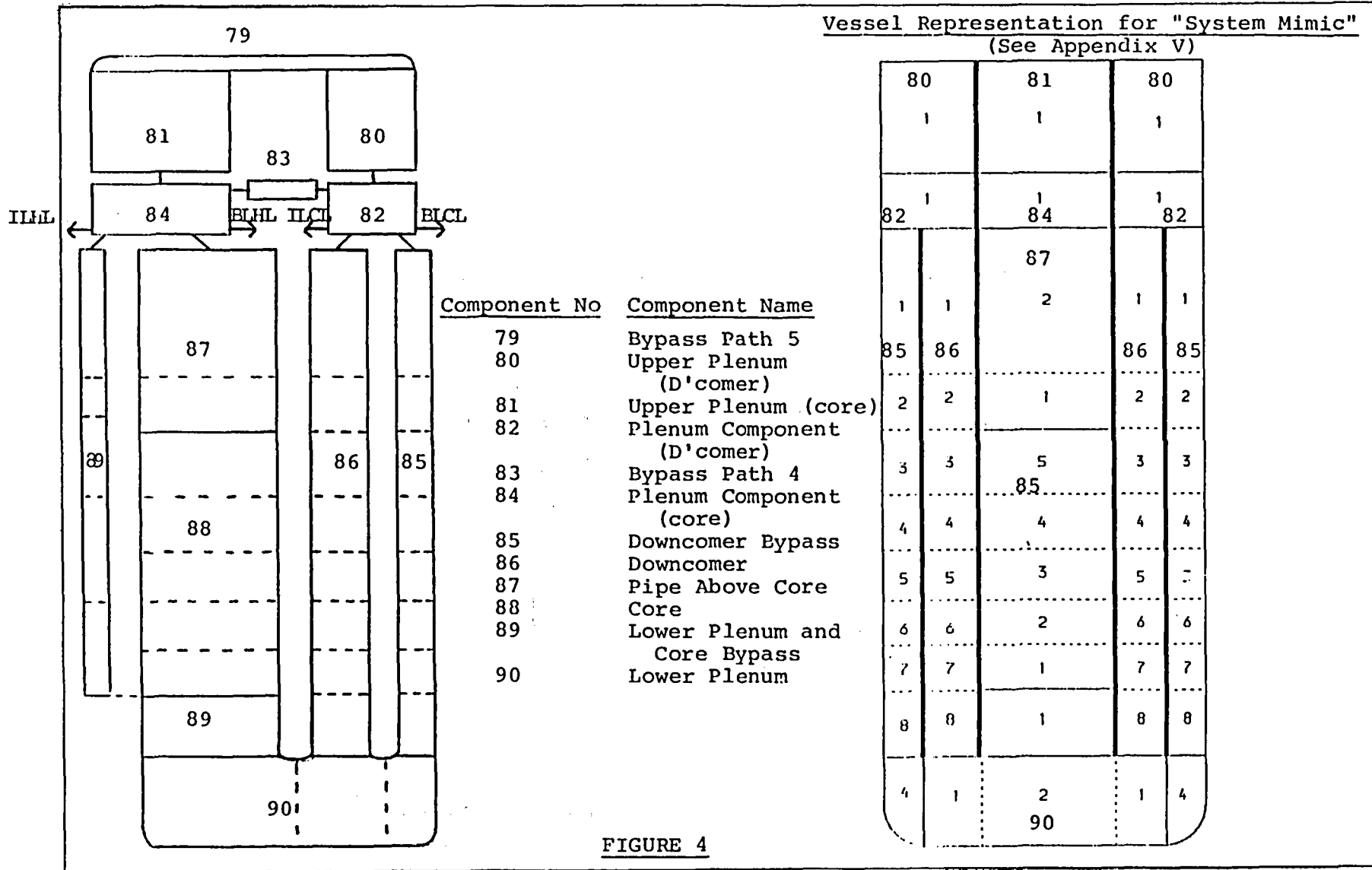
Component No	Component Name
79	Bypass Path 5
80	Upper Plenum (D'comer)
81	Upper Plenum (core)
82	Plenum Component (D'comer)
83	Bypass Path 4
84	Plenum Component (core)
85	Downcomer Bypass
86	Downcomer
87	Pipe Above Core
88	Core
89	Lower Plenum and Core Bypass
90	Lower Plenum

FIGURE 4

TRAC-PF1/MOD1 REACTOR VESSEL NODALISATION DIAGRAM FOR LP-SB-1

MAIN STEAM LINE   23

Cells Numbered	Component No	Component Name
14-19	20	Boiler
28,29,31	21	Steam Dome
21-24,26	22	Downcomer
1-6	23	Steam Line Valve
	27	Main and Auxiliary Feedwater Tee

MAIN FEEDWATER

AUX FEEDWATER
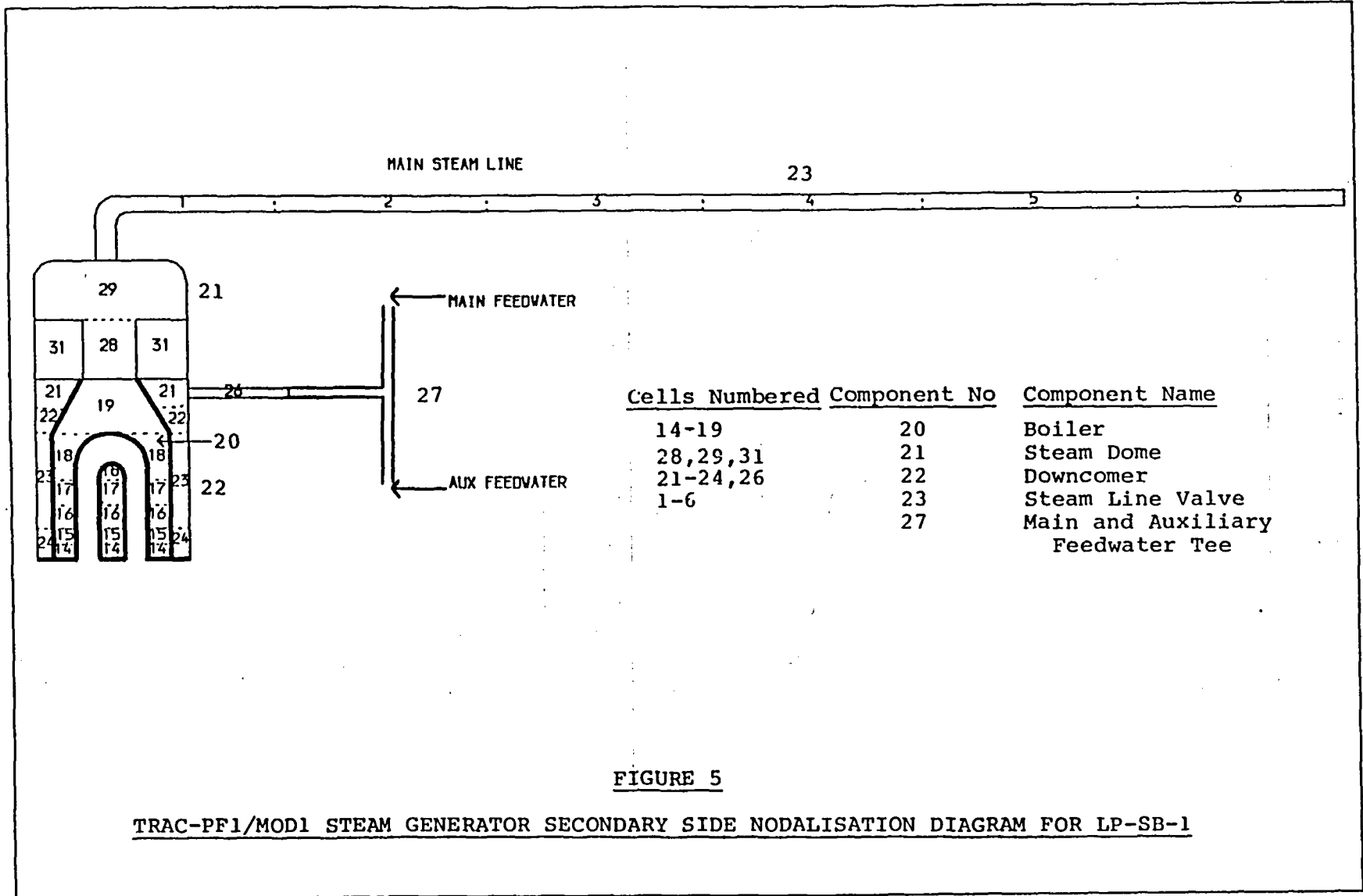
FIGURE 5

TRAC-PF1/MOD1 STEAM GENERATOR SECONDARY SIDE NODALISATION DIAGRAM FOR LP-SB-1

THE FOLLOVING ARE PLOTTED AGAINST REACTOR TIME

TOTAL CPU TIME
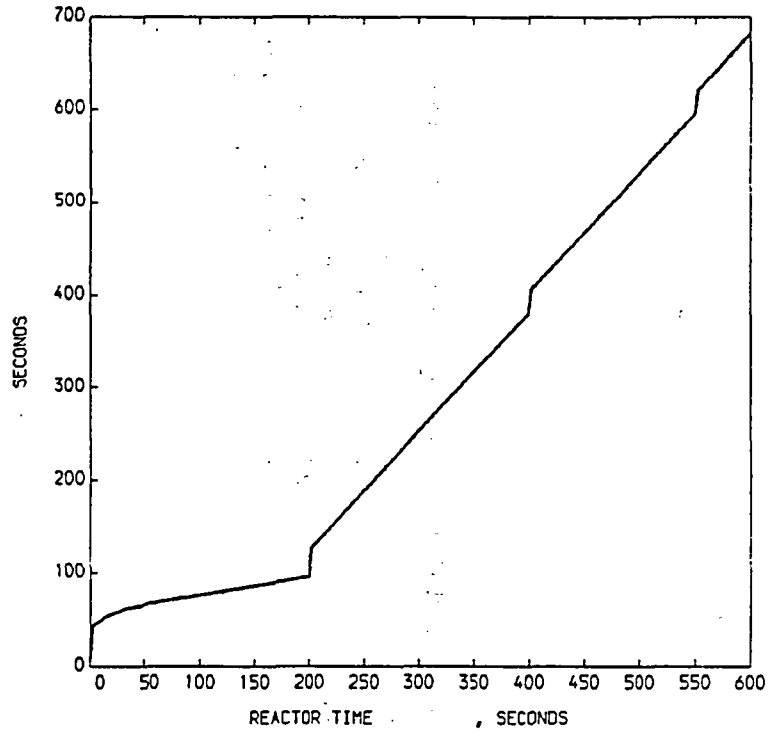
FIGURE 6 - CPU USAGE
LP-SB-1 STEADY STATE CALCULATION

THE FOLLOVING ARE PLOTTED AGAINST REACTOR TIME
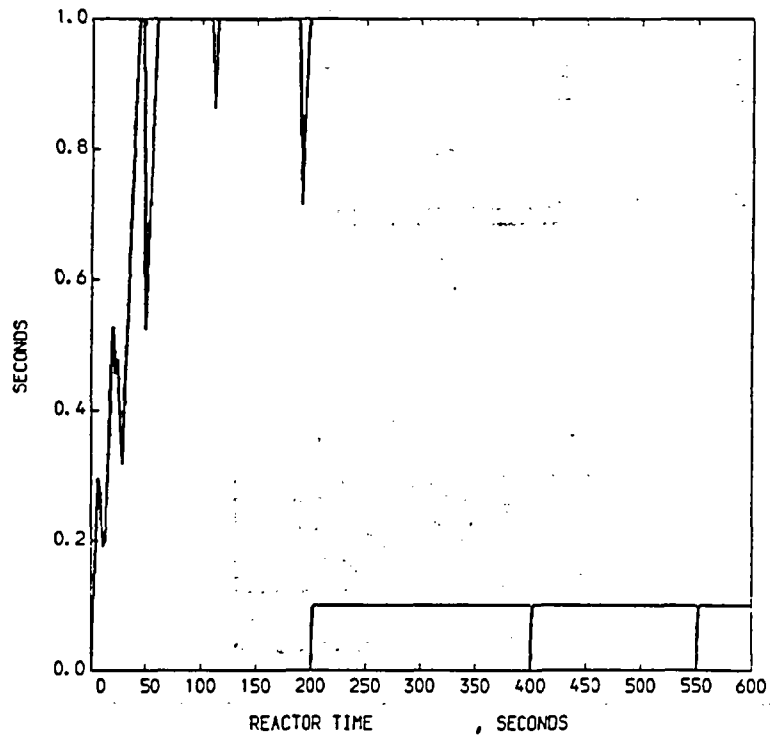
TIME STEP SIZE

FIGURE 7 - TIME STEP SIZE
LP-SB-1 STEADY STATE CALCULATION

AEEW - R 2254
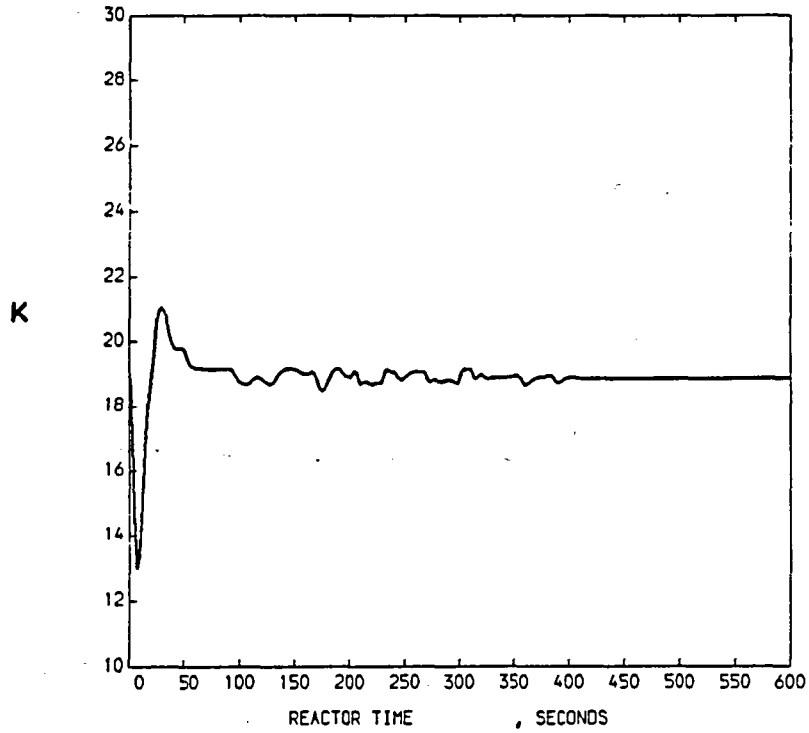
FIGURE 8 - TEMPERATURE DIFFERENCE ACROSS CORE
LP-SB-1 STEADY STATE CALCULATION
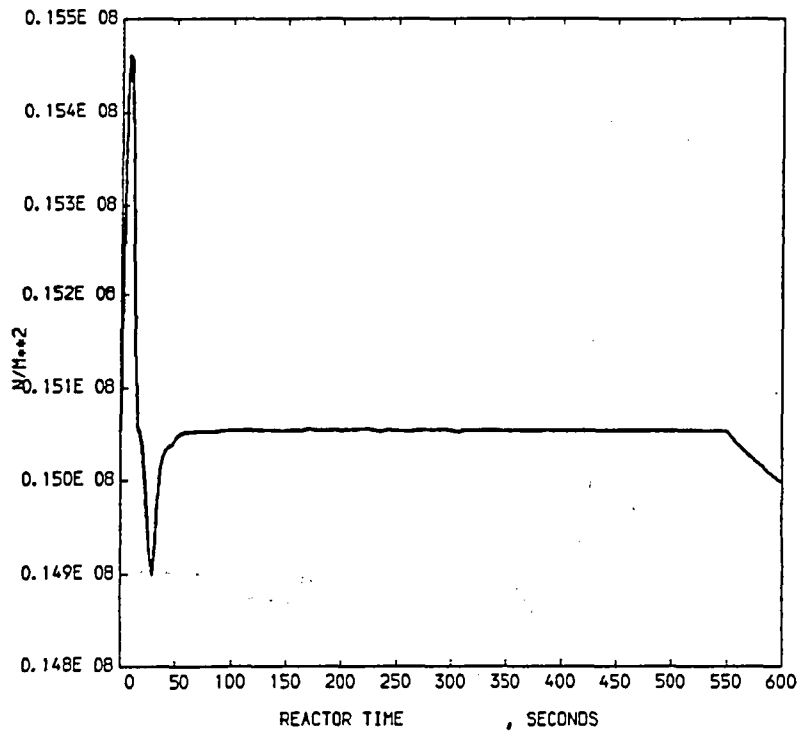
FIGURE 9 - PRIMARY SYSTEM PRESSURE
LP-SB-1 STEADY STATE CALCULATION

AEEW - R 2254
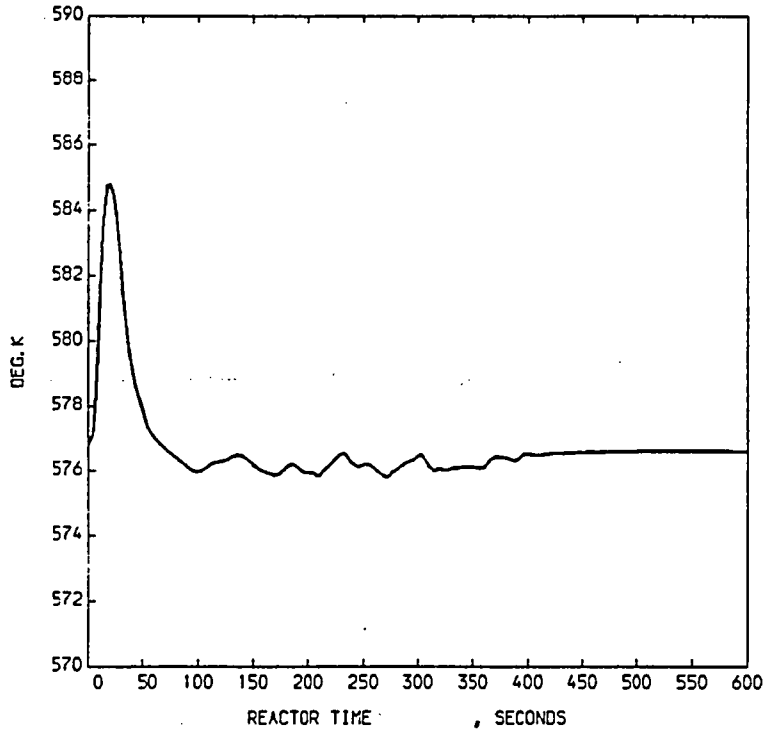
FIGURE 10 - ILHL TEMPERATURE
LP-SB-1 STEADY STATE CALCULATION
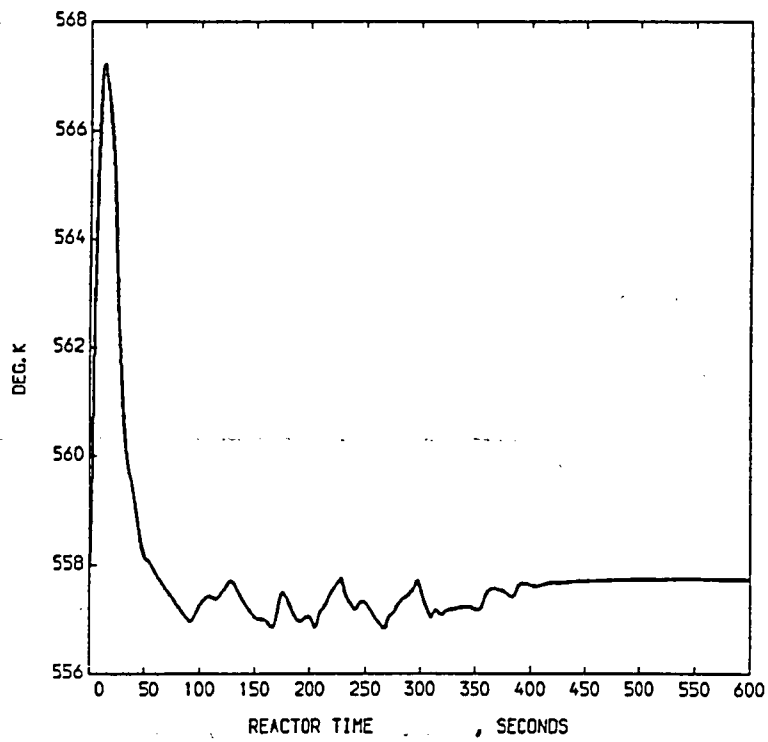
FIGURE 11 - ILCL TEMPERATURE
LP-SB-1 STEADY STATE CALCULATION
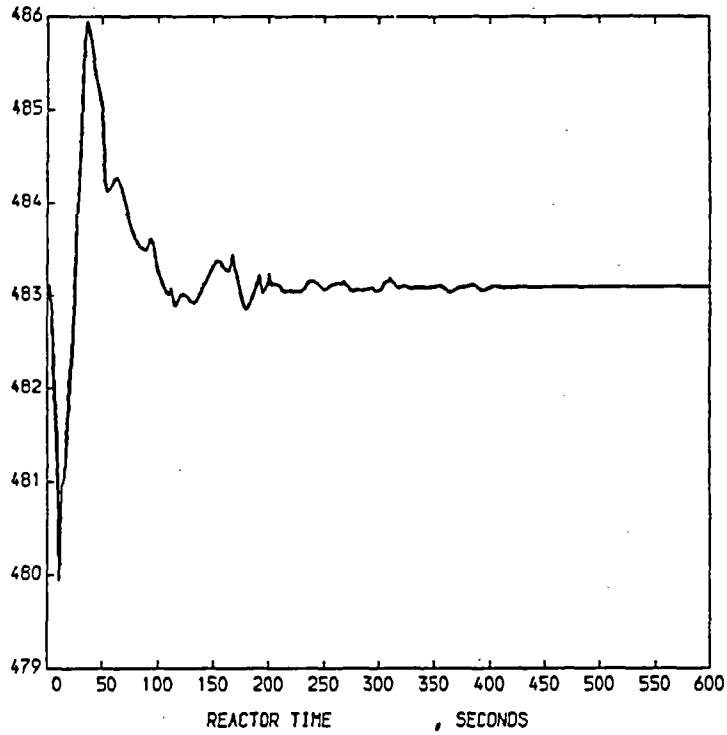
FIGURE 12 - ILHL MASS FLOW RATE (KG/S)
LP-SB-1 STEADY STATE CALCULATION
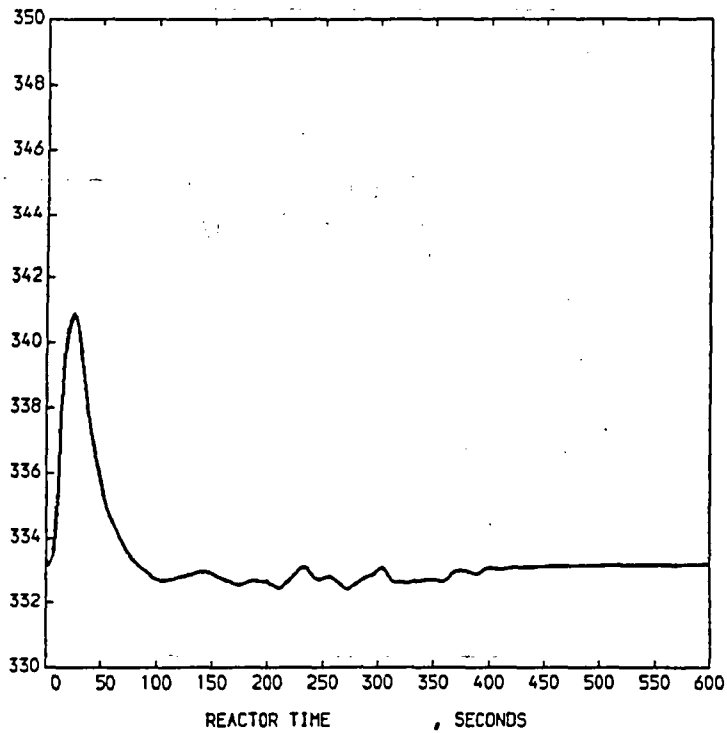
FIGURE 13 - PUMP SPEED (RAD/S)
LP-SB-1 STEADY STATE CALCULATION

AEEW - R 2254
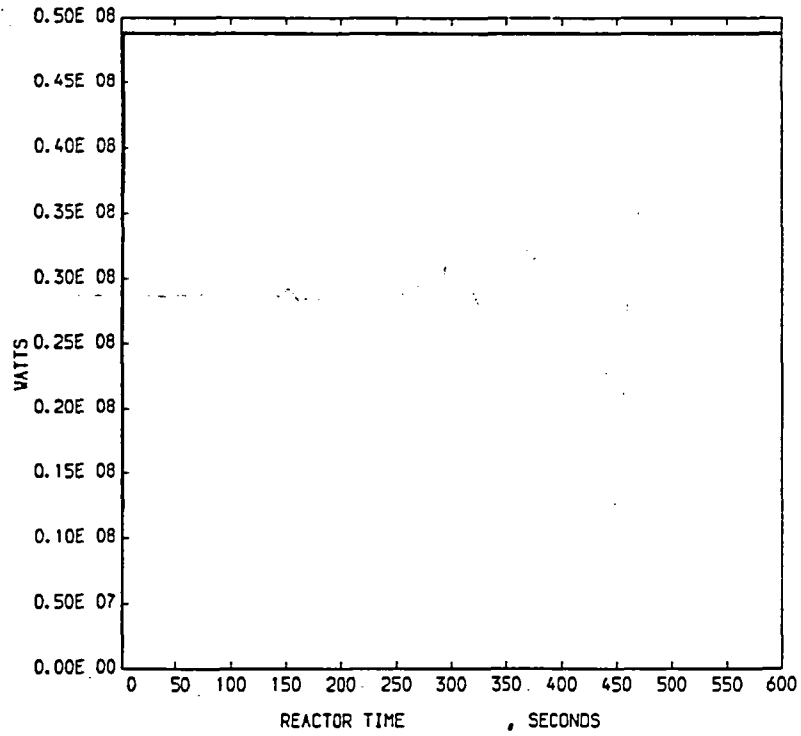
REACTOR POWER

FIGURE 14 – REACTOR POWER
LP-SB-1 STEADY STATE CALCULATION

SIGNAL VAR. NO.   4
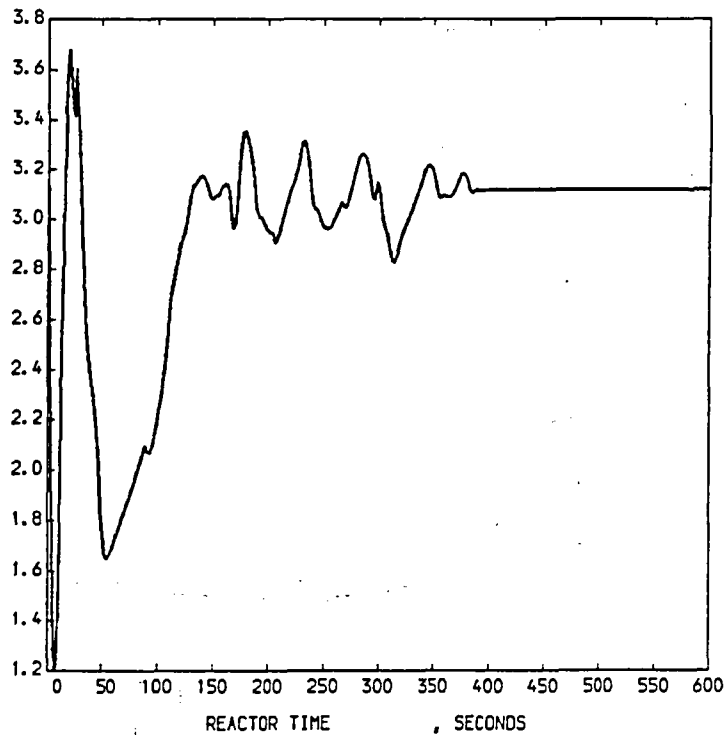
FIGURE 15 – SGS LIQUID LEVEL (M)
LP-SB-1 STEADY STATE CALCULATION

AEEW – R 2254
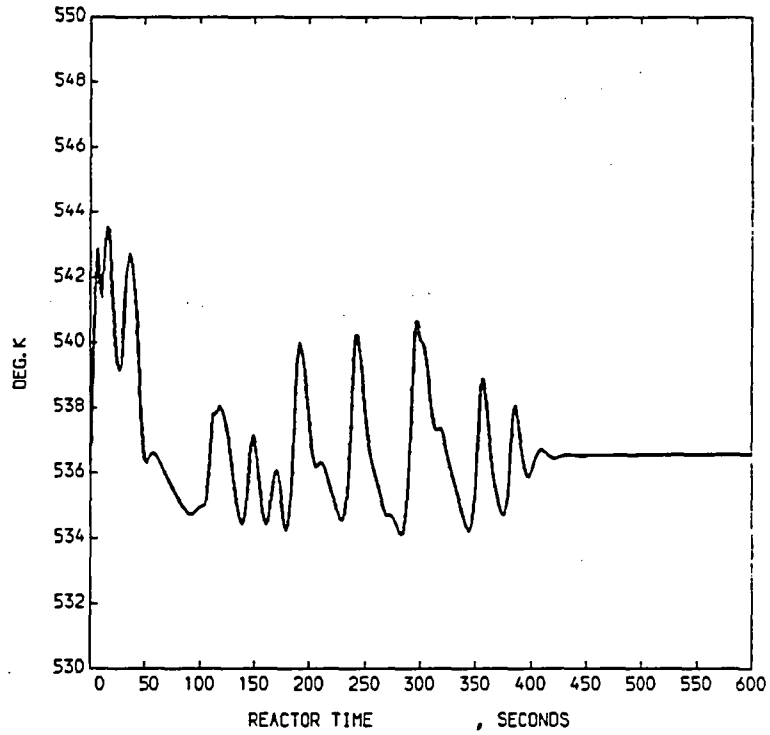
FIGURE 16 - SGS TEMPERATURE (BOTTOM DOWNCOMER)
LP-SB-1 STEADY STATE CALCULATION
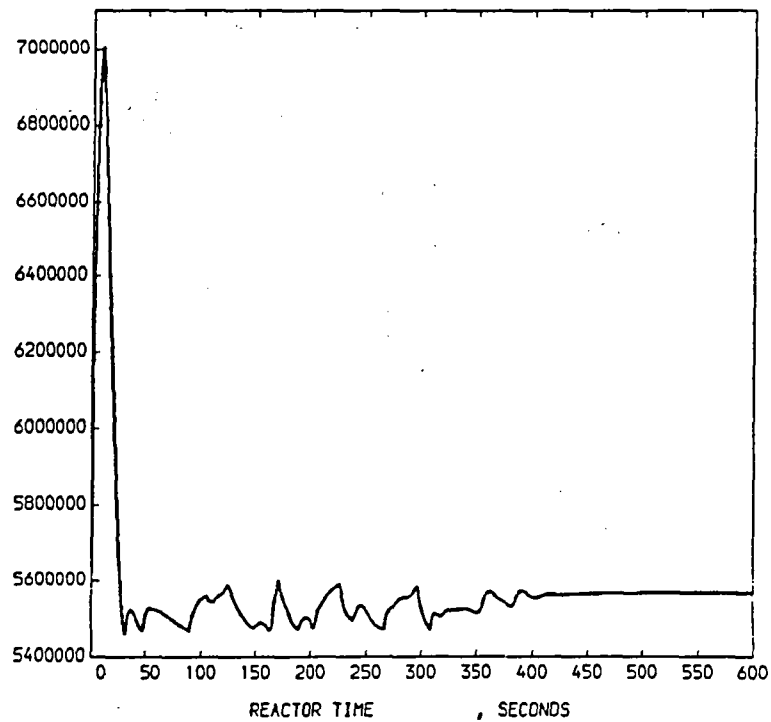
FIGURE 17 - SGS PRESSURE (PA)
LP-SB-1 STEADY STATE CALCULATION

AEEW - R 2254
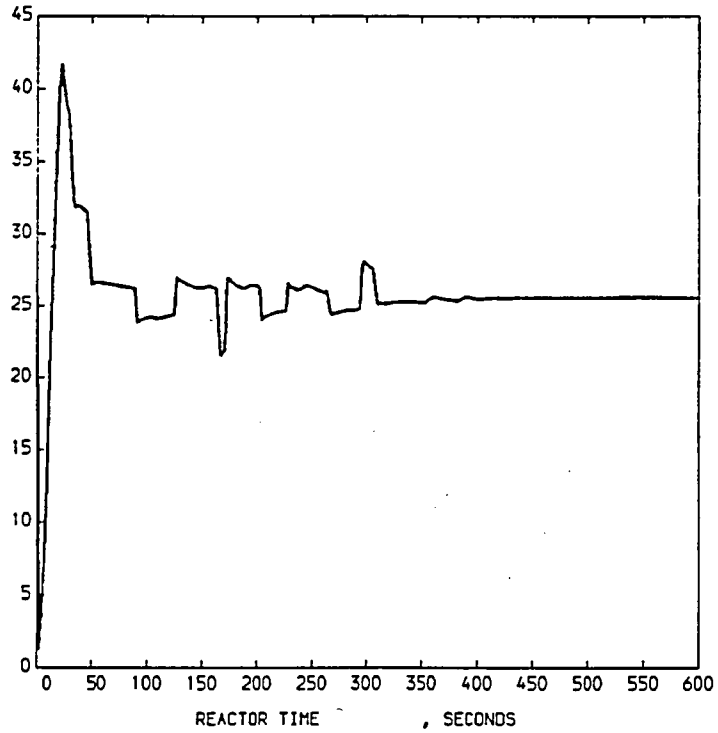
FIGURE 18 - SGS STEAM MASS FLOW RATE (KG/S)
LP-SB-1 STEADY STATE CALCULATION
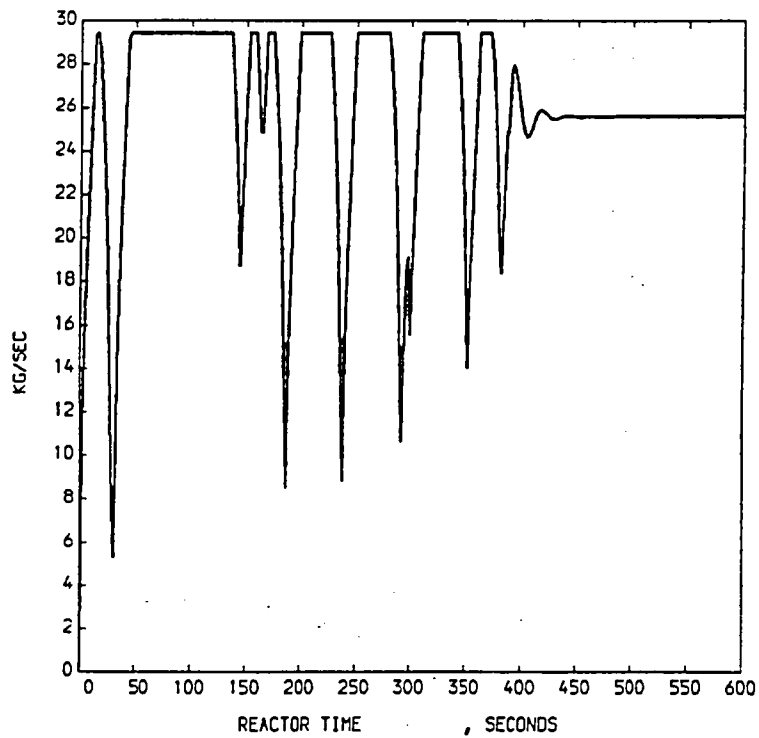
FIGURE 19 - SGS FEEDWATER MASS FLOW RATE
LP-SB-1 STEADY STATE CALCULATION
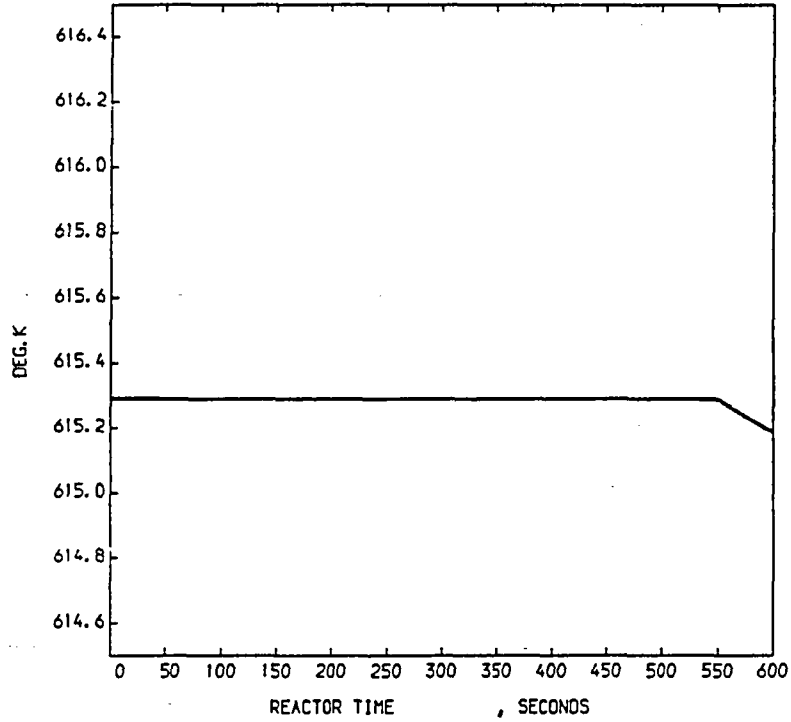
FIGURE 20 - PRESSURIZER LIQUID TEMPERATURE
LP-SB-1 STEADY STATE CALCULATION
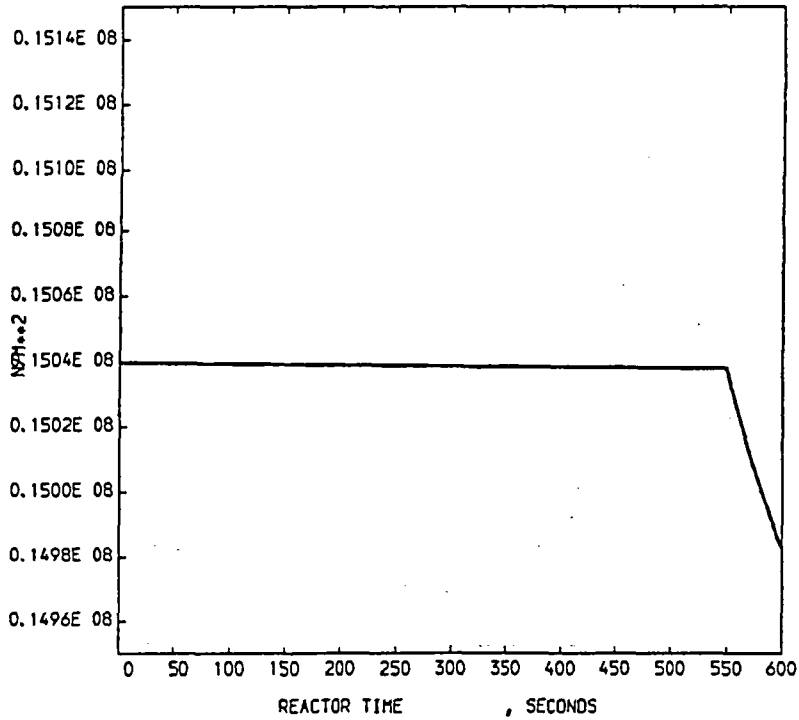
FIGURE 21 - PRESSURIZER PRESSURE
LP-SB-1 STEADY STATE CALCULATION
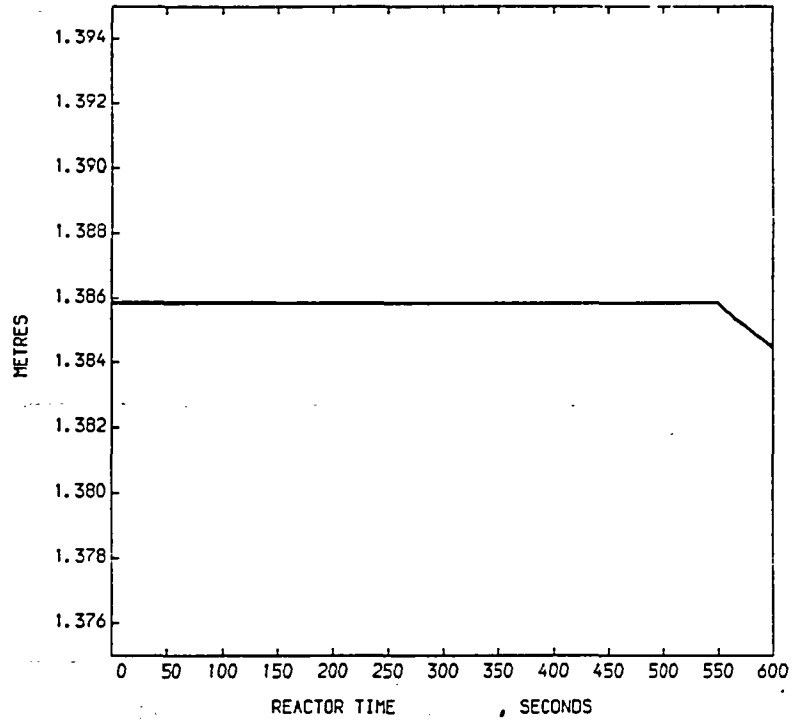
FIGURE 22 - PRESSURIZER LIQUID LEVEL
LP-SB-1 STEADY STATE CALCULATION
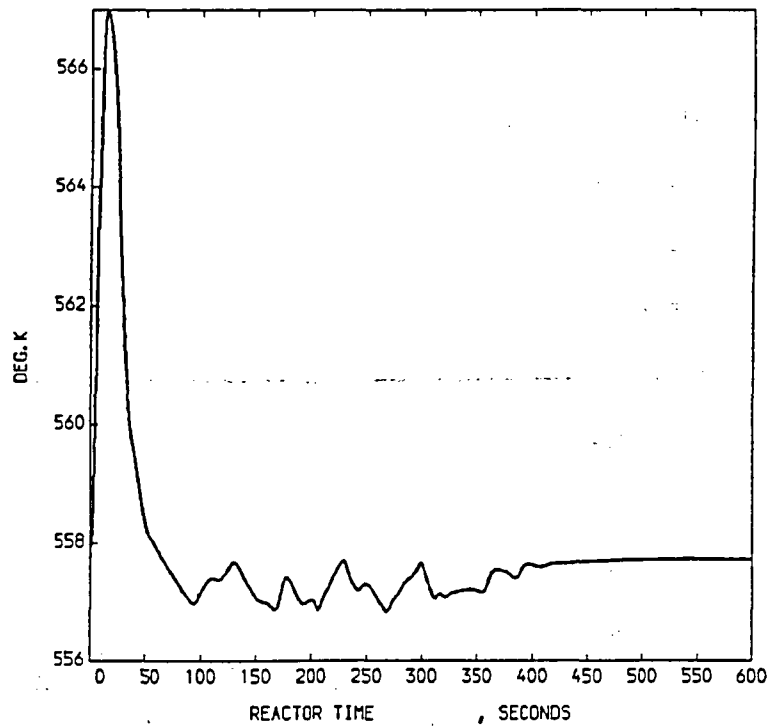
FIGURE 23 - BLCL TEMPERATURE
LP-SB-1 STEADY STATE CALCULATION
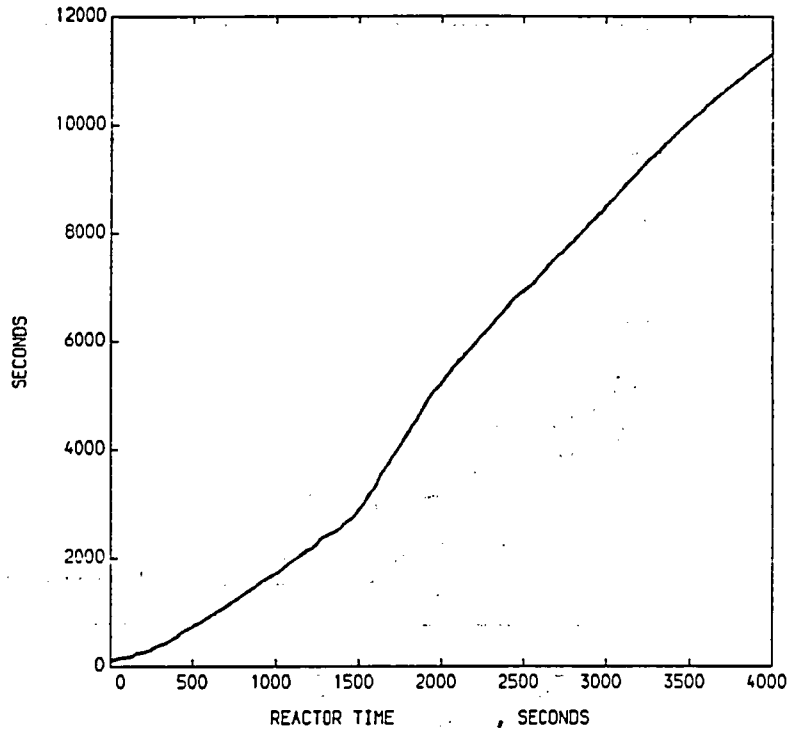
FIGURE 24 - CPU USAGE
LP-SB-1 BASE CASE CALCULATION

THE FOLLOWING ARE PLOTTED AGAINST REACTOR TIME
TIME STEP SIZE
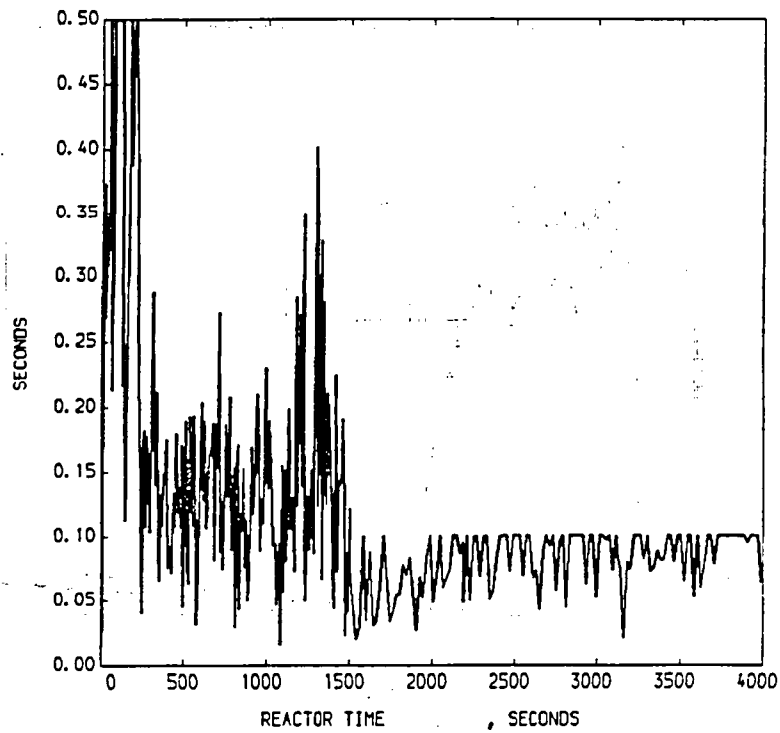
FIGURE 25 - TIME STEP SIZE
LP-SB-1 BASE CASE CALCULATION
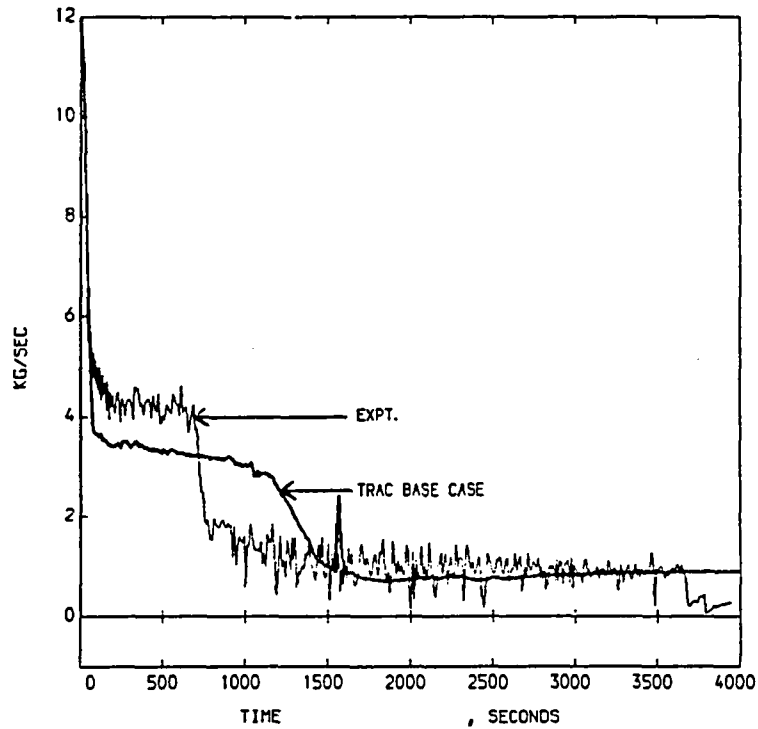
FIGURE 26 - BREAK MASS FLOW RATE
LP-SB-1 BASE CASE CALCULATION
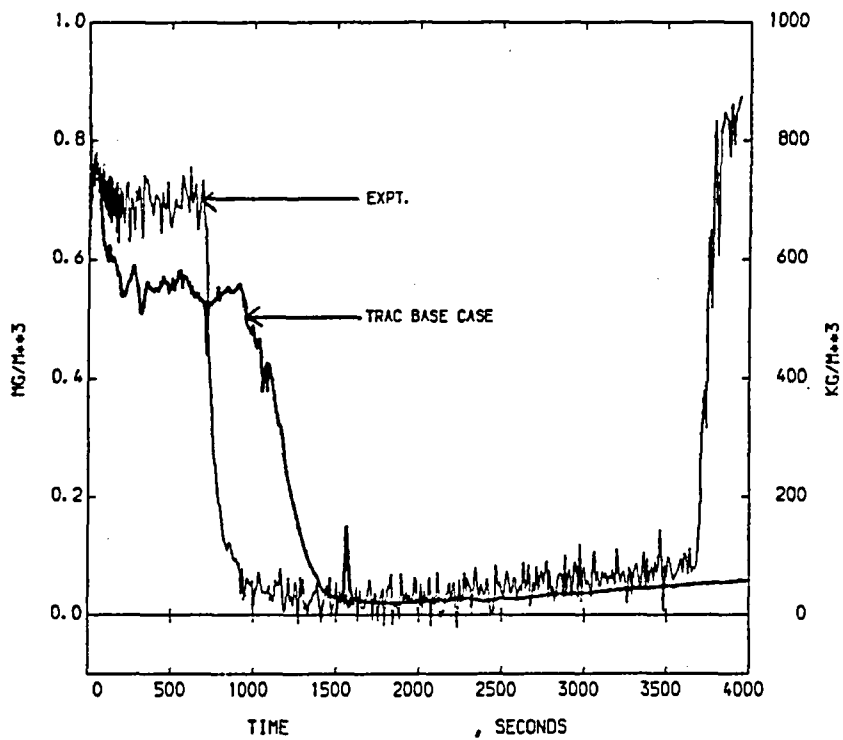
FIGURE 27 - BREAK UPSTREAM DENSITY
LP-SB-1 BASE CASE CALCULATION

AEEW - R 2254
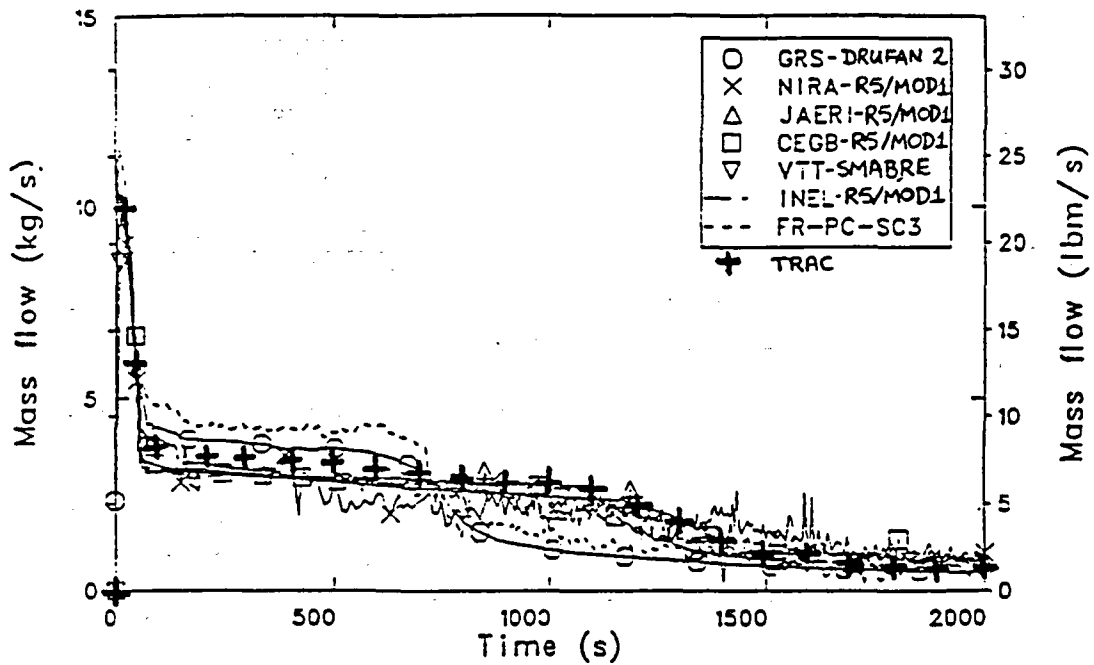
FIGURE 28 - BREAK MASS FLOW RATE, COMPARISON WITH OECD GROUP
LP-SB-1 BASE CASE CALCULATION
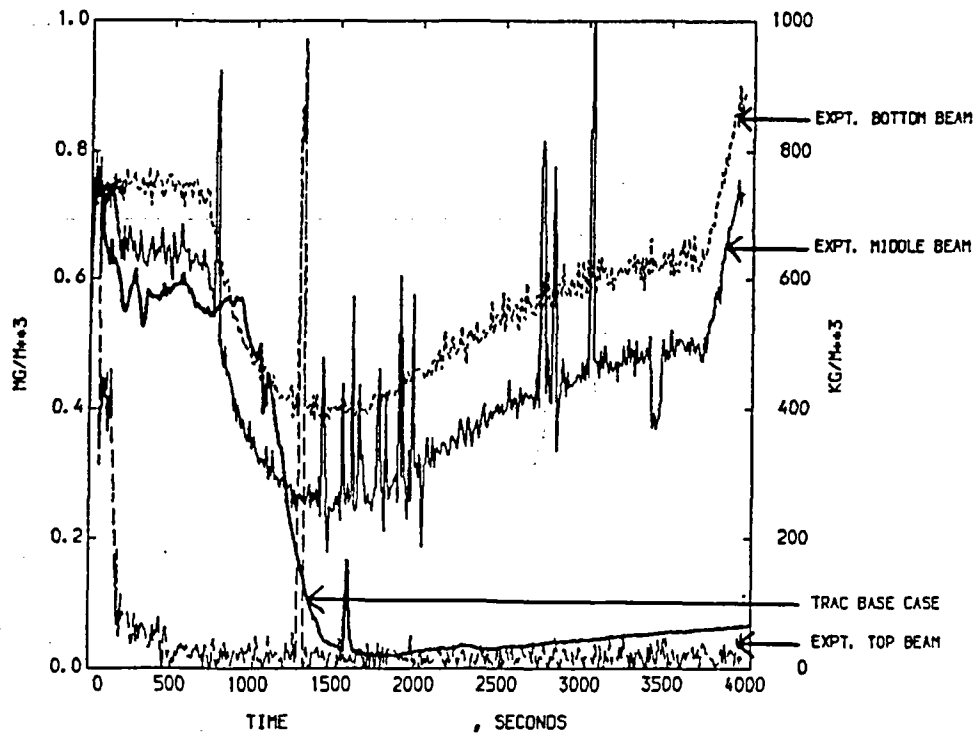
FIGURE 29 - ILHL DENSITY
LP-SB-1 BASE CASE CALCULATION
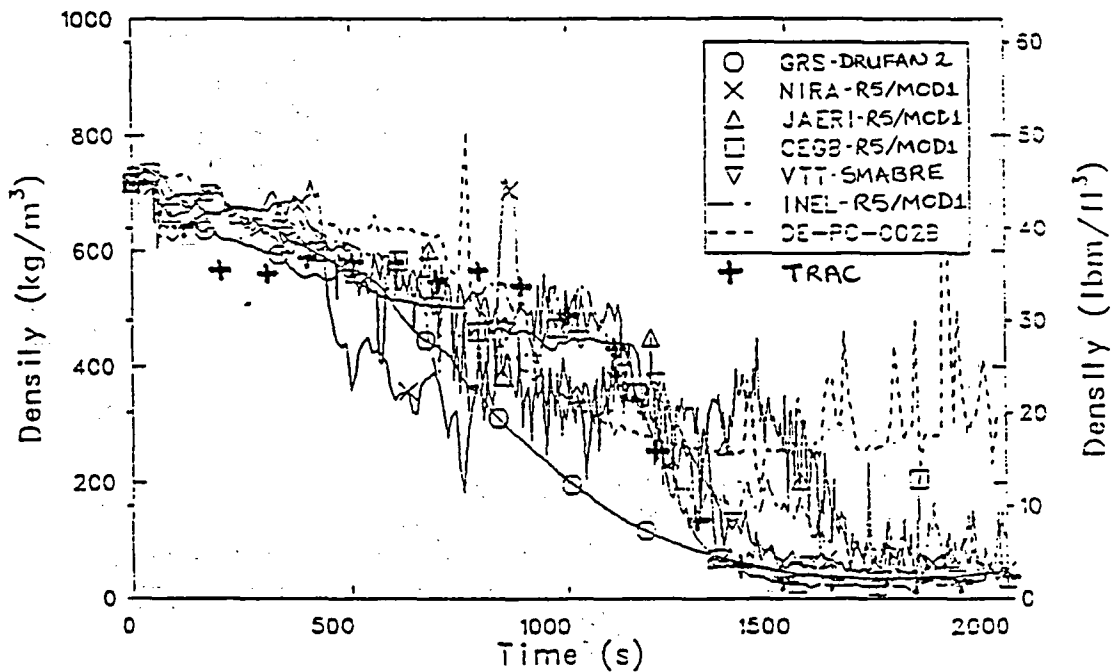
FIGURE 30 - ILHL DENSITY, COMPARISON WITH OECD REVIEW GROUP
LP-SB-1 BASE CASE CALCULATION
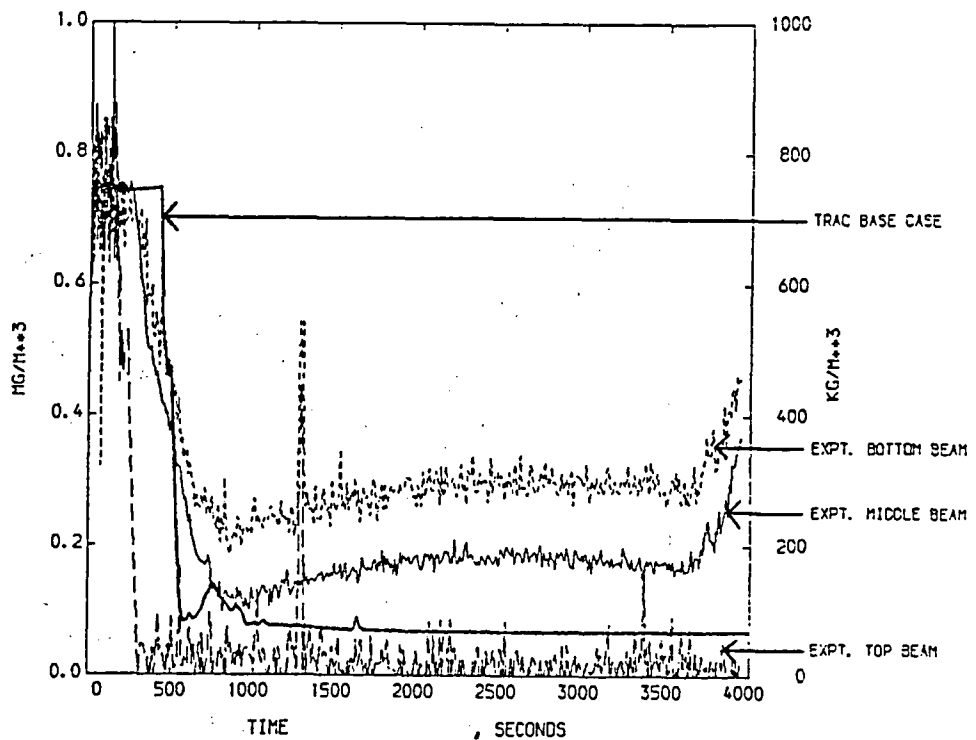
FIGURE 31 - ILCL DENSITY
LP-SB-1 BASE CASE CALCULATION
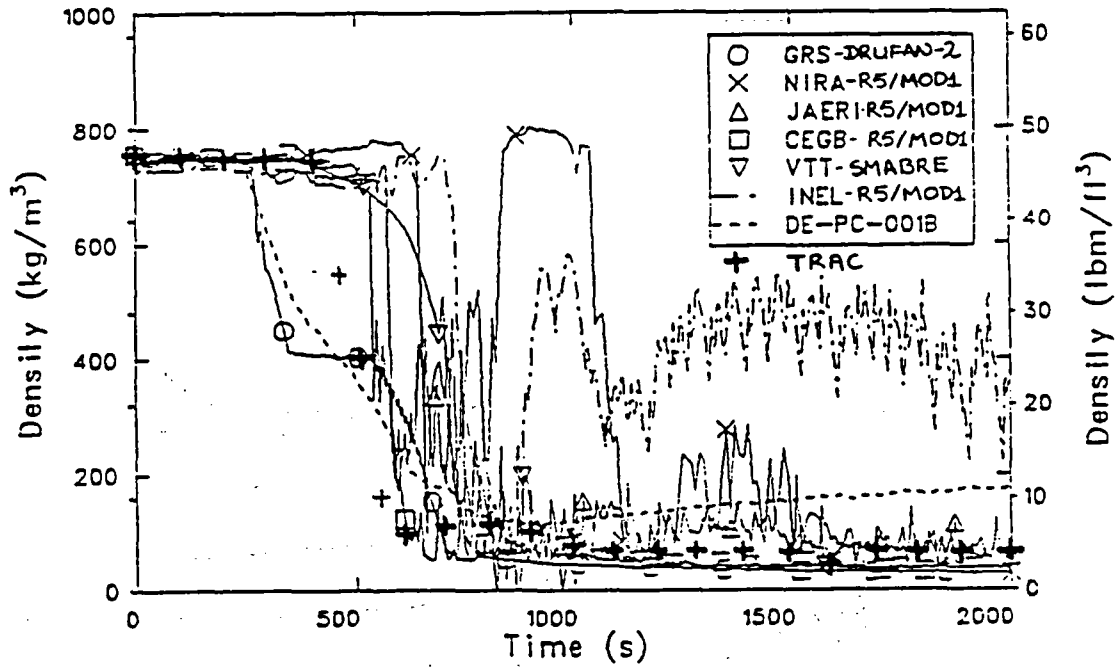
FIGURE 32 - ILCL DENSITY, COMPARISON WITH OECD REVIEW GROUP
LP-SB-1 BASE CASE CALCULATION
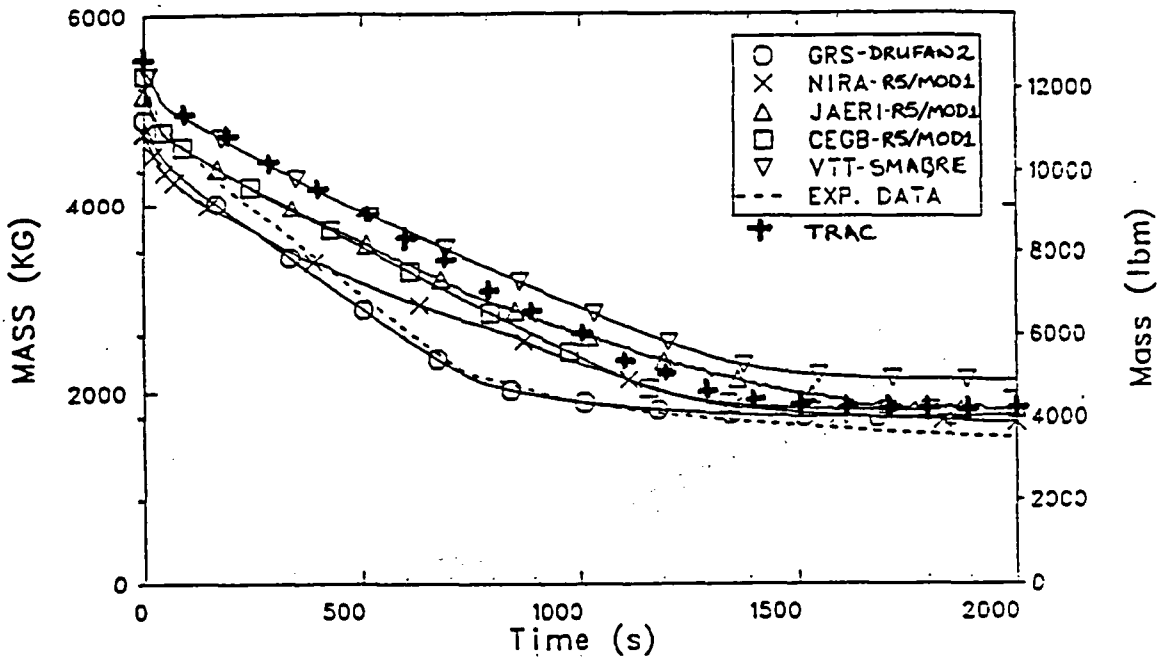
FIGURE 33 - PRIMARY MASS INVENTORY, COMPARISON WITH OECD GROUP
LP-SB-1 BASE CASE CALCULATION

VAPOR FRACTION

FIGURE 34 - CORE VOID FRACTIONS
LP-SB-1 BASE CASE CALCULATION

PE-PC-002   ,PRESSURE
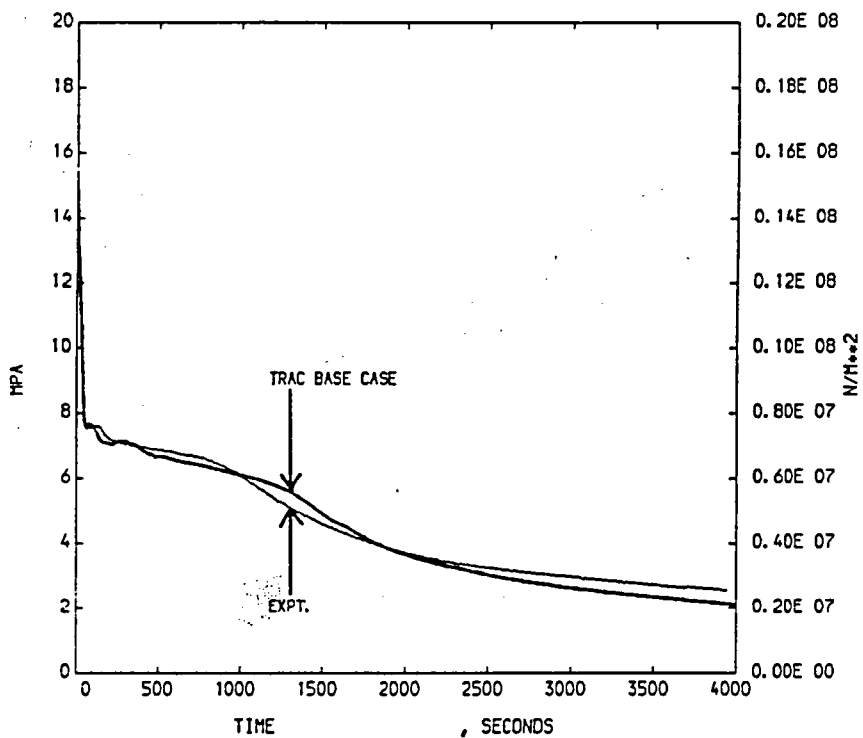
FIGURE 35 - PRIMARY SYSTEM PRESSURE
LP-SB-1 BASE CASE CALCULATION
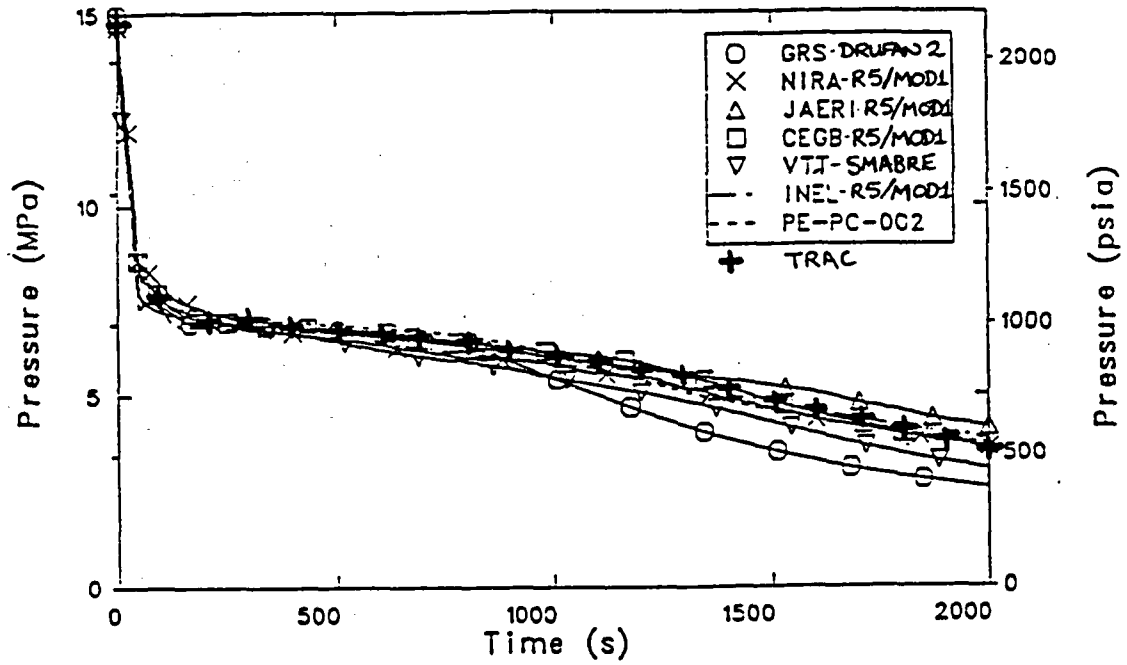
FIGURE 36 - PRIMARY PRESSURE, COMPARISON WITH OECD GROUP
LP-SB-1 BASE CASE CALCULATION

THE FOLLOWING ARE PLOTTED AGAINST TIME

PE-SGS-001   ,SIGNAL VAR. NO.   6
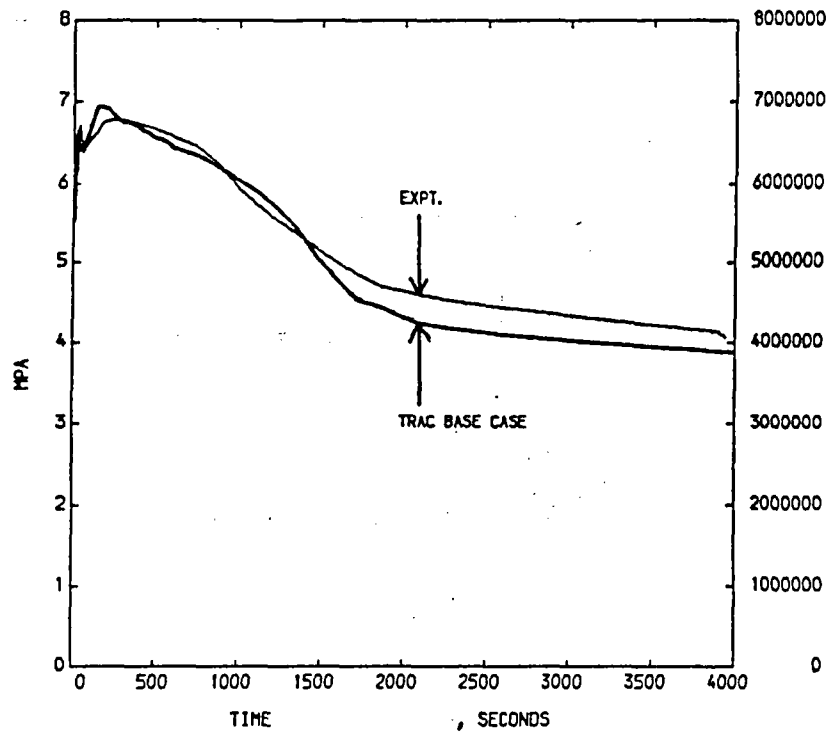
FIGURE 37 - SECONDARY SYSTEM PRESSURE
LP-SB-1 BASE CASE CALCULATION

AEEW - R 2254
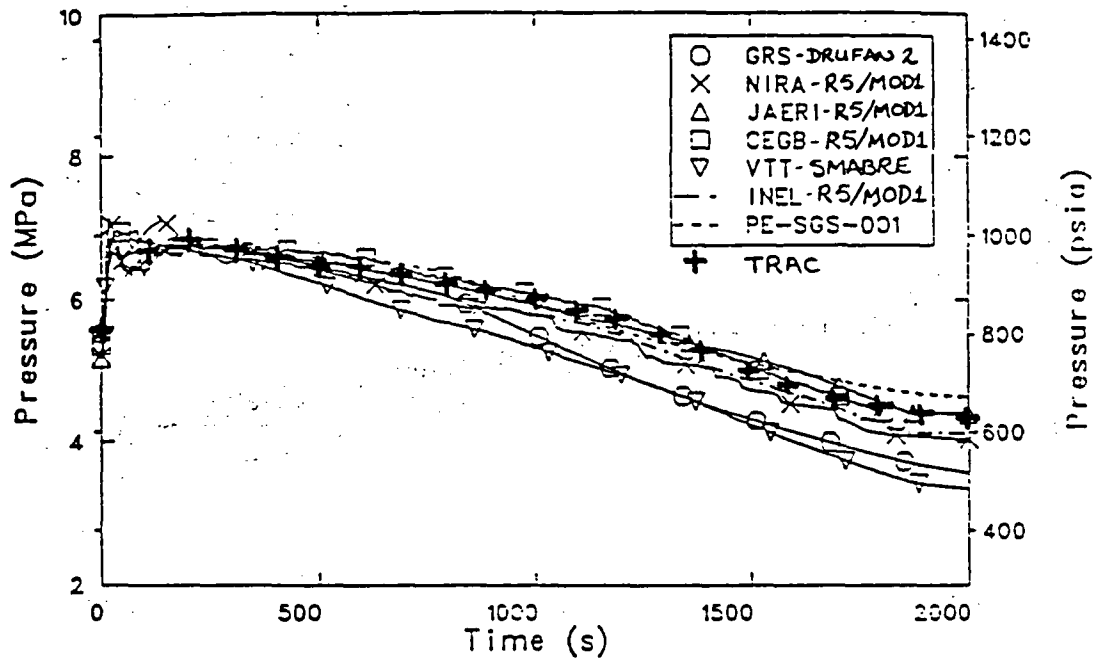
FIGURE 38 - SECONDARY PRESSURE, COMPARISON WITH OECD GROUP
LP-SB-1 BASE CASE CALCULATION

THE FOLLOWING ARE PLOTTED AGAINST REACTOR TIME

VAPOR FRACTION   ,STRATIFIED VOL FLAG ,MASS FLOW RATE
FR-PC-S03
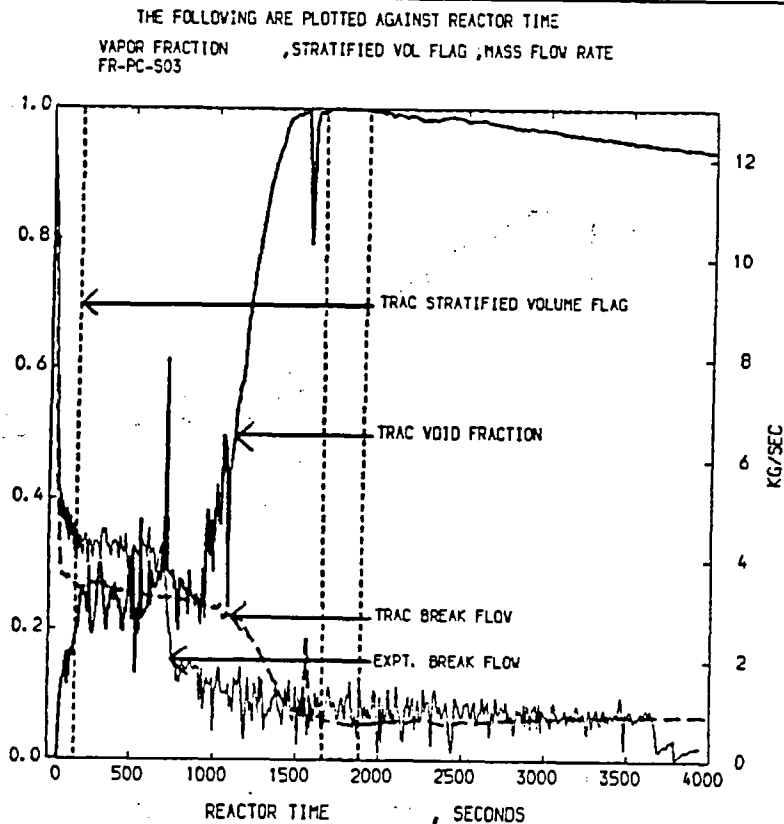
FIGURE 39 - ILHL VOID FRACTION, STRATIFICATION & BREAK FLOW
LP-SB-1 BASE CASE CALCULATION

THE FOLLOWING ARE PLOTTED AGAINST REACTOR TIME
TOTAL CPU TIME
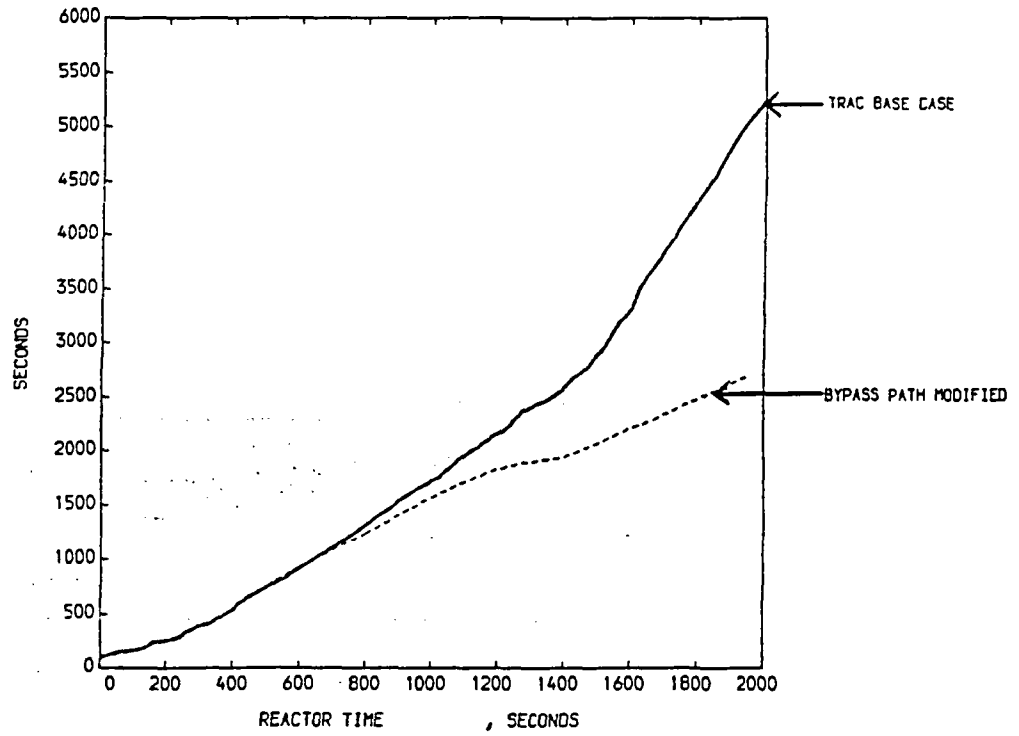
FIGURE 40 - EFFECT OF SIZE OF BYPASS PATH ON RUNNING SPEED
LP-SB-1 BASE CASE CALCULATION

THE FOLLOWING ARE PLOTTED AGAINST TIME
DE-PC-S04B   ,MIXTURE DENSITY
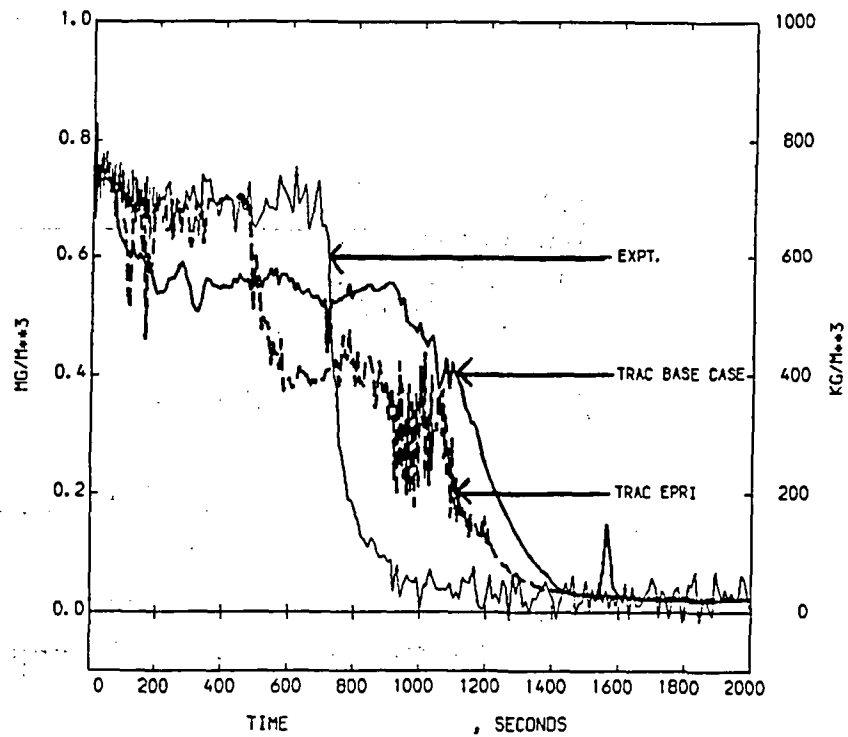
FIGURE 41 - BREAK UPSTREAM DENSITY
LP-SB-1 BASE CASE CALCULATION WITH EPRI CORRELATION

THE FOLLOWING ARE PLOTTED AGAINST TIME

FR-PC-S03   .MASS FLOW RATE
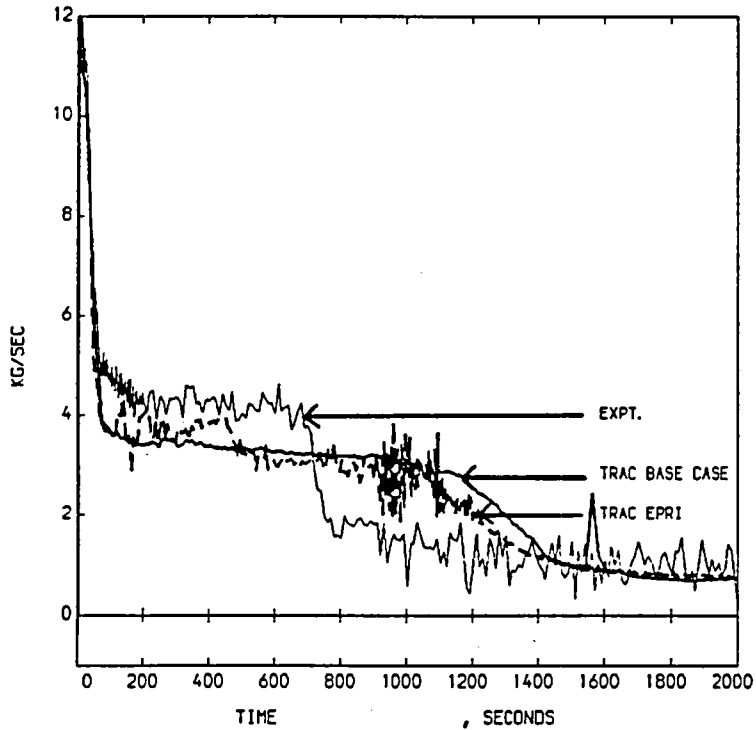
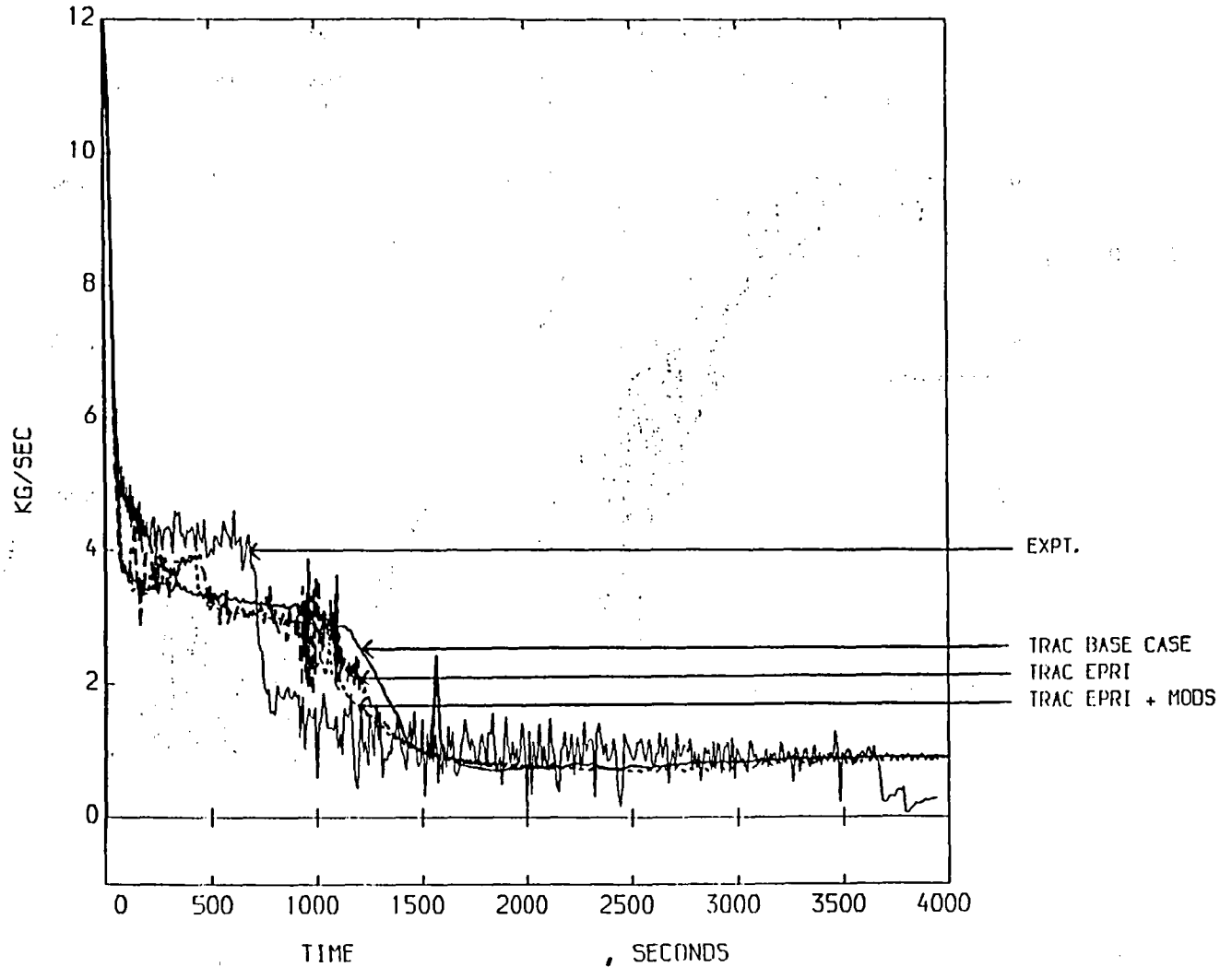FIGURE 42 - BREAK MASS FLOW RATE
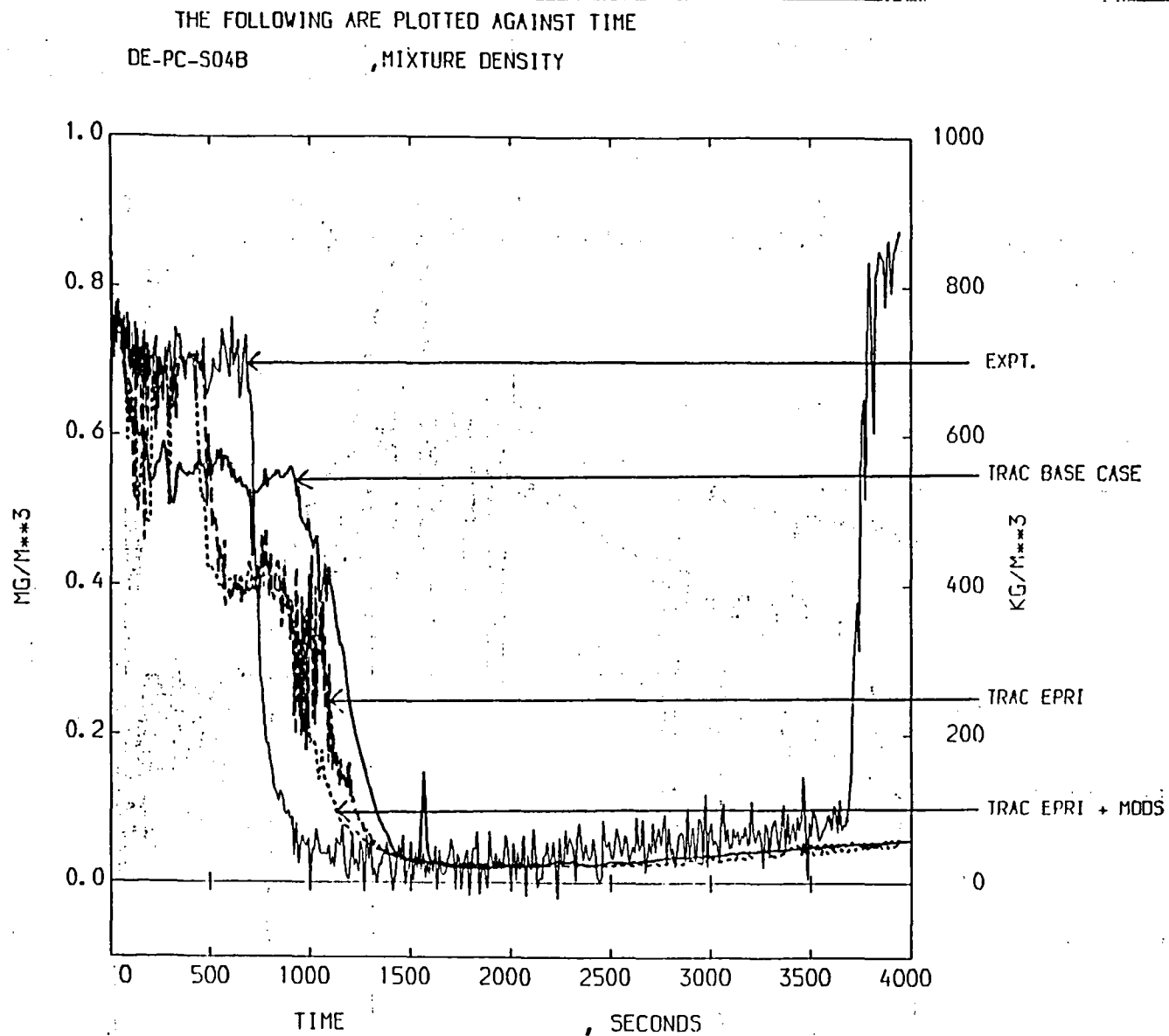LP-SB-1 BASE CASE CALCULATION WITH EPRI CORRELATION

THE FOLLOWING ARE PLOTTED AGAINST TIME

DE-PC-002A   .DE-PC-002B   .DE-PC-002C
MIXTURE DENSITY
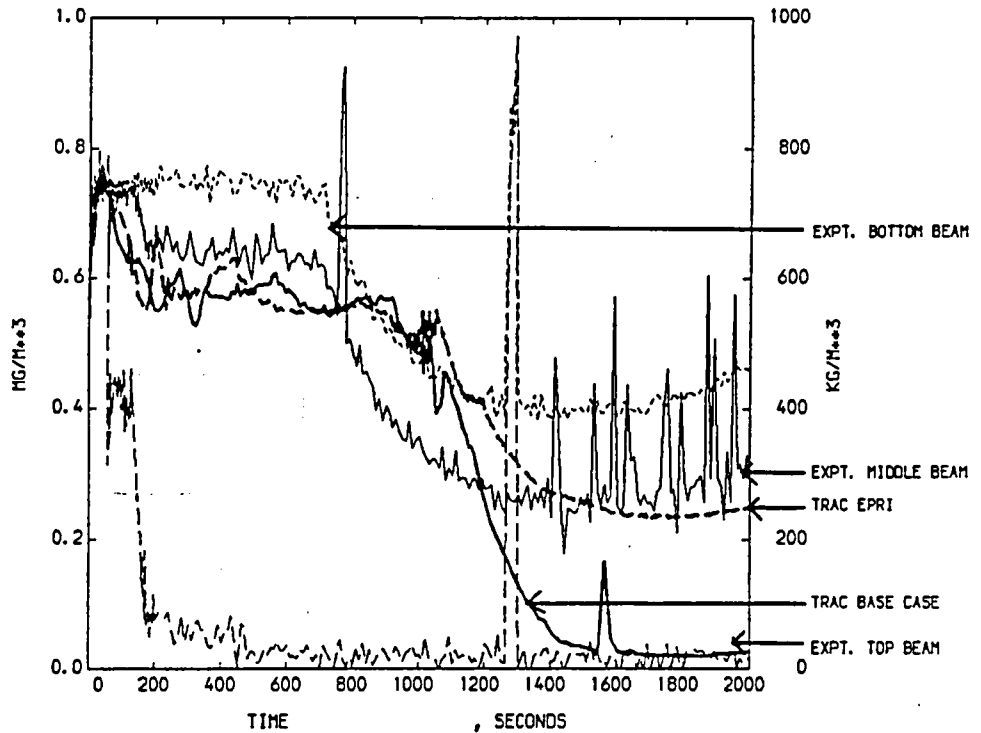
FIGURE 43 - ILHL DENSITY
LP-SB-1 BASE CASE CALCULATION WITH EPRI CORRELATION

AEEW - R 2254

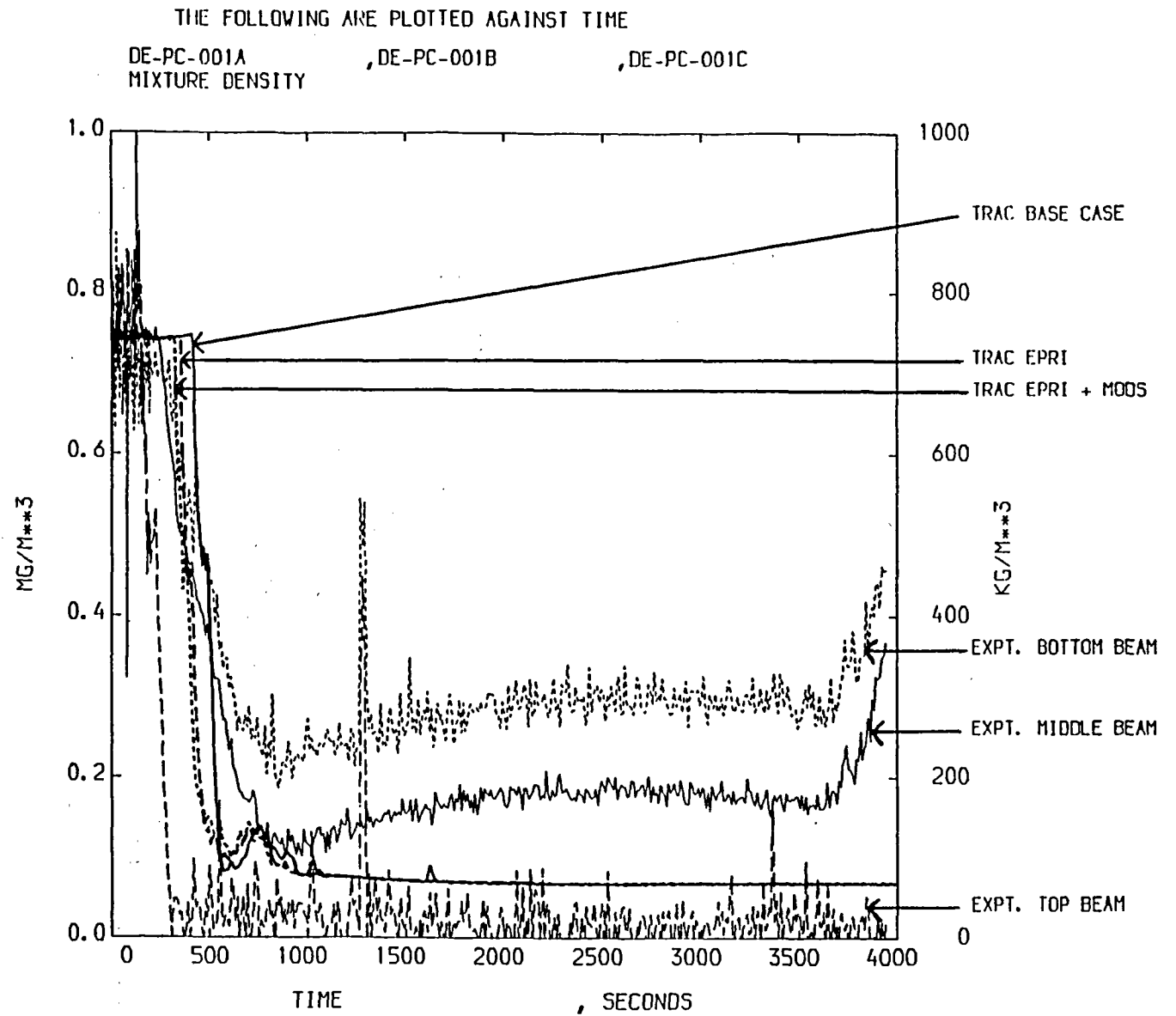DE-PC-001A   ,DE-PC-001B   ,DE-PC-001C
MIXTURE DENSITY
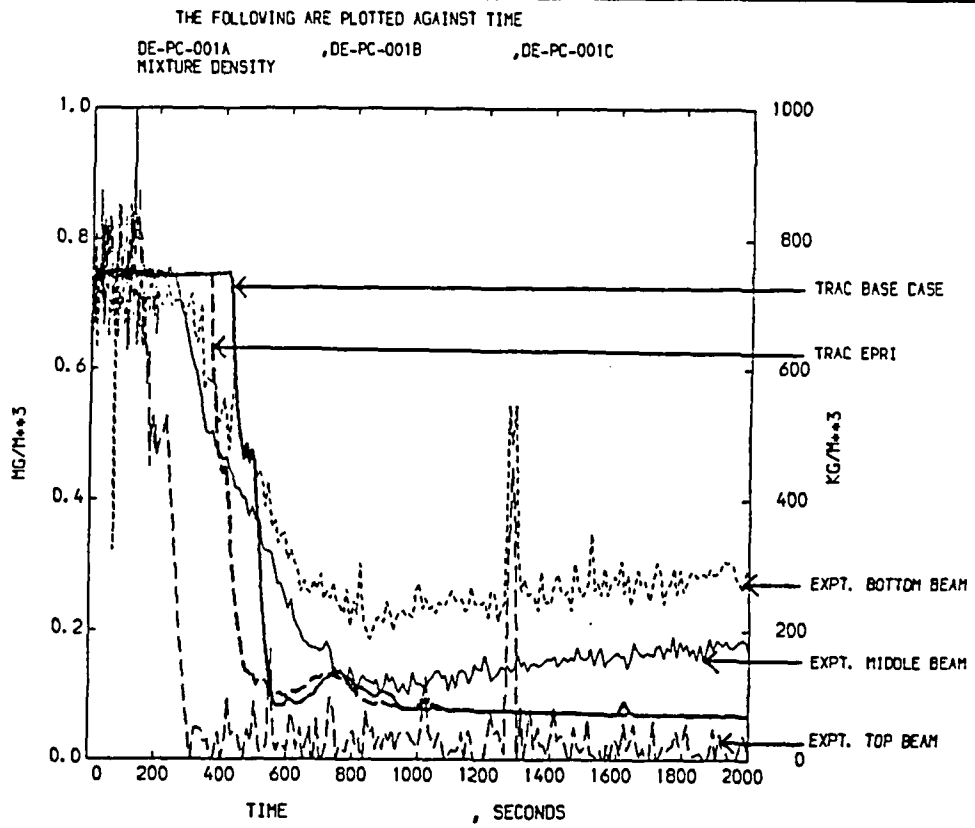
FIGURE 44 - ILCL DENSITY
LP-SB-1 BASE CASE CALCULATION WITH EPRI CORRELATION

THE FOLLOWING ARE PLOTTED AGAINST REACTOR TIME

CONTROL BLK ID   -79,MASS INVENTORY
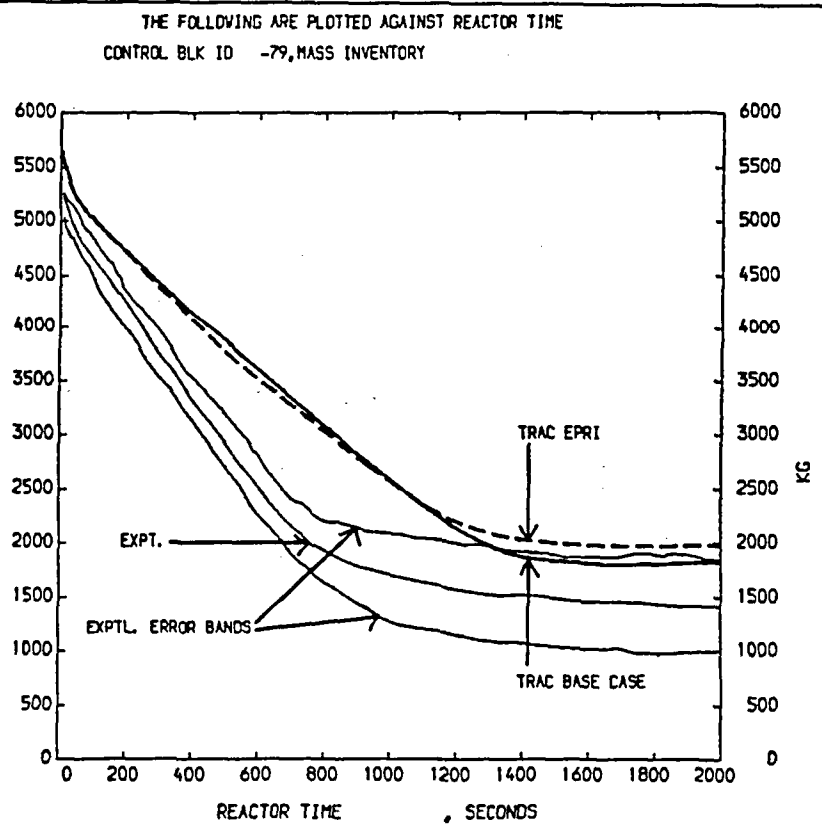
FIGURE 45 - PRIMARY SYSTEM MASS INVENTORY
LP-SB-1 BASE CASE CALCULATION WITH EPRI· CORRELATION
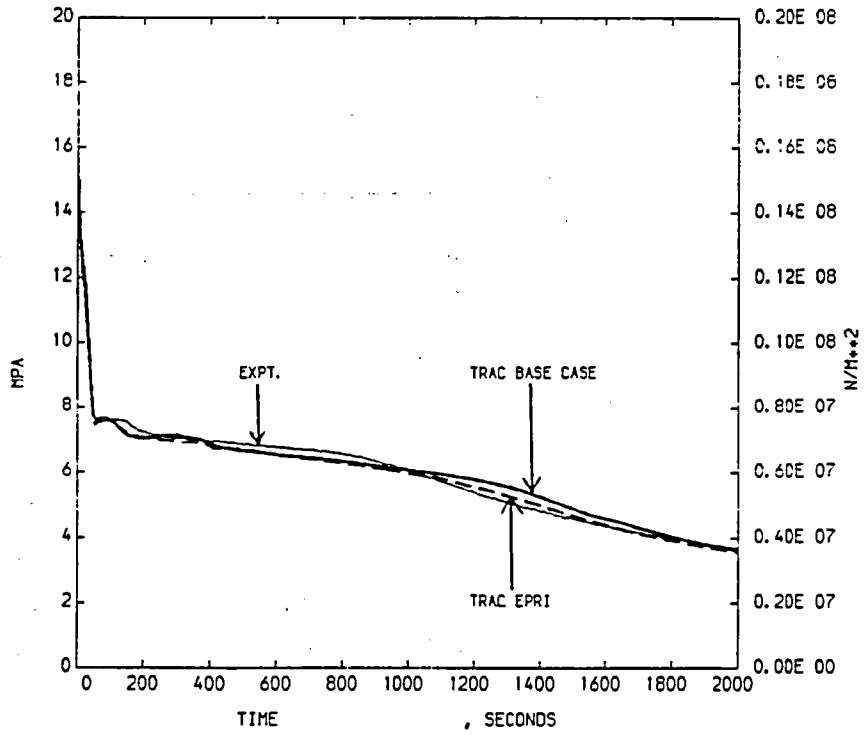
FIGURE 46 - PRIMARY SYSTEM PRESSURE
LP-SB-1 BASE CASE CALCULATION WITH EPRI CORRELATION
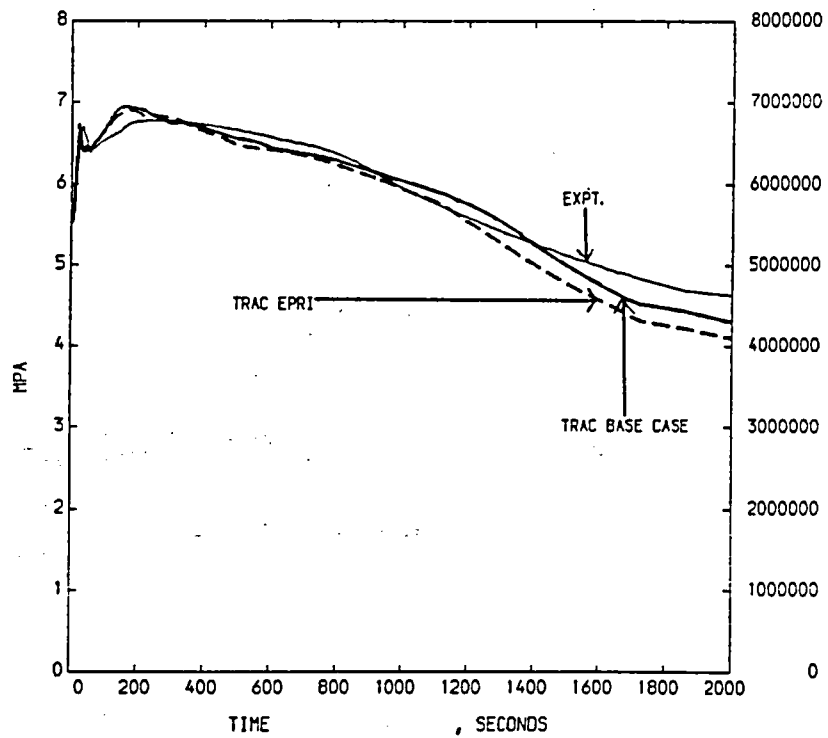
FIGURE 47 - SECONDARY SYSTEM PRESSURE
LP-SB-1 BASE CASE CALCULATION WITH EPRI CORRELATION

THE FOLLOWING ARE PLOTTED AGAINST REACTOR TIME
CONTROL BLK ID -33,CONTROL BLK ID -32
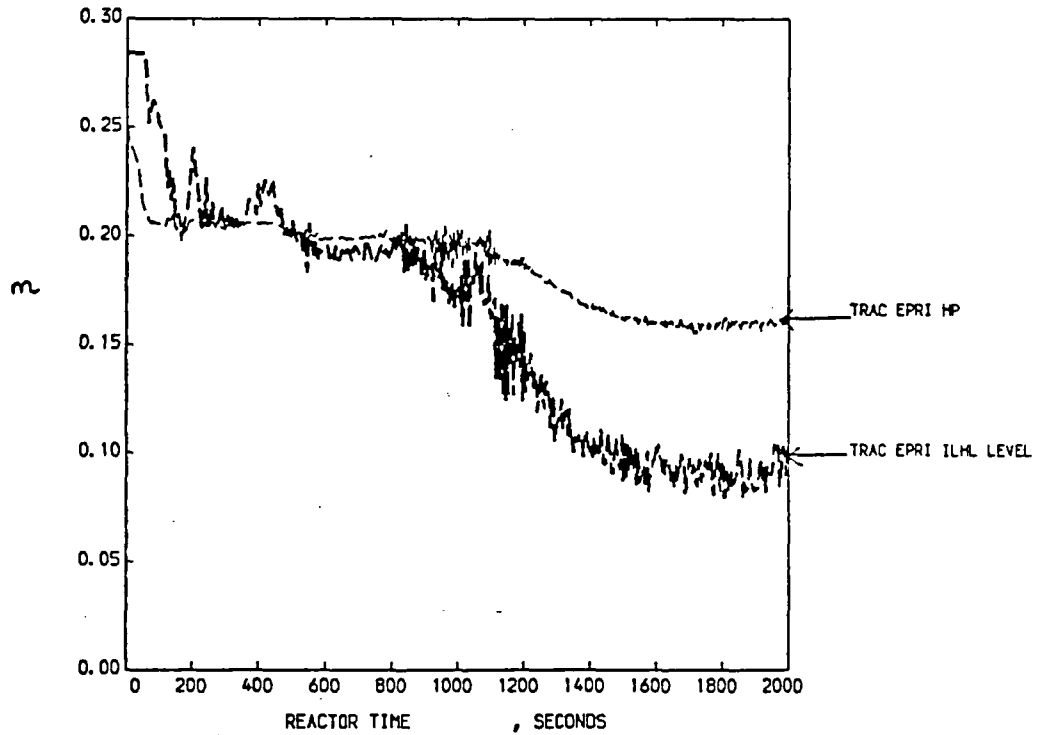
FIGURE 48 - ILHL AND VAPOUR PULL THROUGH LEVELS
LP-SB-1 BASE CASE CALCULATION WITH EPRI CORRELATION

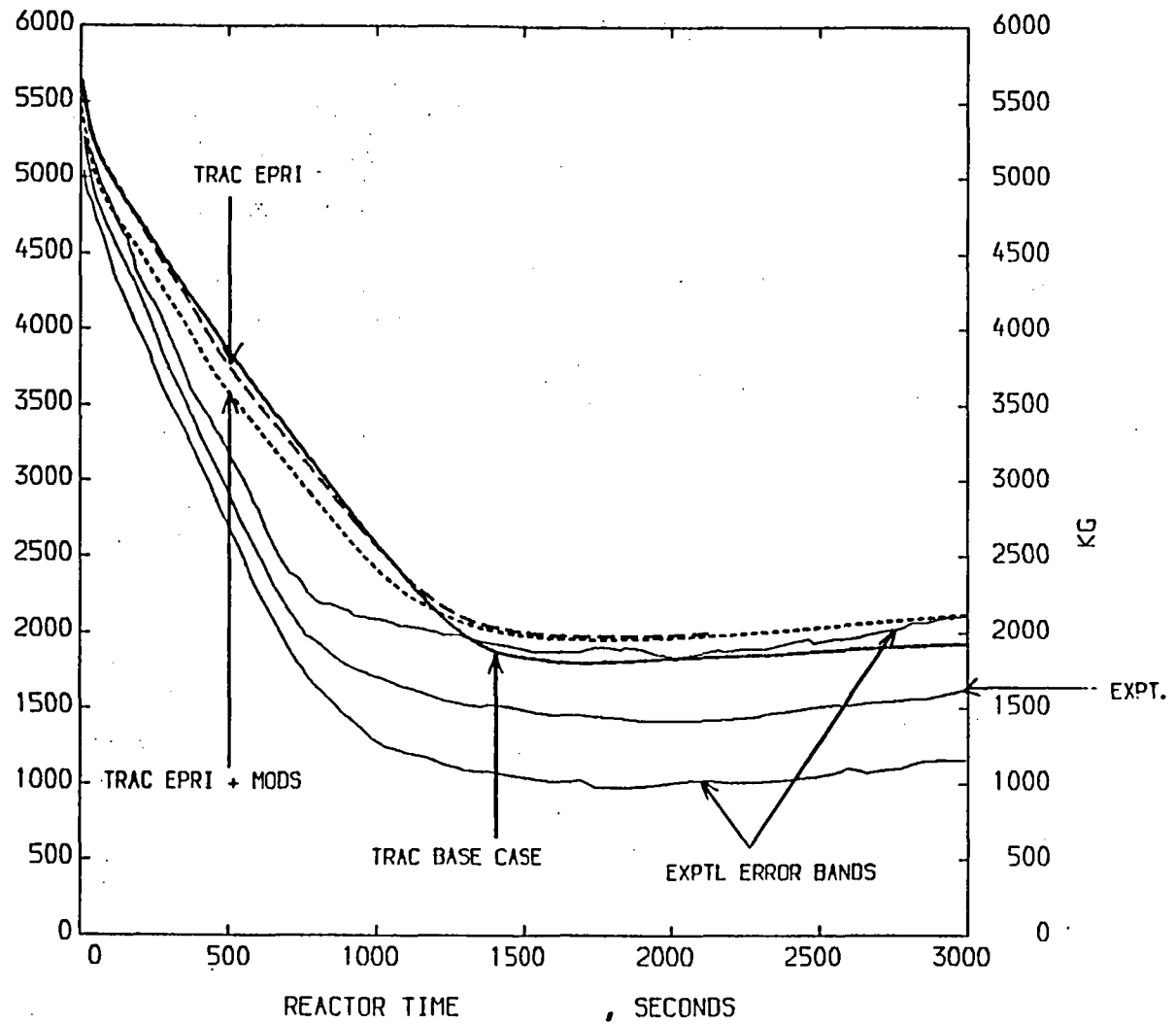THE FOLLOWING ARE PLOTTED AGAINST REACTOR TIME
CONTROL BLK ID -33,LIQUID LEVEL IN H.L.
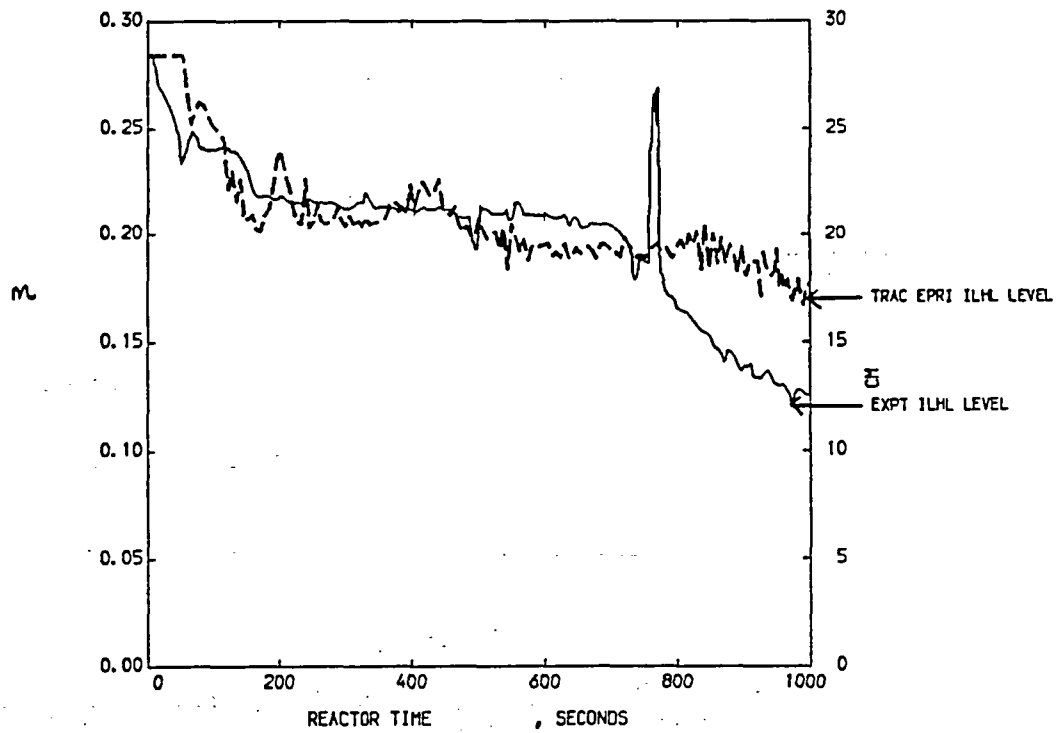
FIGURE 49 - MEASURED AND PREDICTED ILHL LEVELS
LP-SB-1 BASE CASE CALCULATION WITH EPRI CORRELATION

AEEW - R 2254
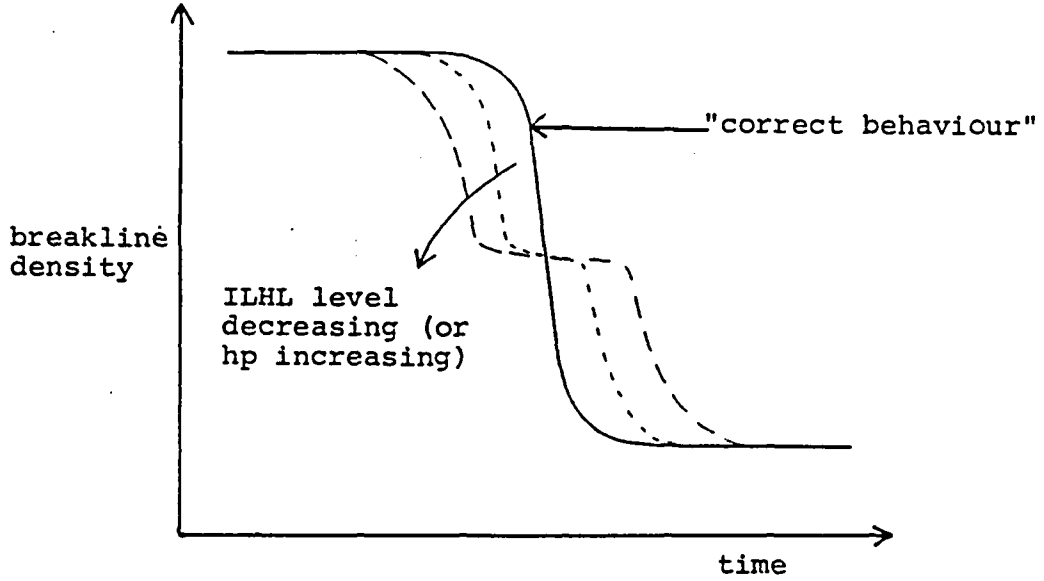
FIGURE 50a

Effect, on Breakline Density, of the ILHL Liquid Level
(or the Level at which Vapour Pull-Through is Predicted
to Occur)
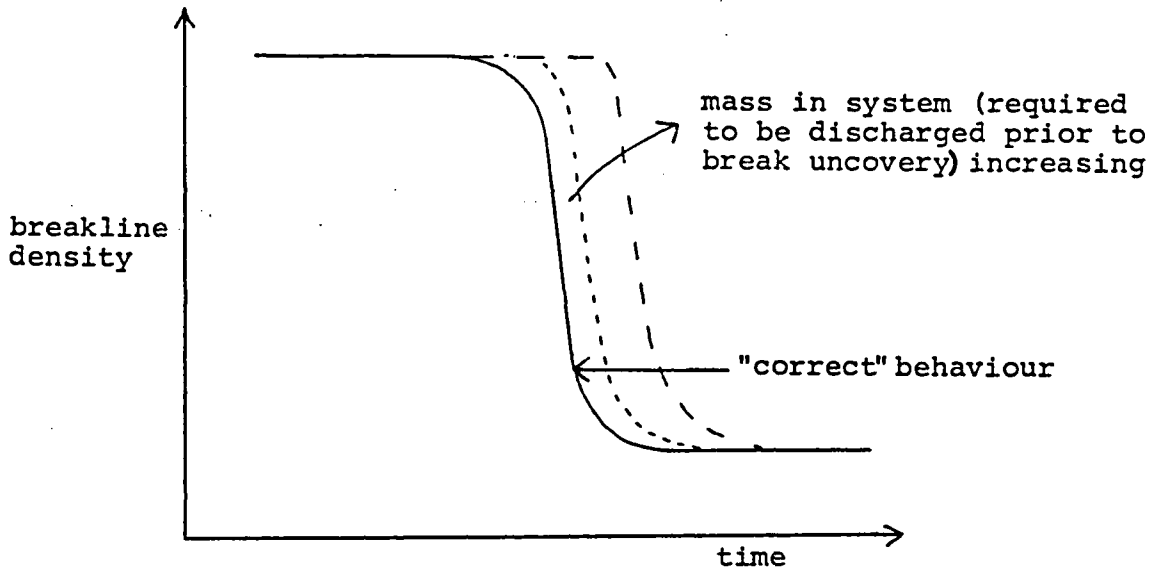
FIGURE 50b

Effect, on Breakline Density, of the Amount of Mass
in the System Required to be Discharged Prior to
Break Uncovery

THE FOLLOWING ARE PLOTTED AGAINST TIME

DE-PC-S04B   ,MIXTURE DENSITY
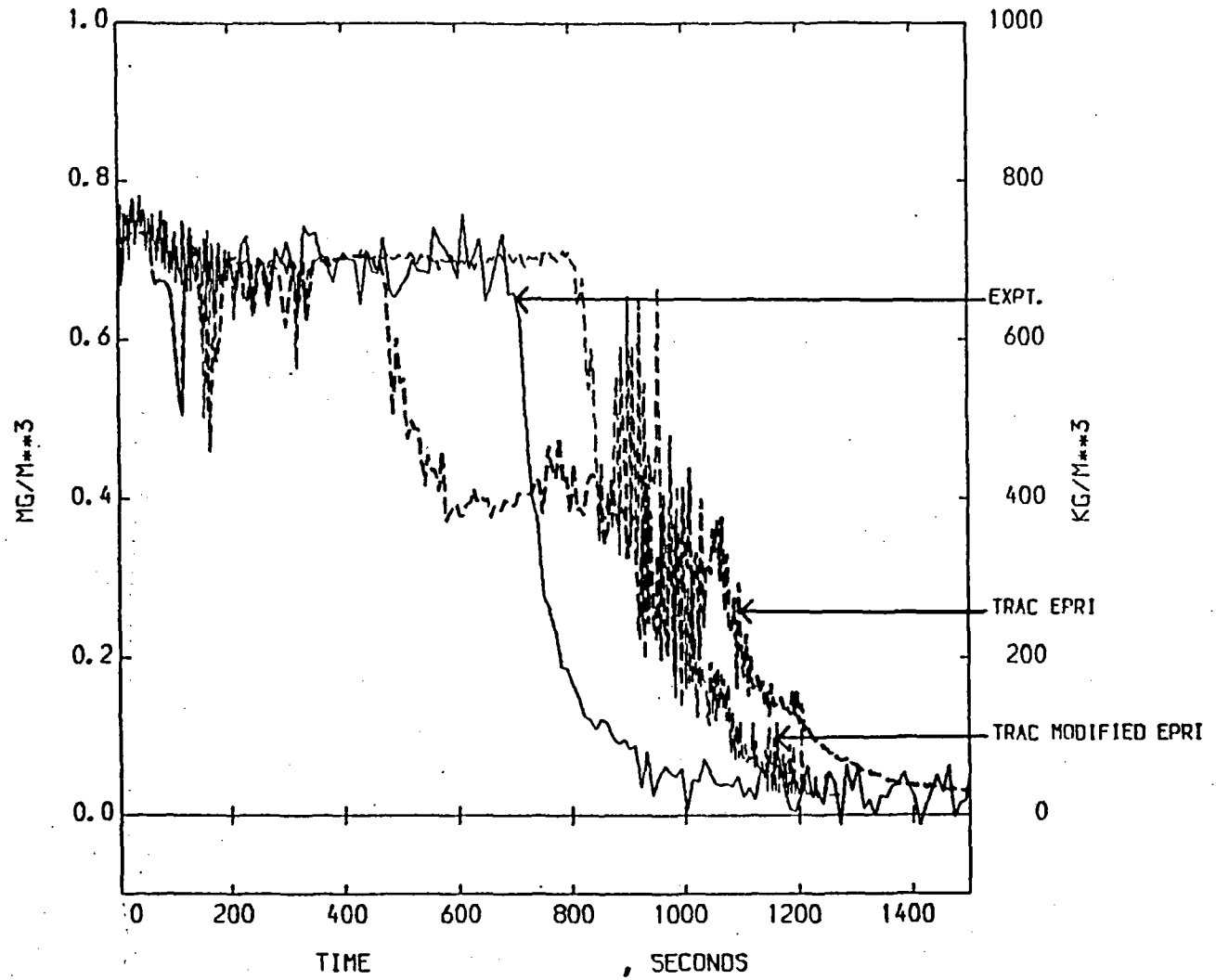
FIGURE 51 - VAPOUR PULL THROUGH EFFECT ON BREAK LINE DENSITY
LP-SB-1 BASE CASE CALCULATION WITH EPRI CORRELATION

THE FOLLOWING ARE PLOTTED AGAINST TIME

FR-PC-S03   ,MASS FLOW RATE

FIGURE 52   —   BREAK MASS FLOW RATE
LP-SB-1 BASE CASE CALCULATION WITH EPRI CORRELN & INPUT MODS

THE FOLLOWING ARE PLOTTED AGAINST TIME

DE-PC-S04B   ,MIXTURE DENSITY

FIGURE 53 — BREAK UPSTREAM DENSITY
LP-SB-1 BASE CASE CALCULATION WITH EPRI CORRELN & INPUT MODS

THE FOLLOWING ARE PLOTTED AGAINST TIME

DE-PC-002A   ,DE-PC-002B   ,DE-PC-002C
MIXTURE DENSITY
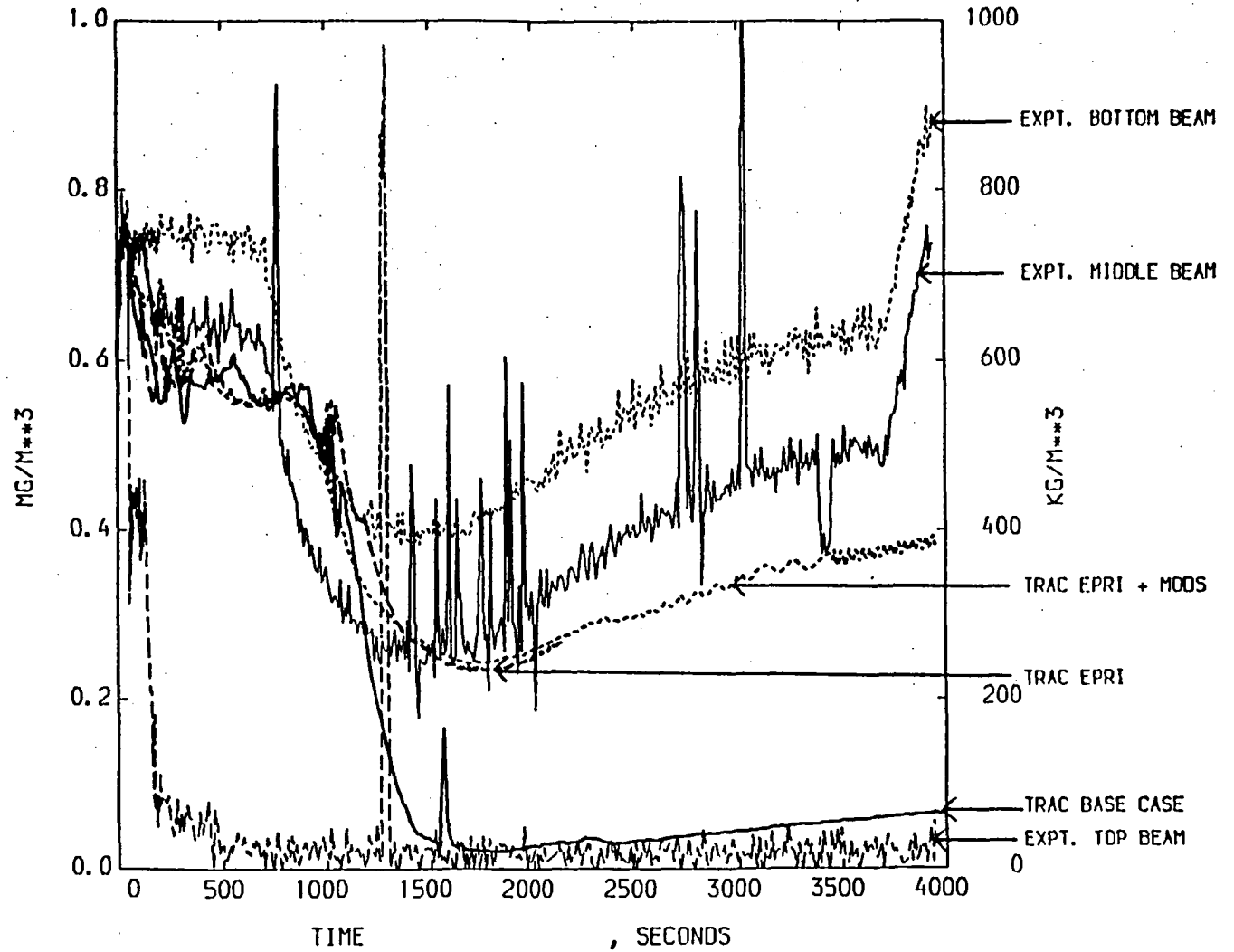
FIGURE 54   –   ILHL DENSITY
LP-SB-1 BASE CASE CALCULATION WITH EPRI CORRELN & INPUT MODS

THE FOLLOWING ARE PLOTTED AGAINST TIME

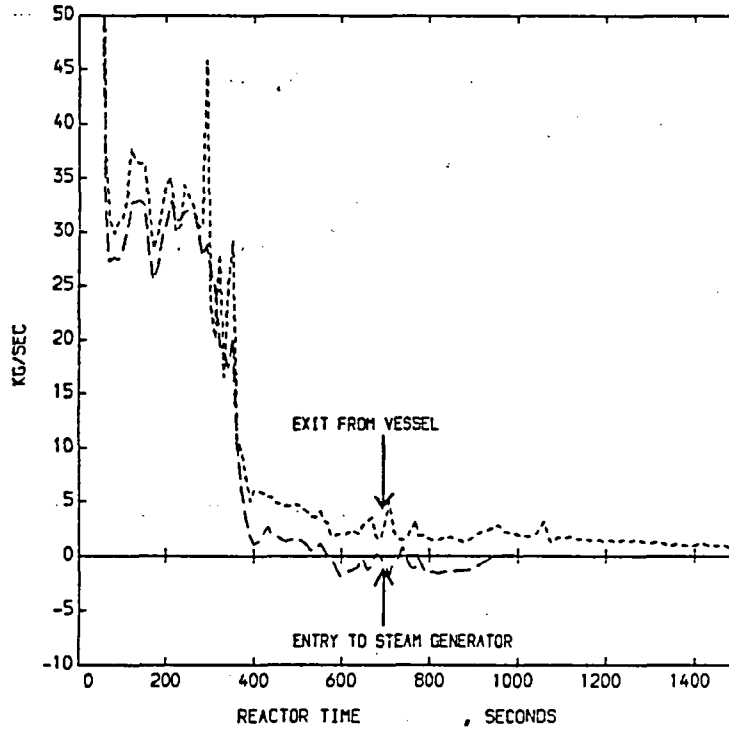DE-PC-001A   , DE-PC-001B   , DE-PC-001C
MIXTURE DENSITY

FIGURE 55 – ILCL DENSITY
LP-SB-1 BASE CASE CALCULATION WITH EPRI CORRELN & INPUT MODS
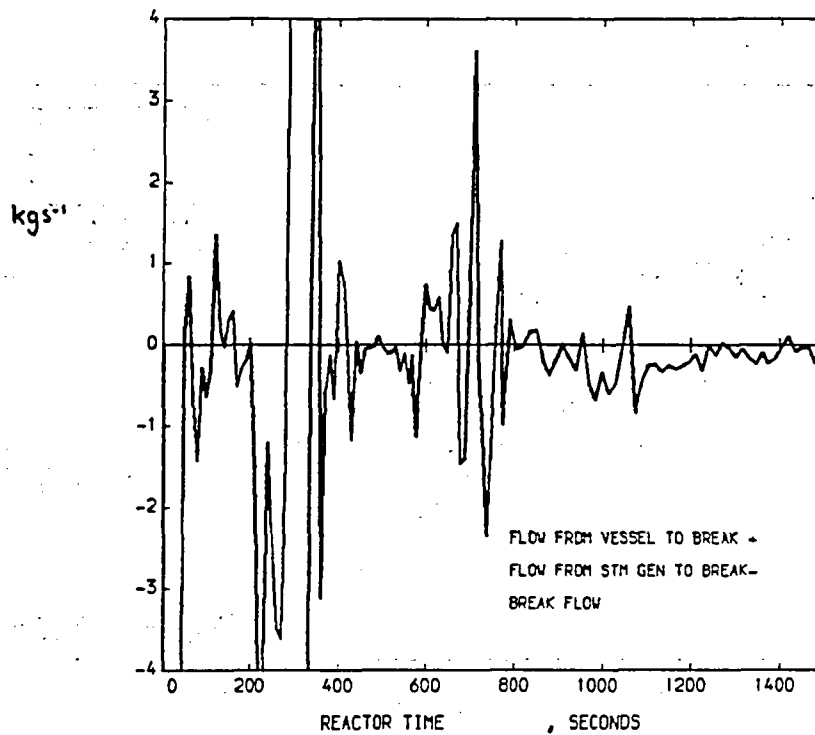
THE FOLLOWING ARE PLOTTED AGAINST REACTOR TIME

CONTROL BLK ID   -79, MASS INVENTORY

FIGURE 56 — PRIMARY SYSTEM MASS INVENTORY
LP-SB-1 BASE CASE CALCULATION WITH EPRI CORRELATION & INPUT MODS
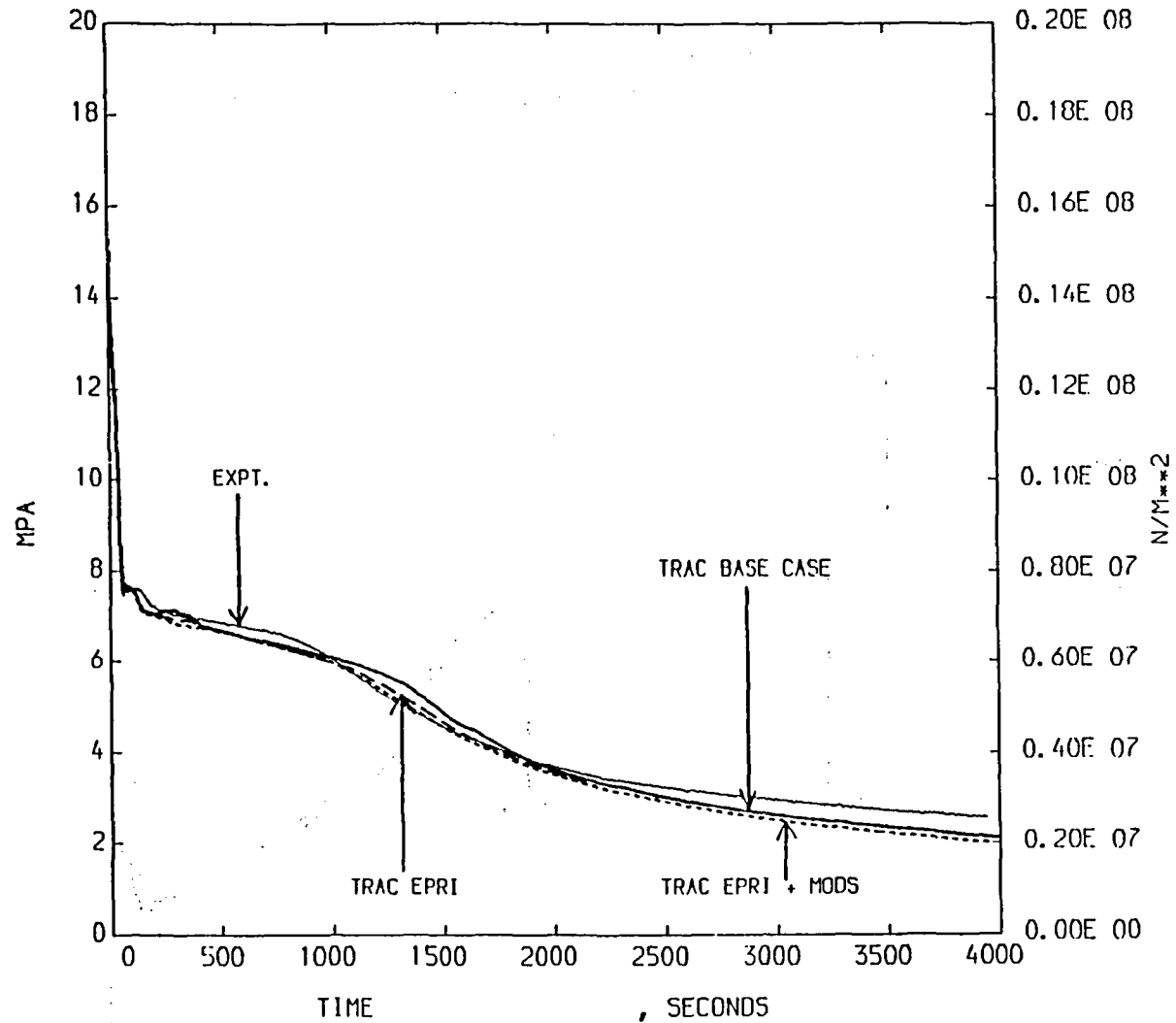
FIGURE 57 – PRIMARY SYSTEM PRESSURE
LP-SB-1 BASE CASE CALCULATION WITH EPRI CORRELN & INPUT MODS

THE FOLLOWING ARE PLOTTED AGAINST TIME

PE-SGS-001   ,SIGNAL VAR. NO.   6
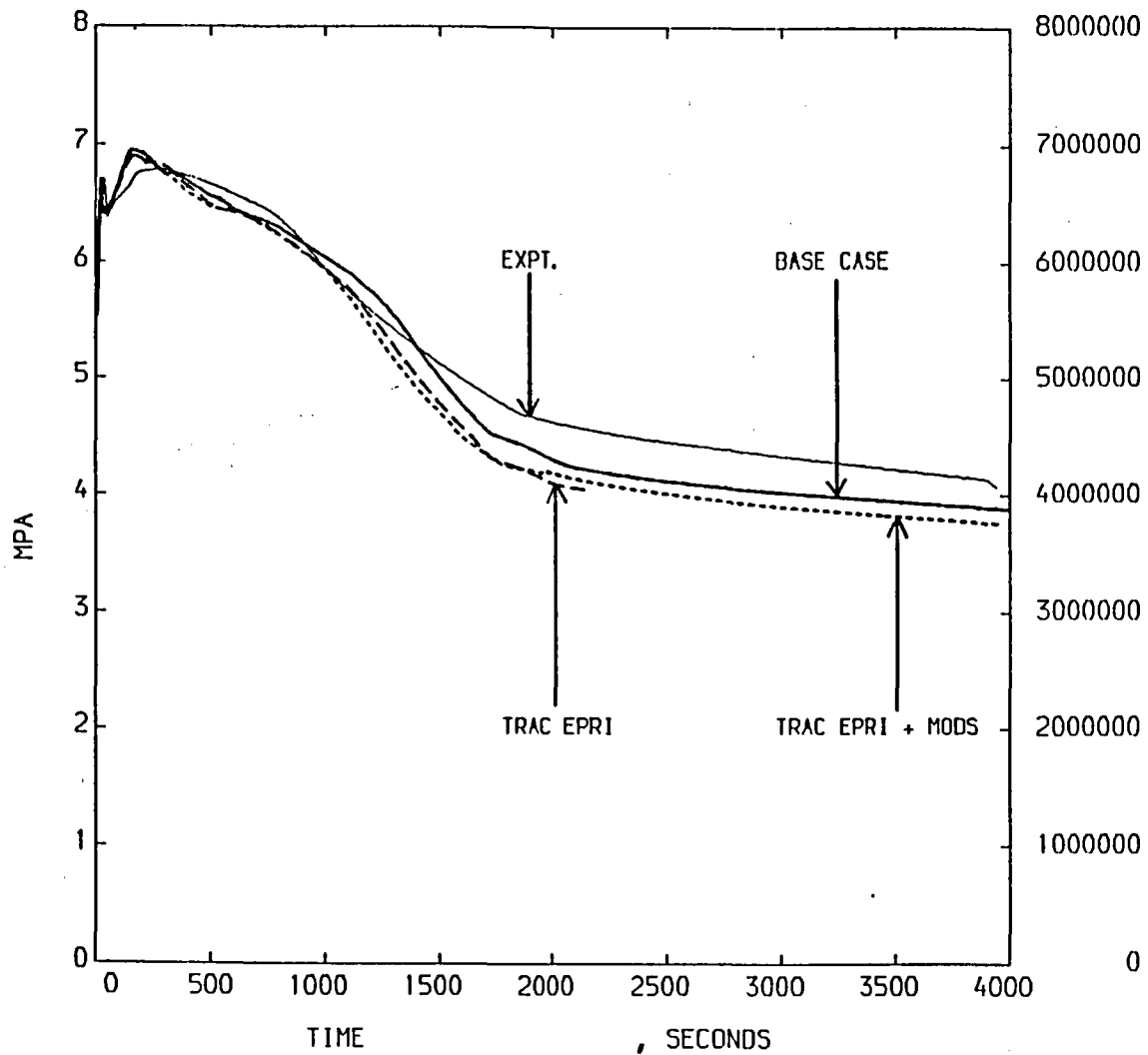
FIGURE 58 — SECONDARY SYSTEM PRESSURE
LP-SB-1 BASE CASE CALCULATION WITH EPRI CORRELN & INPUT MODS
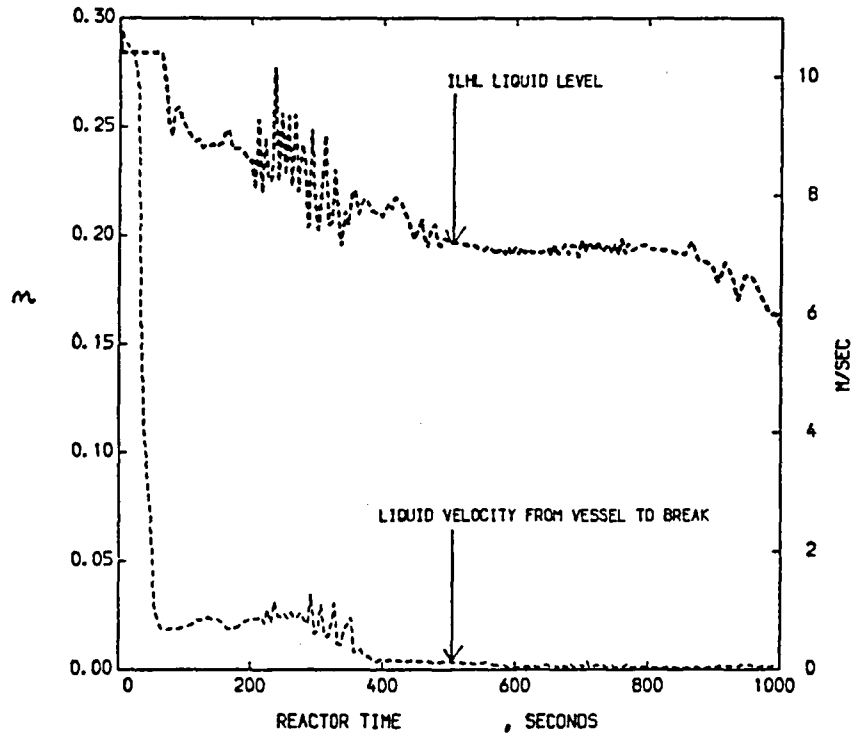
FIGURE 59 - ILHL LIQUID LEVEL AND NATURAL CIRCULATION
LP-SB-1 BASE CASE CALCULATION WITH EPRI CORRELATION & INPUT MODS
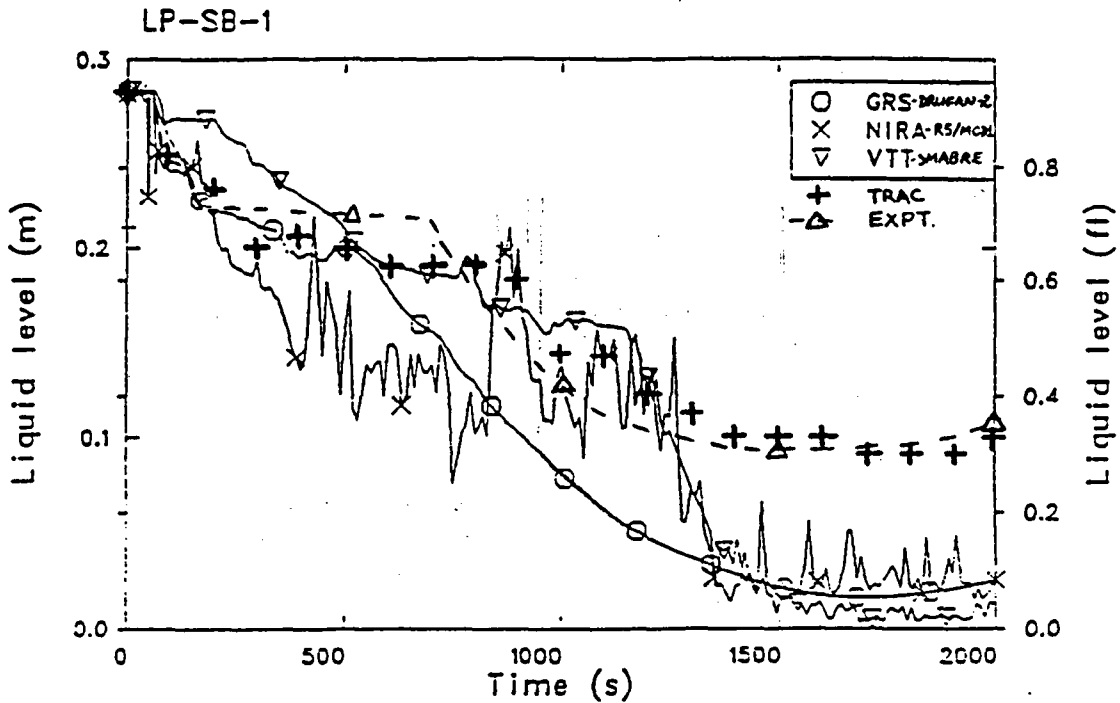
FIGURE 60 - ILHL LEVEL, COMPARISON WITH OECD REVIEW GROUP
LP-SB-1 BASE CASE CALCULATION WITH EPRI CORRELATION & INPUT MODS

MASS FLOW RATE

FIGURE 61 - ILHL MASS FLOW RATES
LP-SB-1 BASE CASE CALCULATION WITH EPRI CORRELN & INPUT MODS

FUNCTION

FIGURE 62 - ILHL MASS FLOW BALANCE
LP-SB-1 BASE CASE CALCULATION WITH EPRI CORRELN & INPUT MODS

THE FOLLOWING ARE PLOTTED AGAINST TIME

DE-PC-S04B   ,MIXTURE DENSITY
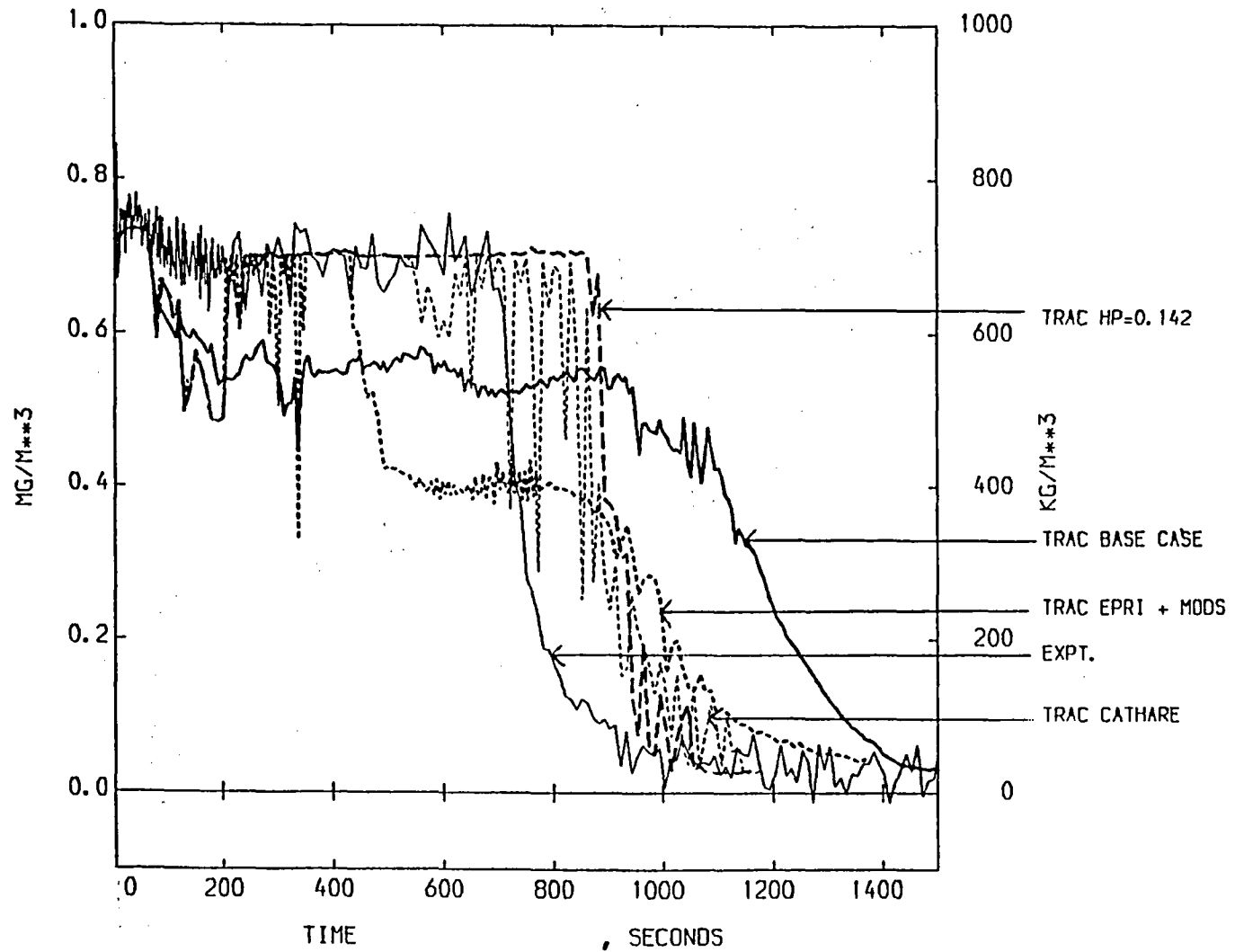
FIGURE 63 – EFFECT OF CORRELATION CHOICE ON BREAKLINE DENSITY
LP-SB-1 BASE CASE CALCULATION WITH EPRI CORRELATION & INPUT MODS
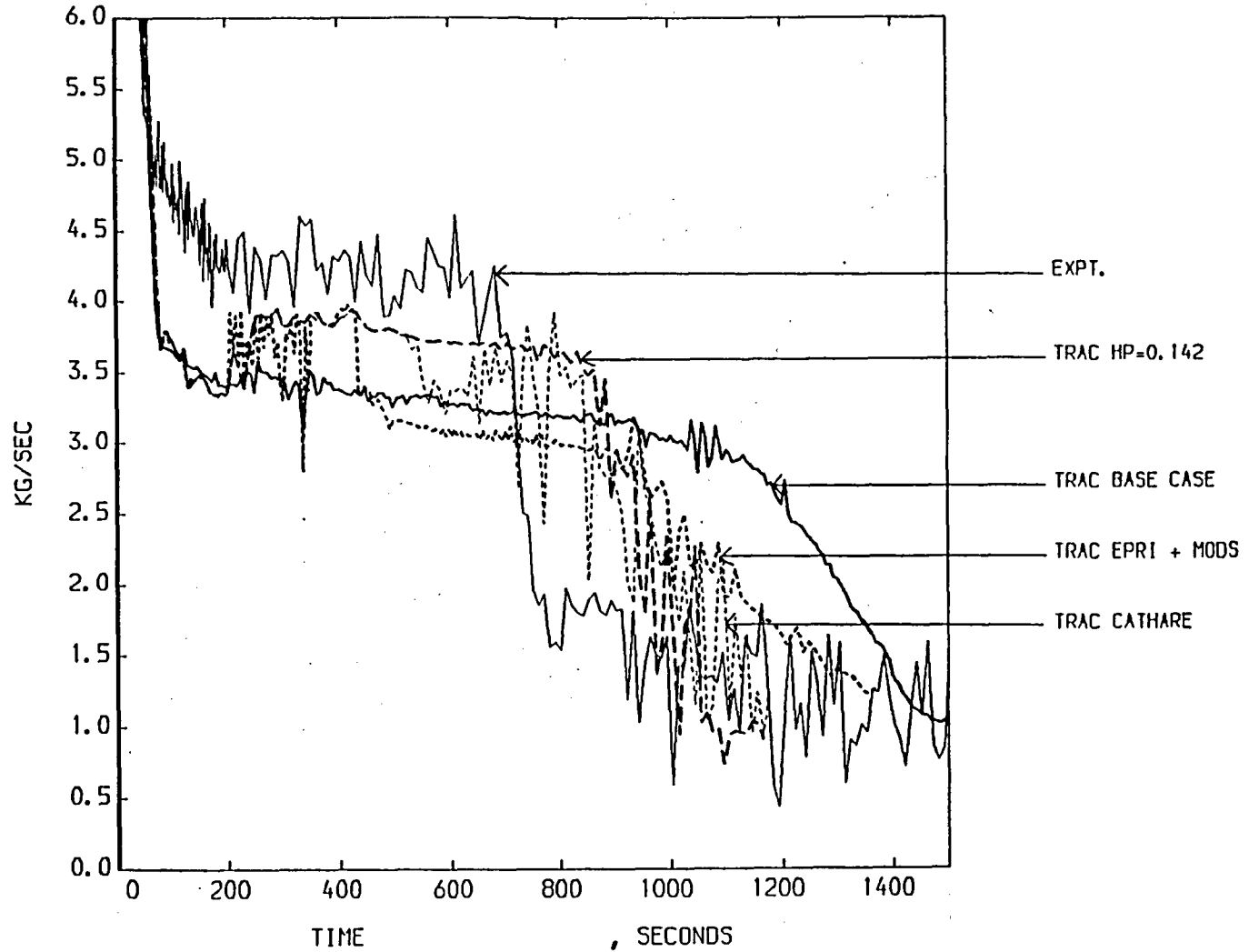
THE FOLLOWING ARE PLOTTED AGAINST TIME

FR-PC-S03   ,MASS FLOW RATE

FIGURE 64 — EFFECT OF CORRELATION CHOICE ON BREAK MASS FLOW
LP-SB-1 BASE CASE CALCULATION WITH EPRI CORRELATION & INPUT MODS

THE FOLLOWING ARE PLOTTED AGAINST REACTOR TIME
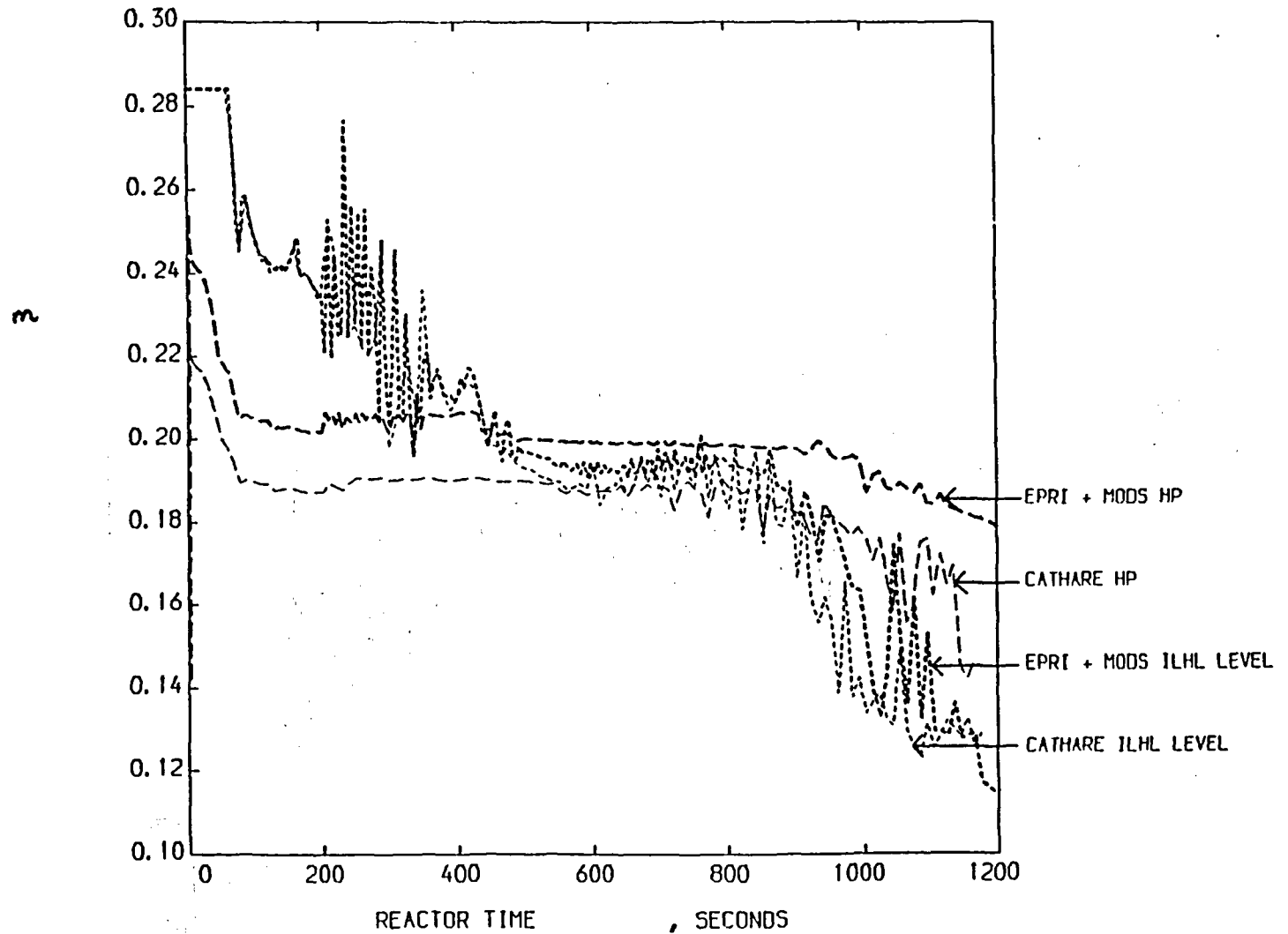
CONTROL BLK ID   -33, CONTROL BLK ID   -32

FIGURE 65 - EFFECT OF CORRELATION CHOICE ON ILHL LEVEL
LP-SB-1 BASE CASE CALCULATION WITH EPRI CORRELATION & INPUT MODS

THE FOLLOWING ARE PLOTTED AGAINST TIME
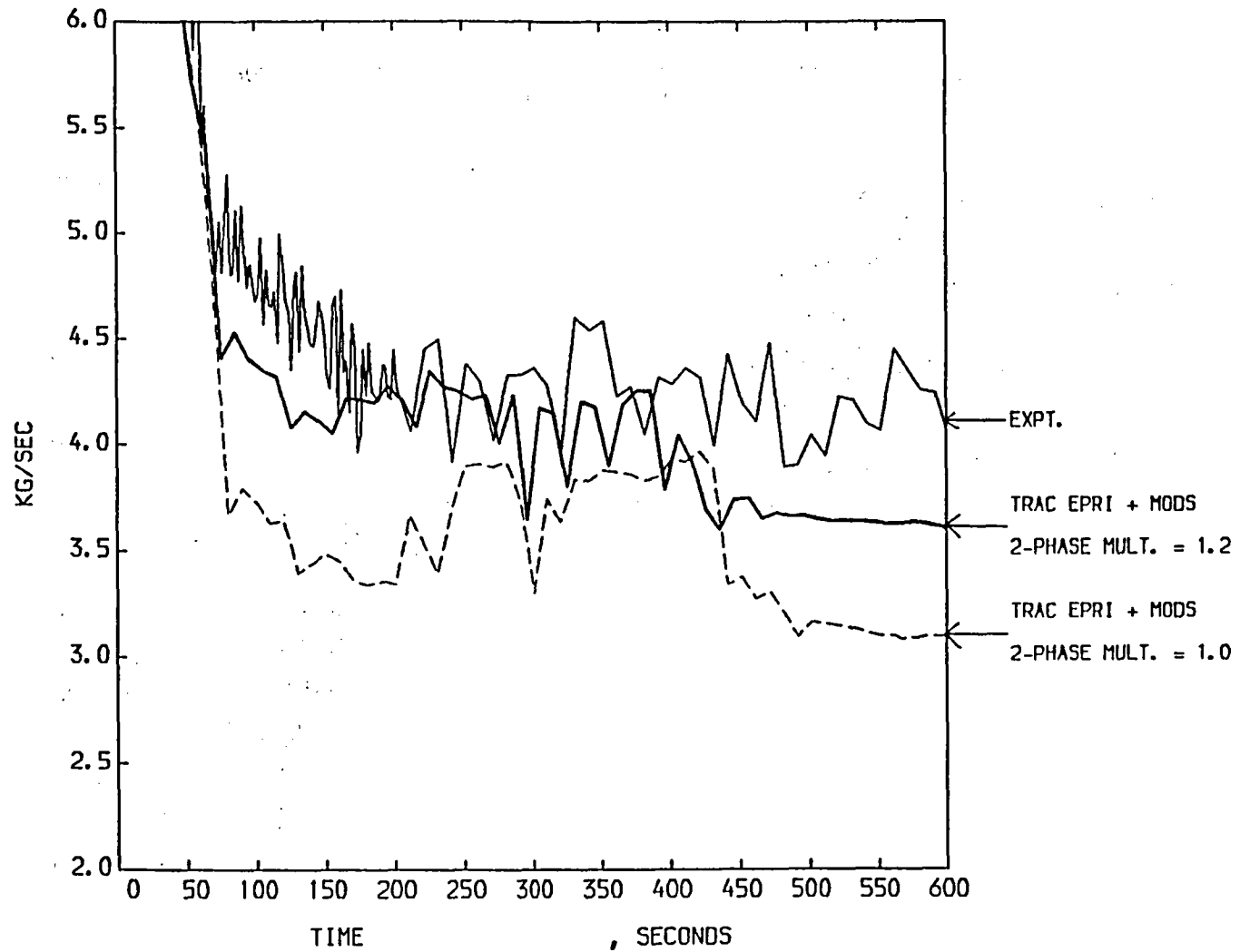
FR-PC-S03   ,MASS FLOW RATE

FIGURE 66 – EFFECT OF 2-PHASE MULTIPLIER CHOICE ON BREAK FLOW
LP-SB-1 BASE CASE CALCULATION WITH EPRI CORRELN & INPUT MODS

APPENDIX I

MICROFICHE LISTING OF THE TRAC-PF1/MOD1 INPUT DECK FOR LP-SB-1 (USED FOR THE STEADY STATE CALCULATION)

(See inside back cover pocket for microfiche)

THE EPRI CORRELATION FOR BRANCHLINE FLOW QUALITY AS A FUNCTION OF MAINLINE STRATIFIED LIQUID LEVEL

Experiments performed in the Two-Phase Flow Loop (TPFL) at the Idaho National Engineering Laboratory (INEL), during 1984, investigated the liquid entrainment/vapour pull-through phenomena of a tee with a large mainline to branchline diameter ratio and the effect of these phenomena on the flow rate in the branchline (19). As a result of the experimental work, correlations (recommended for use in codes) for predicting the liquid levels for the onset of vapour pull-through and liquid entrainment and the resulting branchline flow quality were derived as follows:

$$\frac{h_e}{D} = \frac{1}{2} - \frac{C_e}{D} \left[\frac{\dot{m}_g^2}{g\rho_g (\rho_f - \rho_g)} \right]^{0.2}$$

$$\frac{h_p}{D} = \frac{1}{2} + \frac{C_p}{D} \left[\frac{\dot{m}_f^2}{g\rho_f (\rho_f - \rho_g)} \right]^{0.2}$$

$$X = 0 \text{ if } h > h_p$$

$$X = \exp \left[C_x \left(\frac{h - h_e}{h_p - h_e} \right) \right] \qquad \text{if} \quad h_e < h < h_p$$

$$X = 1 \text{ if } h < h_e$$

where h_e = liquid level at which liquid entrainment begins (m)

h_p = liquid level at which vapour pull-through begins (m)

D = mainline internal diameter (m)

C_e = constant obtained from experimental data (0.62)

C_p = constant obtained from experimental data (0.82)

$\dot{m}_g$ = gas mass flow rate in branchline (kg s^{-1})

$\dot{m}_f$ = liquid mass flow rate in branchline (kg s^{-1})
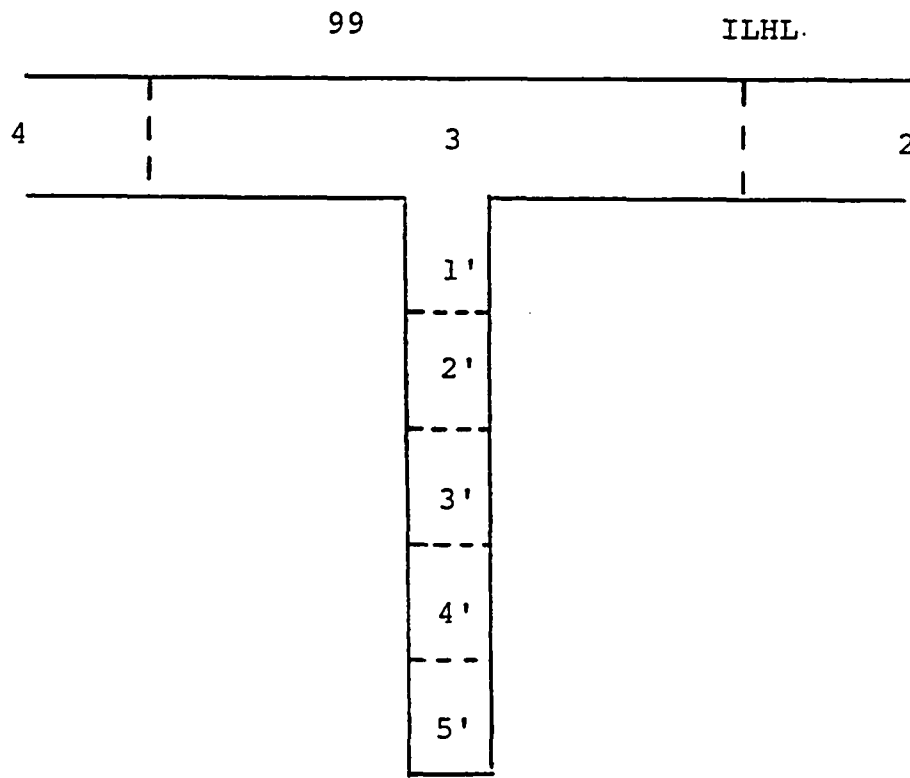
g = acceleration due to gravity (ms^{-2})

ρ_g = gas density (kg m^{-3})
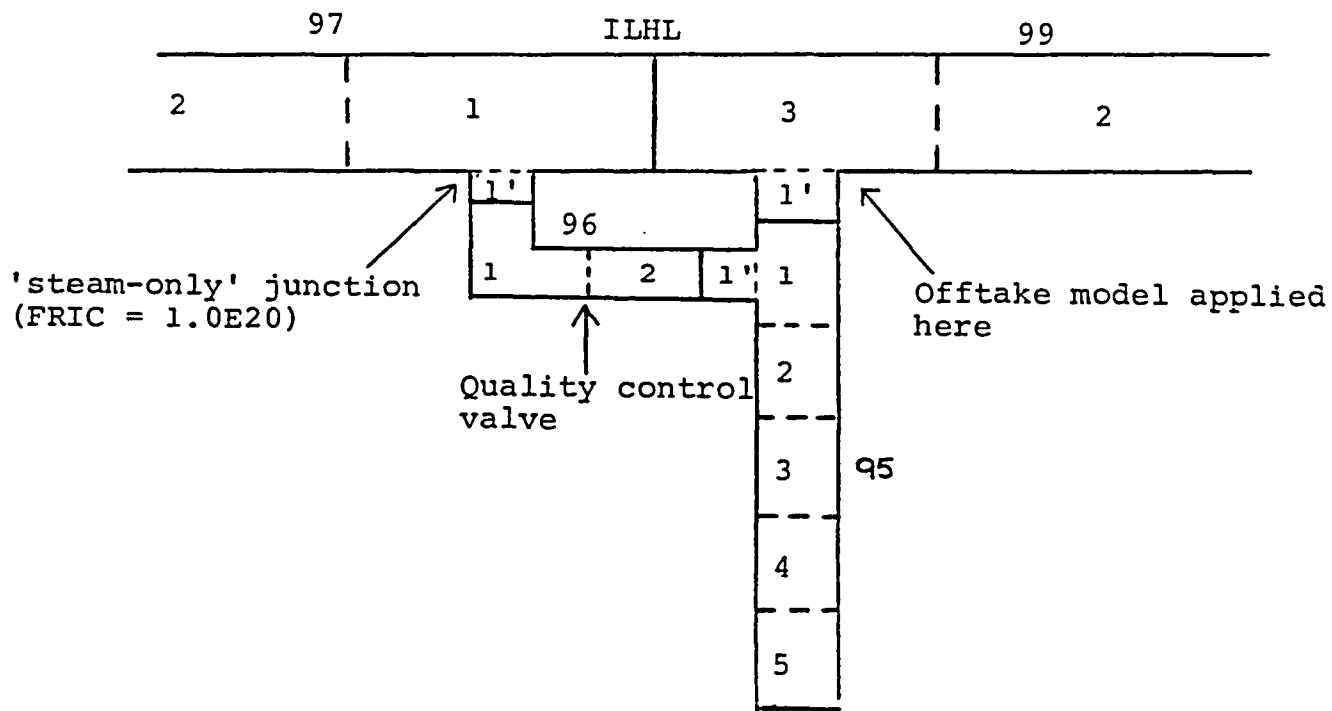
ρ_f = liquid density (kg m^{-3})

X = branchline flow quality

C_X = constant obtained from experimental data (- 3.4)

Implementing the correlation for branchline flow quality as a function of stratified liquid level involved modifying the LP-SB-1 input model as shown in Figure AII.1. A VALVE component was introduced in order to control the amount of steam entering the branchline and Version BØ2C of the TRAC-PF1/MOD1 code - employing a branch offtake quality model for stratified flow - was used.

99   ILHL.

4 | 3 | 2

1'

2'

3'

4'

5'

BREAK

(a) Base Case Calculation

97   ILHL   99

2 | 1   3 | 2

1'   1'
         96
1   2   1" 1
                      1
'steam-only' junction   2
(FRIC = 1.0E20)   Offtake model applied
                                         here
                           3   95
Quality control
valve   4

                           5

BREAK

(b) EPRI Correlation Calculations

FIGURE AII.1

Nodalization Modification for Implementation of Breakline
Quality Control

AEEW - R 2254

APPENDIX III

EFFECT OF DEFICIENCIES IN THE TRAC-PF1/MOD1 INTERPHASE DRAG MODEL ON THE PREDICTION OF THE CORE DENSITY FOR LP-SB-1

An assessment of the interphase drag correlation used for modelling vertical two-phase flows in TRAC-PF1/MOD1 is described in Reference 20. The assessment compared void fractions calculated by the code with those predicted by standard correlations in order that an estimate might be made of the void fraction errors likely to arise, in a particular application, due to deficiencies in the code's modelling of interphase drag.

The plot of percentage error in the density predicted by the code (when compared with that predicted by the Wilson-Rooney correlation) as a function of void fraction (20) is reproduced in Figure A.III.1. (The Figure is applicable to zero liquid flow rates - under which circumstances errors were found to be largest).

In order to gain an indication of the likely magnitude, and effect, of errors in the densities predicted by TRAC-PF1/MOD1 for LP-SB-1, Figure A.III.1 was applied at a particular point in the transient. Figure A.III.2 shows the fluid conditions in the core (component number 88) and the pipe above the core (component number 87) at ~ 800 seconds as predicted by the "Base Case + EPRI Correlation" calculation of LP-SB-1.

In cell numbers 87/1, 87/2, 88/5 and 88/4, the fluid conditions are such that the error in density (defined as $(\rho_2 - \rho_1)/\rho_1$ x 100%, where ρ_1 = density calculated by Wilson Rooney correlation and ρ_2 = density predicted by the code) is ~ - 10%, ie the density in these cells is underestimated, by TRAC-PF1/MOD1, by ~ 10%. For the remaining cells (88/1, 88/2 and 88/3) the density error is negligible.

Had the density in parts of the core and the pipe above the core not been underestimated, the additional gravitational head available to balance the fluid in the downcomer would have been:

$$\sum (h\rho) \times g \times 10\%$$

$$= (1.446 \times 486 + 0.476 \times 544 + 0.457 \times 564 + 0.457 \times 591) \times 9.81 \times 0.1$$

$$= 1461 \text{ kg m}^{-1} \text{ s}^{-2}$$

This would be equivalent to increasing the density in the top cell of the downcomer by $\dfrac{1461}{9.81 \times 1.446}$ kg m^{-3} ie 103 kg m^{-3}.

Therefore, had the density not been underpredicted, additional fluid of the order of

$(0.46762 \times 486 + 0.15393 \times 544 + 8.0499 \times 10^{-2} \times 564 + 8.0499 \times 10^{-2} \times 591) \times 0.1 + 0.19192 \times 103*$

$$= 60 \text{ kg}$$

* $\sum (\text{Vol} \times \Delta\rho)$

would have remained in the vessel. It would have been necessary
to expel less fluid from the break and break uncovery could be
expected to have occurred ~ 20 seconds earlier.

ERRORS IN MEAN TWO-PHASE MIXTURE DENSITY FOR $j_\ell = 0$

(a) $D_h = 0.01$m
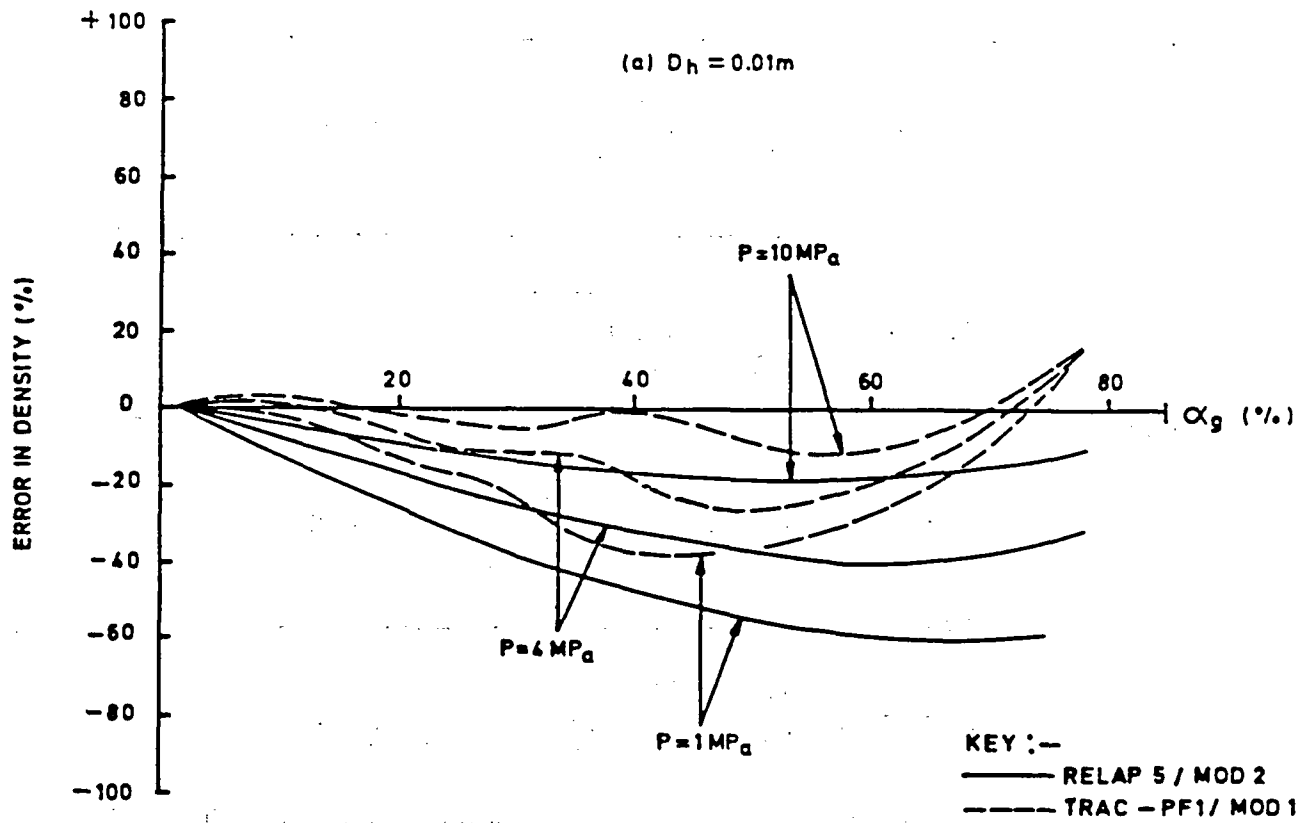
FLUID CONDITIONS IN THE CORE AND THE PIPE ABOVE THE CORE AT ~ 800 SECONDS

jg $(\alpha_g u_g)$	u_g		CELL	u_ℓ	$j\ell$ $(1-\alpha_g)u_\ell$
0.225	0.6054			0.2583	0.16
	1.446 m	$\rho m = 486$ kgm^{-3} $\alpha_g = 0.372$ VOL $= 0.46762$ m^3	87/2		
0.14	0.3761 X			0.1184	0.07
	0.476 m	$\rho m = 544$ kgm^{-3} $\alpha_g = 0.2925$ VOL $= 0.15393$ m^3	87/1		
0.10	0.3512 X			0.09877	0.07
	0.457 m	$\rho m = 564$ kgm^{-3} $\alpha_g = 0.265$ VOL $= 8.0499 \times 10^{-2}$ m^3	88/5		
0.09	0.3481 X			0.09487	0.07
	0.457 m	$\rho m = 591$ kgm^{-3} $\alpha_g = 0.2275$ VOL $= 8.0499 \times 10^{-2}$ m^3	88/4		
0.08	0.3436 X			0.08604	0.07
		$\alpha_g = 0.131$ VOL $= 4.0337 \times 10^{-2}$ m^3	88/3		
0.05	0.3457			0.08109	0.07
		$\alpha_g = 0.06781$ VOL $= 4.0161 \times 10^{-2}$ m^3	88/2		
0.02	0.3463			0.07751	0.07
		$\alpha_g = 0.01798$ VOL $= 5.3724 \times 10^{-2}$ m^3	88/1		
0.01	0.3467			0.07588	0.07

Pressure ~ 6.3 MPa
Hydraulic diameter = 0.0122 m

APPENDIX IV

MODIFICATIONS TO LP-SB-1 BASE CASE INPUT DECK FOR FINAL TRANSIENT CALCULATION

1 Correction of GRAVs in Lower Plenum (Component Number 90)

	GRAV	
	Base Case Calculation	Final Calculation[1]
Main Branch	-1.0, 0.0, 1.0	-1.0, -0.182245, 1.0
Side Branch	0.0, 1.0	-0.0824089, 1.0

2 Correction of Effective Cell Lengths for Plenum Components (Component Numbers 82 and 84)

Component	EFFECTIVE PLENUM SIDE CELL LENGTHS	
	Base Case Calculation	Final Calculation[2]
82	0.142,0.0705,0.0705, 0.142,0.142,0.0705	0.284,0.141,0.141, 0.284,0.284,0.141
84	0.142,0.329,0.142, 0.142,0.329,0.329	0.284,0.658,0.284, 0.284,0.658,0.658

[1] data obtained by running TRAC-PF1/MOD1 with elevation data and allowing the code to compute the GRAV terms.

[2] the code expects the total height (and width) of the plenum and not half the height (and half the width) as was specified for the Base Case Calculation.

APPENDIX IV

MODIFICATIONS TO LP-SB-1 BASE CASE INPUT DECK FOR FINAL TRANSIENT CALCULATION

1   Correction of GRAVs in Lower Plenum (Component Number 90)

	GRAV	
	Base Case Calculation	Final Calculation[1]
Main Branch	-1.0, 0.0, 1.0	-1.0, -0.182245, 1.0
Side Branch	0.0, 1.0	-0.0824089, 1.0

2   Correction of Effective Cell Lengths for Plenum Components (Component Numbers 82 and 84)

Component	EFFECTIVE PLENUM SIDE CELL LENGTHS	
	Base Case Calculation	Final Calculation[2]
82	0.142,0.0705,0.0705, 0.142,0.142,0.0705	0.284,0.141,0.141, 0.284,0.284,0.141
84	0.142,0.329,0.142, 0.142,0.329,0.329	0.284,0.658,0.284, 0.284,0.658,0.658

[1] data obtained by running TRAC-PF1/MOD1 with elevation data and allowing the code to compute the GRAV terms.

[2] the code expects the total height (and width) of the plenum and not half the height (and half the width) as was specified for the Base Case Calculation.

6 Renodalisation of Reflood Assist Bypass Line[6]

(i) Broken Loop Hot leg (Component Number 31)

			Base Case Calculation	Final Calculation
Side Branch		RAD	0.10795 m	0.111 m
"	"	TH	0.02858 m	0.0255 m
"	"	DX	1.389 m, 0.814 m, 5.1044 m	1.687 m, 0.726 m, 1.849 m
"	"	VOL	0.054 m^3, 0.0314 m^3, 0.1986 m^3	0.0658 m^3, 0.0283 m^3, 0.0721 m^3
"	"	FA	R3 0.0388 m^2, 0.02119 m^2	R3 0.039 m^2, 0.013 m^2
"	"	GRAV	0.0, 0.2242, 0.1912, 0.0	0.0, 1.0, 0.0, 0.0
"	"	HD	R3 0.2223 m, 1.41E-3 m	R3 0.2228 m, 1.41E-3 m

(ii) Broken Loop Cold Leg (Component Number 41)

			Base Case Calculation	Final Calculation
Side Branch		RAD	0.10795 m	0.111 m
"	"	TH	0.02858 m	0.0255 m
"	"	DX	0.885 m, 7.2834 m	2.129 m, 3.27 m
"	"	VOL	0.03033 m^3, 0.2768 m^3	0.0830 m^3, 0.1275 m^3
"	"	FA	R2 0.0388 m^2, 0.02119 m^2	R2 0.039 m^2, 0.013 m^2
"	"	GRAV	0.0, 0.199, 0.0	1.0, 0.0, 0.0
"	"	HD	R2 0.2223 m, 1.41E-3 m	R2 0.2228 m 1.41E-3 m

[6] Size of Reflood Assist Bypass Line decreased (2).

LP-SB-1 BASE CASE CALCULATIONS WITH EPRI CORRELATION AND INPUT MODEL MODIFICATIONS - SERIES OF PICTURES SHOWING PREDICTED SYSTEM CONDITIONS THROUGHOUT THE TRANSIENT

The following series of pictures shows, at 200 second intervals, the predicted void fraction distribution, the liquid and vapour velocities and the occurrences of stratified flow conditions throughout the system. The nodalisation may be compared with that of Figures 3a, 3b, 4 and 5. The pictures were produced from the final calculations - Base Case + EPRI Correlation + Input Modifications - and include the break line quality control valve (see Figure AII.1).

S.M.A.R.T. SYSTEM MIMIC FOR ANALYSIS OF REACTOR TRANSIENTS

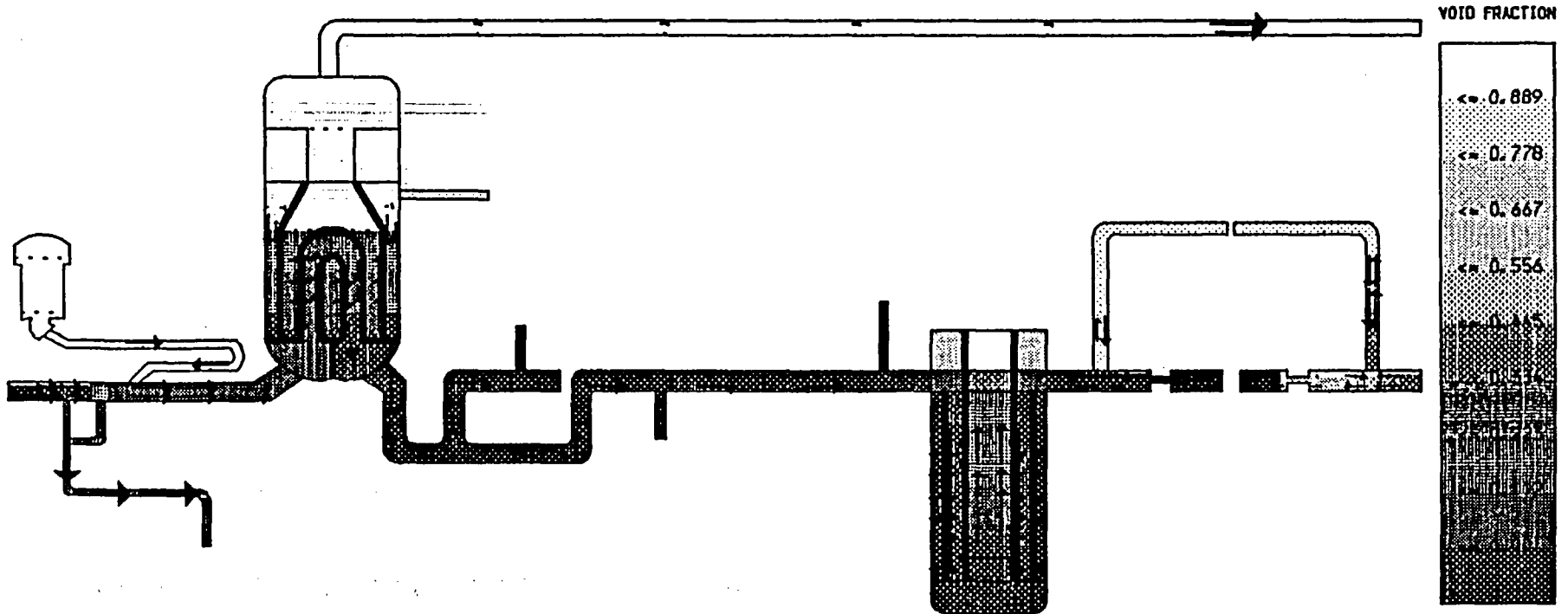TITLE OF FRAME:- TRAC PREDICTION OF LOFT SB-1 (BASE + EPRI CORRELN + INPUT MODS)

T: 0.1

VLIQ ⟶

(5.00)

VVAP ⟶

(5.00)

VOID FRACTION

<= 0.889

<= 0.778

<= 0.667

<= 0.556
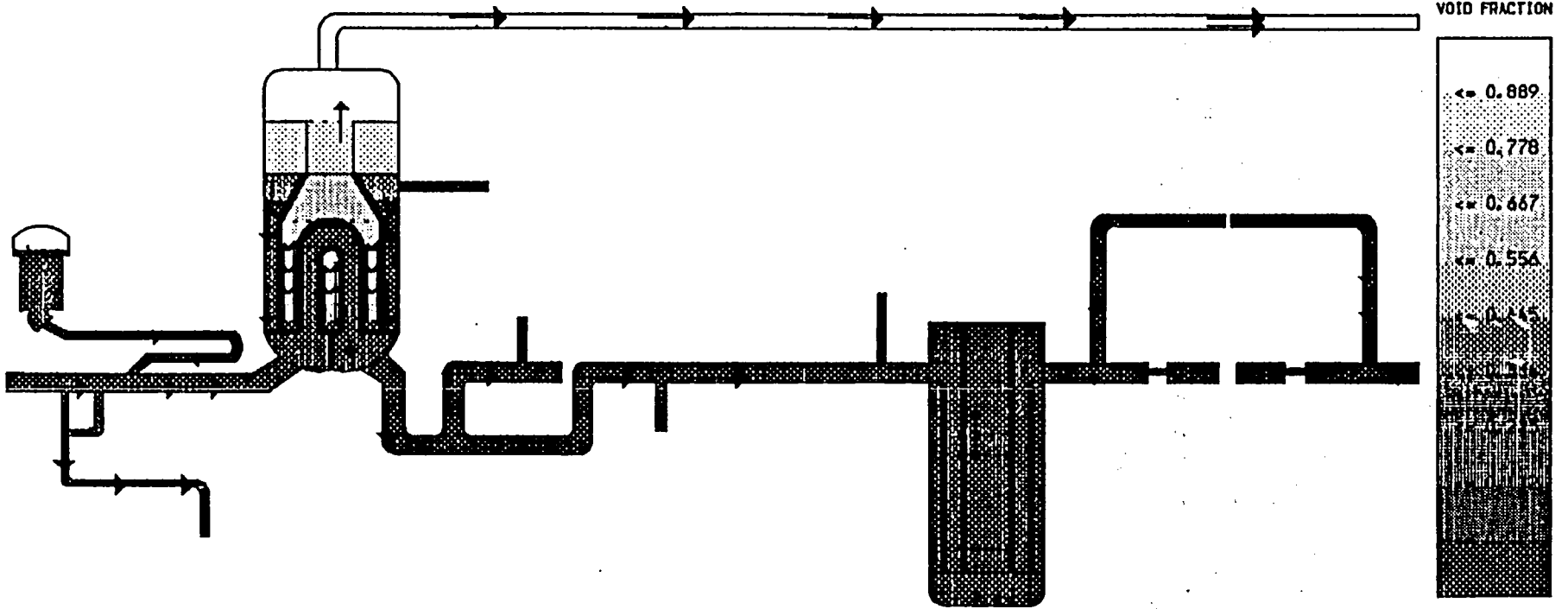
S. M. A. R. T. SYSTEM MIMIC FOR ANALYSIS OF REACTOR TRANSIENTS

TITLE OF FRAME.- TRAC PREDICTION OF LOFT SB-1 (BASE + EPRI CORRELN + INPUT MODS)

T₁ 229.2

VLIQ ⟶
(5.00)
VVAP ⟶
(5.00)

VOID FRACTION

<= 0.889

<= 0.778

<= 0.667

<= 0.556

S. M. A. R. T. SYSTEM MIMIC FOR ANALYSIS OF REACTOR TRANSIENTS

TITLE OF FRAME:- TRAC PREDICTION OF LOFT SB-1 (BASE + EPRI CORRELN + INPUT MODS)

T: 409.6

VLIQ ⟶

(5.00)

VVAP ⟶

(5.00)

VOID FRACTION

<= 0.889

<= 0.778

<= 0.667

<= 0.556

S. M. A. R. T. SYSTEM MIMIC FOR ANALYSIS OF REACTOR TRANSIENTS

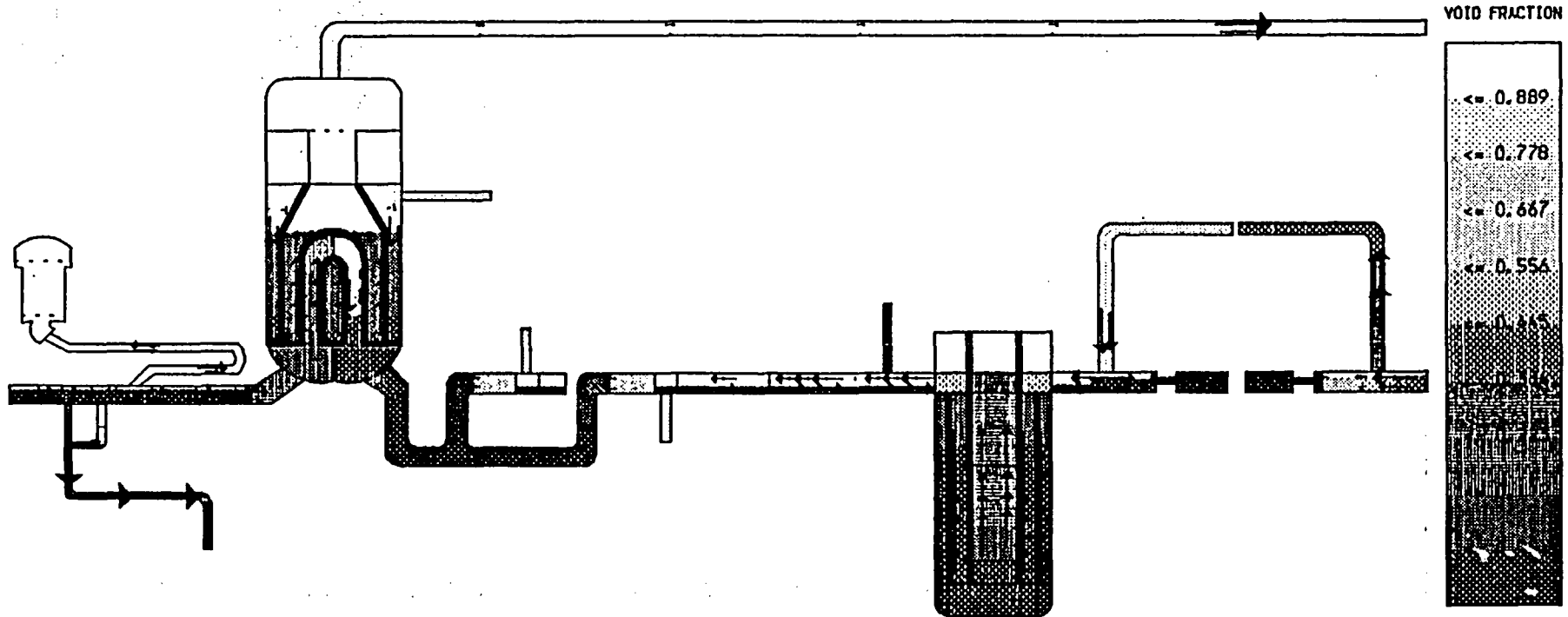TITLE OF FRAME:- TRAC PREDICTION OF LOFT SB-1 (BASE + EPRI CORRELN + INPUT MODS)

T: 626.2

VLIQ ⟶

(5.00)

VVAP ⟶

(5.00)

VOID FRACTION

<= 0.889

<= 0.778

<= 0.667

<= 0.556

S. M. A. R. T. SYSTEM MIMIC FOR ANALYSIS OF REACTOR TRANSIENTS

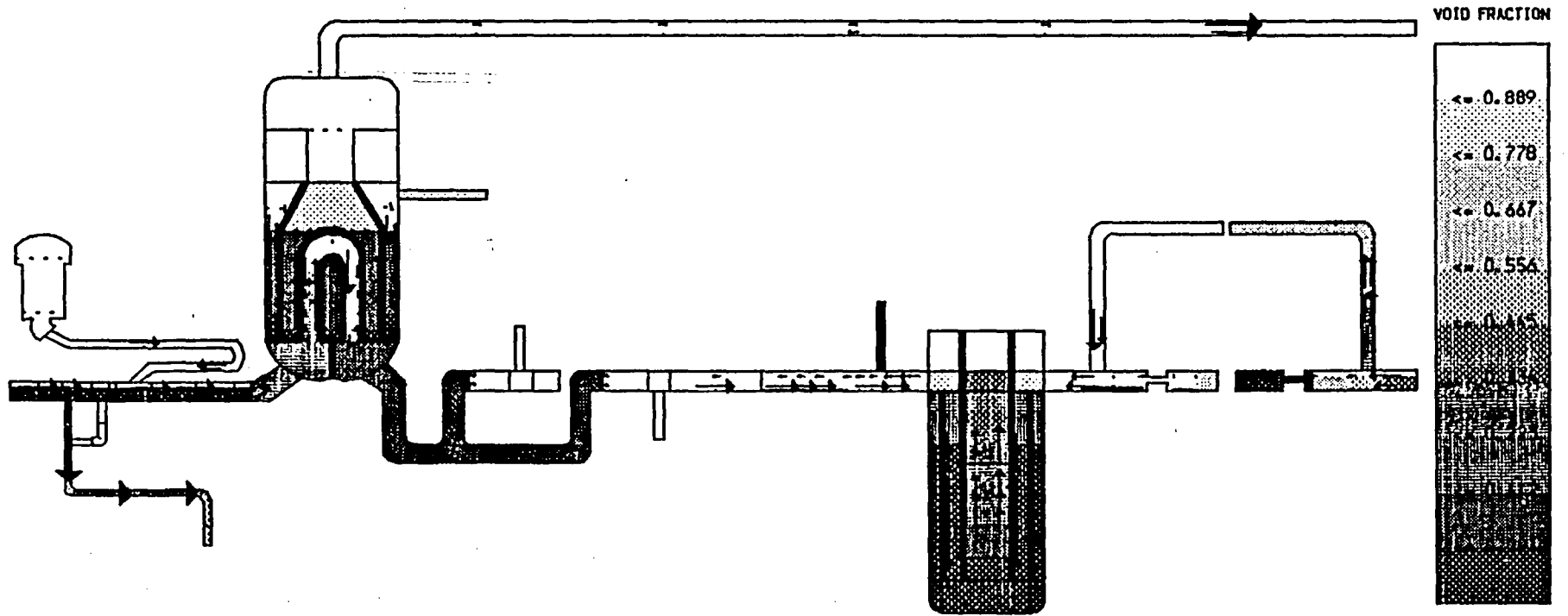TITLE OF FRAME:- TRAC PREDICTION OF LOFT SB-1 (BASE + EPRI CORRELN + INPUT MODS)

T: 802.0

VLIQ ⟶

(5.00)

VVAP ⟶

(5.00)

VOID FRACTION

<= 0.889

<= 0.778

<= 0.667

<= 0.556

S.M.A.R.T. SYSTEM MIMIC FOR ANALYSIS OF REACTOR TRANSIENTS

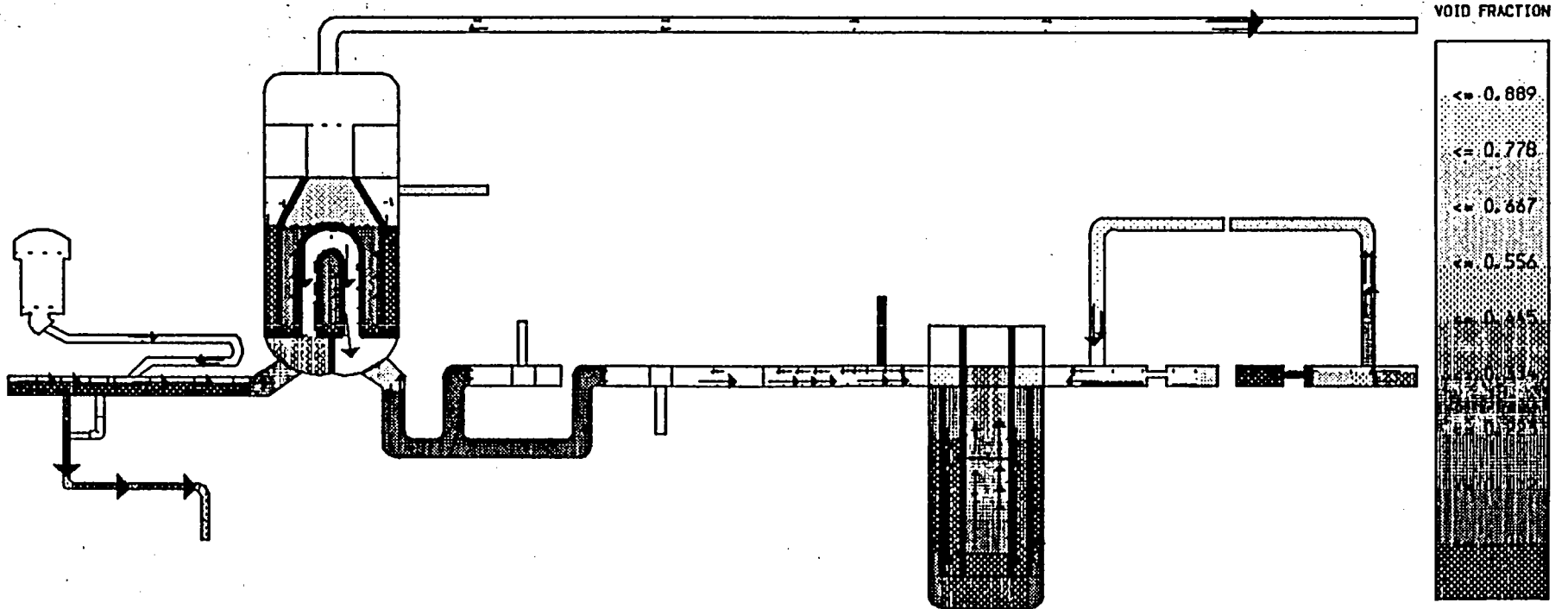TITLE OF FRAME:- TRAC PREDICTION OF LOFT SB-1 (BASE + EPRI CORRELN + INPUT MODS)

T: 1012.9
VLIQ —→
(5.00)
VVAP ——→
(5.00)

VOID FRACTION

<= 0.889
<= 0.778
<= 0.667
<= 0.556
<= 0.445

S.M.A.R.T. SYSTEM MIMIC FOR ANALYSIS OF REACTOR TRANSIENTS

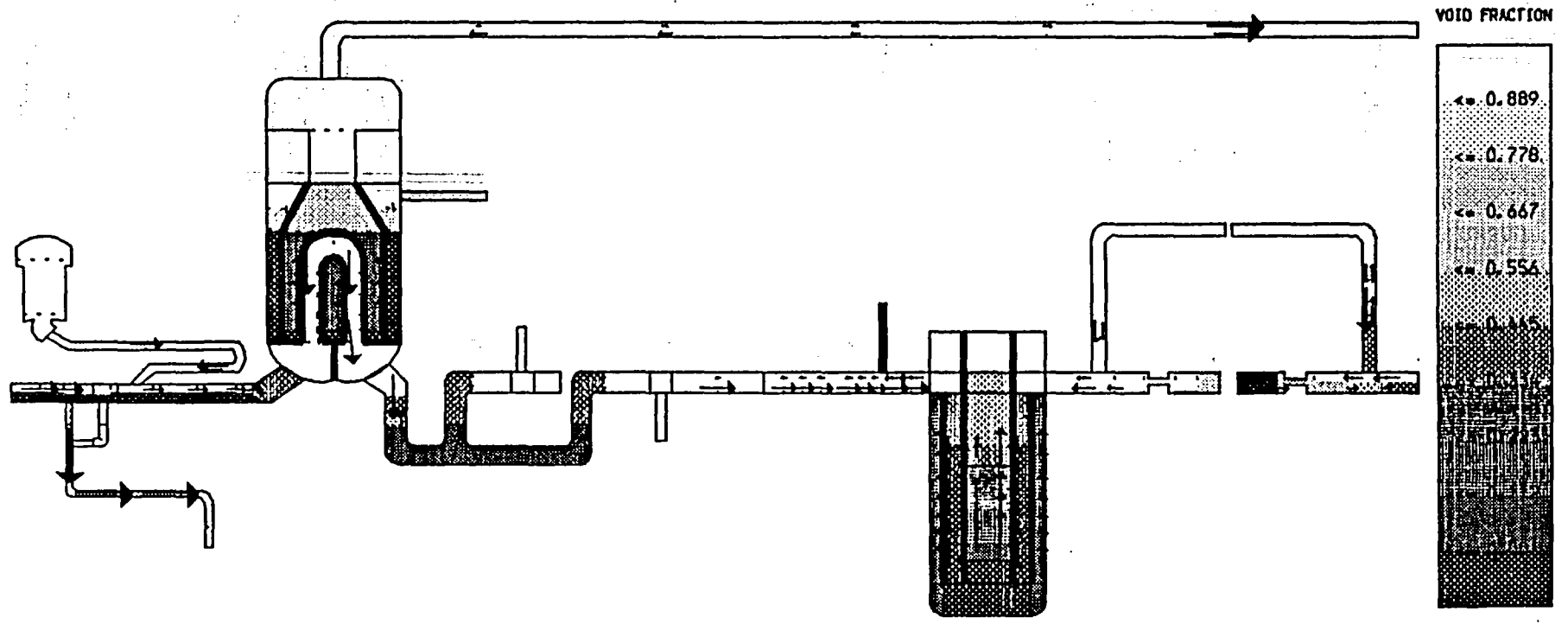TITLE OF FRAME:- TRAC PREDICTION OF LOFT SB-1 (BASE + EPRI CORRELN + INPUT MODS)

T: 1223.9

VLIQ ⟶
(5.00)

VVAP ⟶
(5.00)

VOID FRACTION

<= 0.889

<= 0.778

<= 0.667

<= 0.556

S.M.A.R.T. SYSTEM MIMIC FOR ANALYSIS OF REACTOR TRANSIENTS

TITLE OF FRAME:- TRAC PREDICTION OF LOFT SB-1 (BASE + EPRI CORRELN + INPUT MODS)
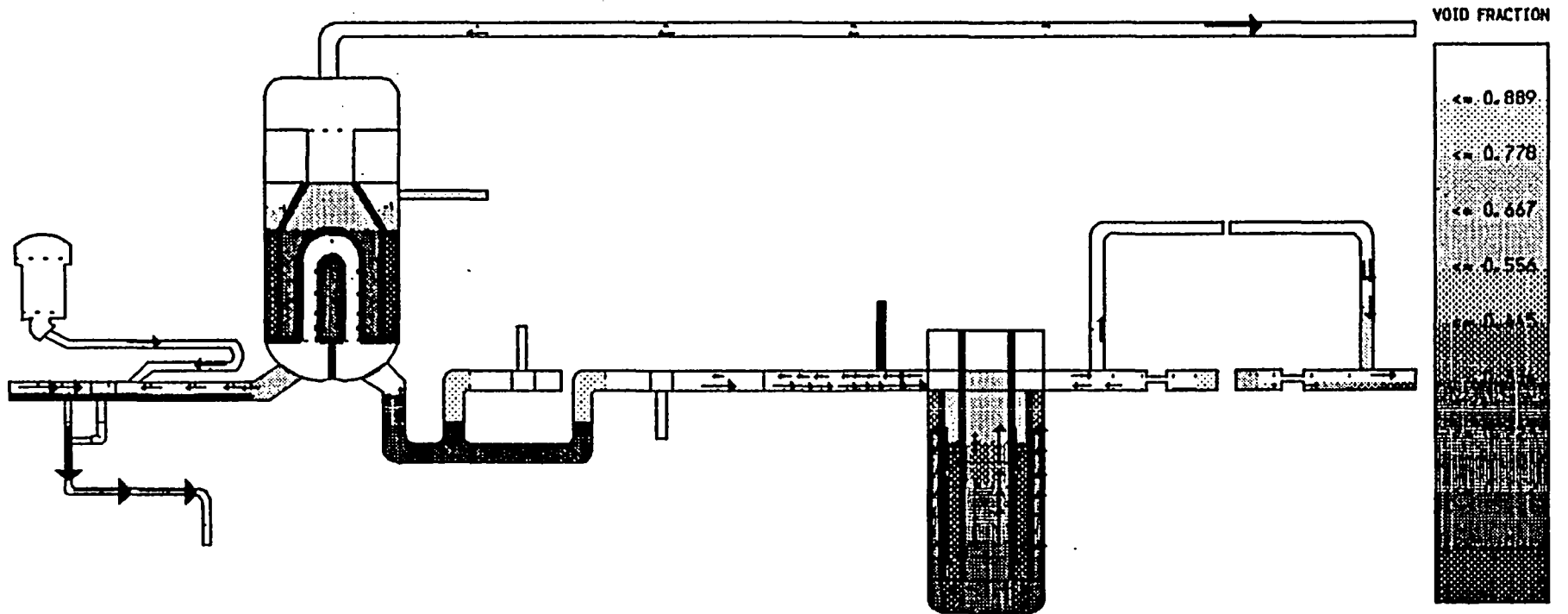
T: 1402.2

VLIQ ⟶
(5.00)

VVAP ⟶
(5.00)

VOID FRACTION

<= 0.889

<= 0.778

<= 0.667

<= 0.554

S. M. A. R. T. SYSTEM MIMIC FOR ANALYSIS OF REACTOR TRANSIENTS

TITLE OF FRAME:- TRAC PREDICTION OF LOFT SB-1 (BASE + EPRI CORRELN + INPUT MODS)

Ti 1613.2

VLIQ ⟶
(5.00)

VVAP ⟶
(5.00)

VOID FRACTION

<= 0.889

<= 0.778

<= 0.667

<= 0.556

S.M.A.R.T. SYSTEM MIMIC FOR ANALYSIS OF REACTOR TRANSIENTS

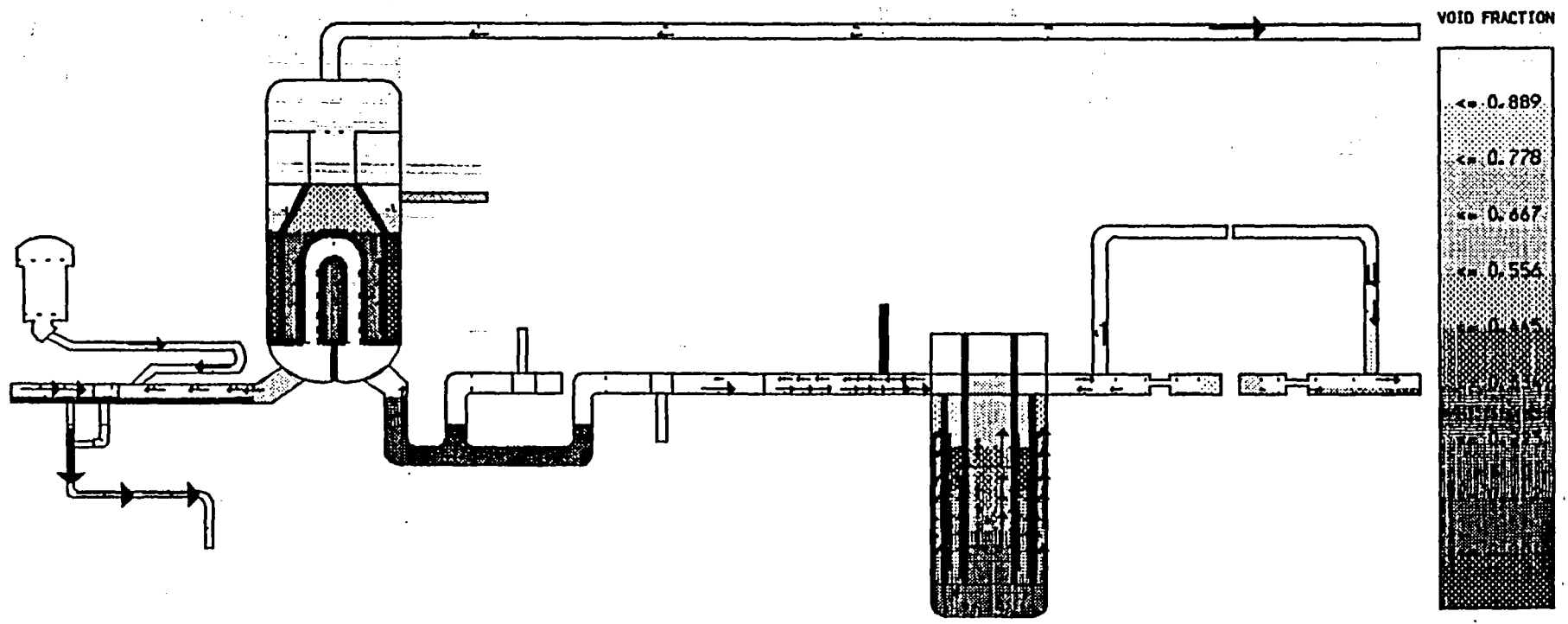TITLE OF FRAME:- TRAC PREDICTION OF LOFT SB-1 (BASE + EPRI CORRELN + INPUT MODS)

T: 1824.7

VLIQ ⟶
(5.00)

VVAP ⟶
(5.00)

VOID FRACTION

<= 0.889

<= 0.778

<= 0.667

<= 0.556

0.445

S. M. A. R. T. SYSTEM MIMIC FOR ANALYSIS OF REACTOR TRANSIENTS

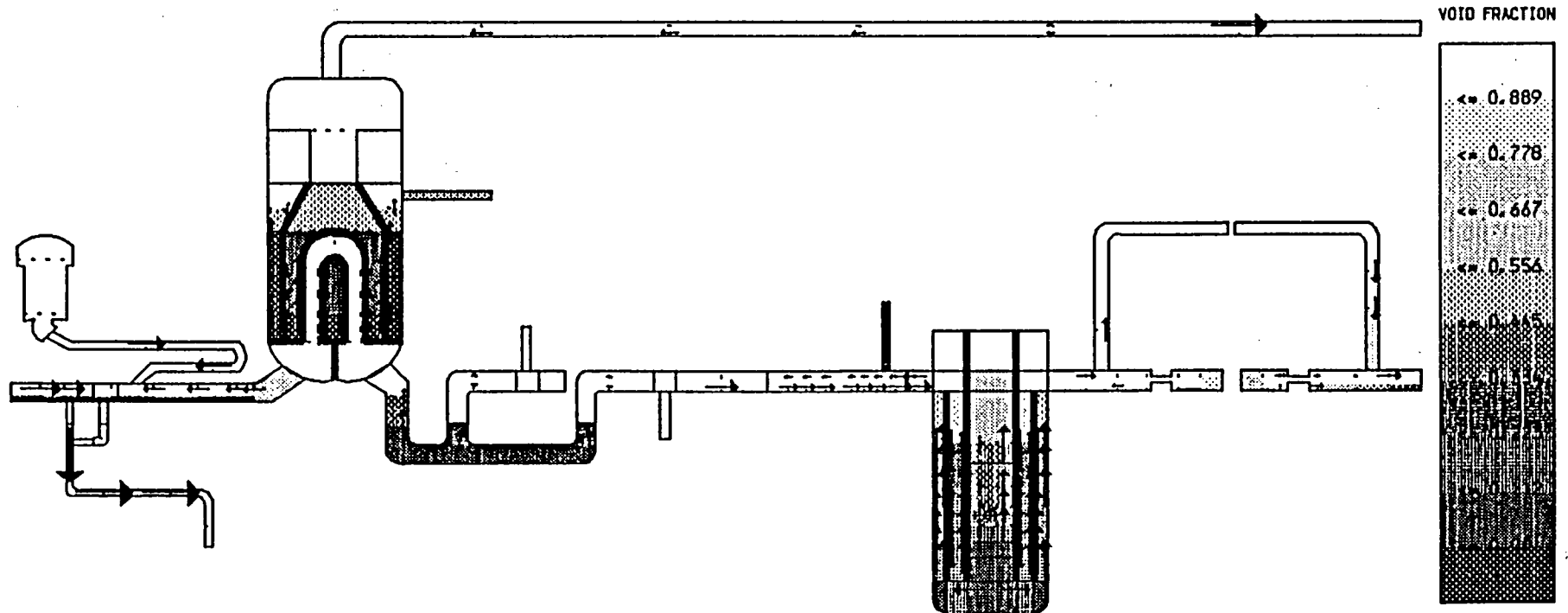TITLE OF FRAME.- TRAC PREDICTION OF LOFT SB-1 (BASE + EPRI CORRELN + INPUT MODS)

T¡ 2010.5

VLIQ ⟶

(5.00)

VVAP ⟶

(5.00)

VOID FRACTION

<= 0.889

<= 0.778

<= 0.667

<= 0.556

S. M. A. R. T. SYSTEM MIMIC FOR ANALYSIS OF REACTOR TRANSIENTS

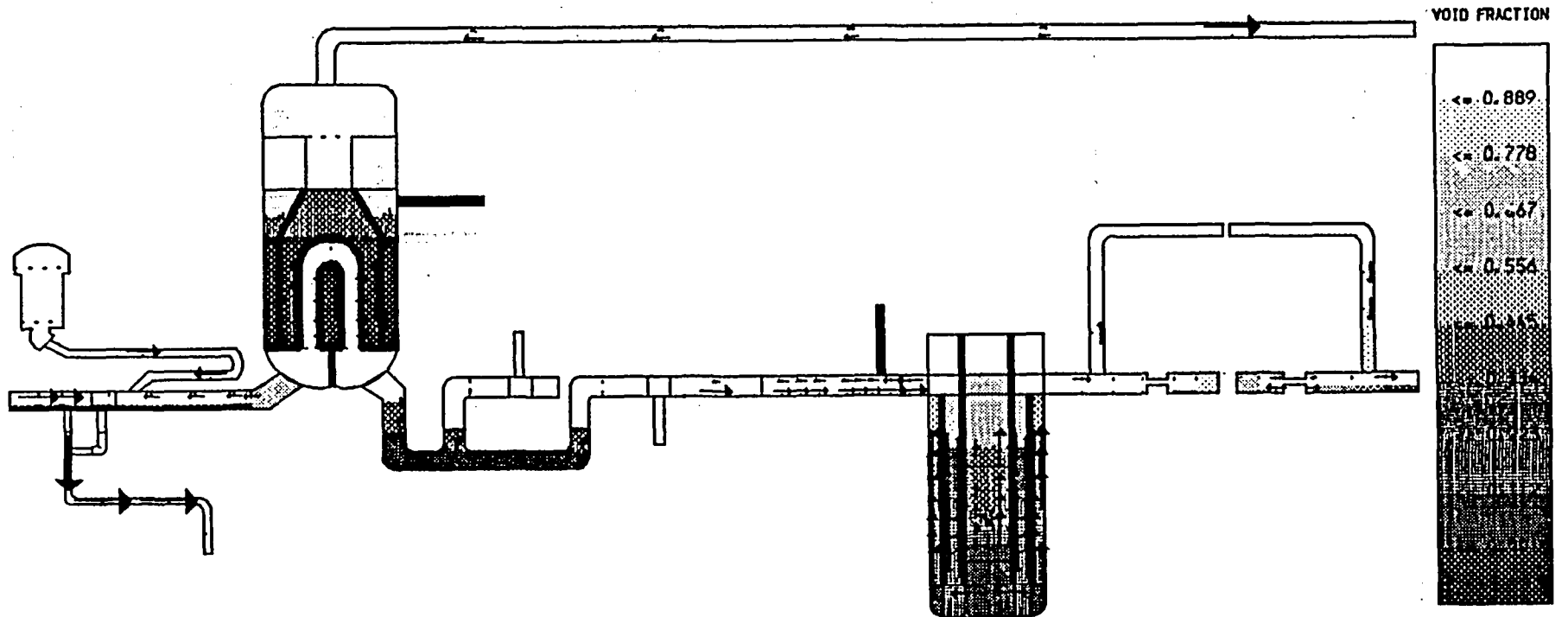TITLE OF FRAME:- TRAC PREDICTION OF LOFT SB-1 (BASE + EPRI CORRELN + INPUT MODS)

T: 2221.9

VLIQ ──→
(5.00)

VVAP ──→
(5.00)

VOID FRACTION

<= 0.889

<= 0.778

<= 0.667

<= 0.556

S. M. A. R. T. SYSTEM MIMIC FOR ANALYSIS OF REACTOR TRANSIENTS

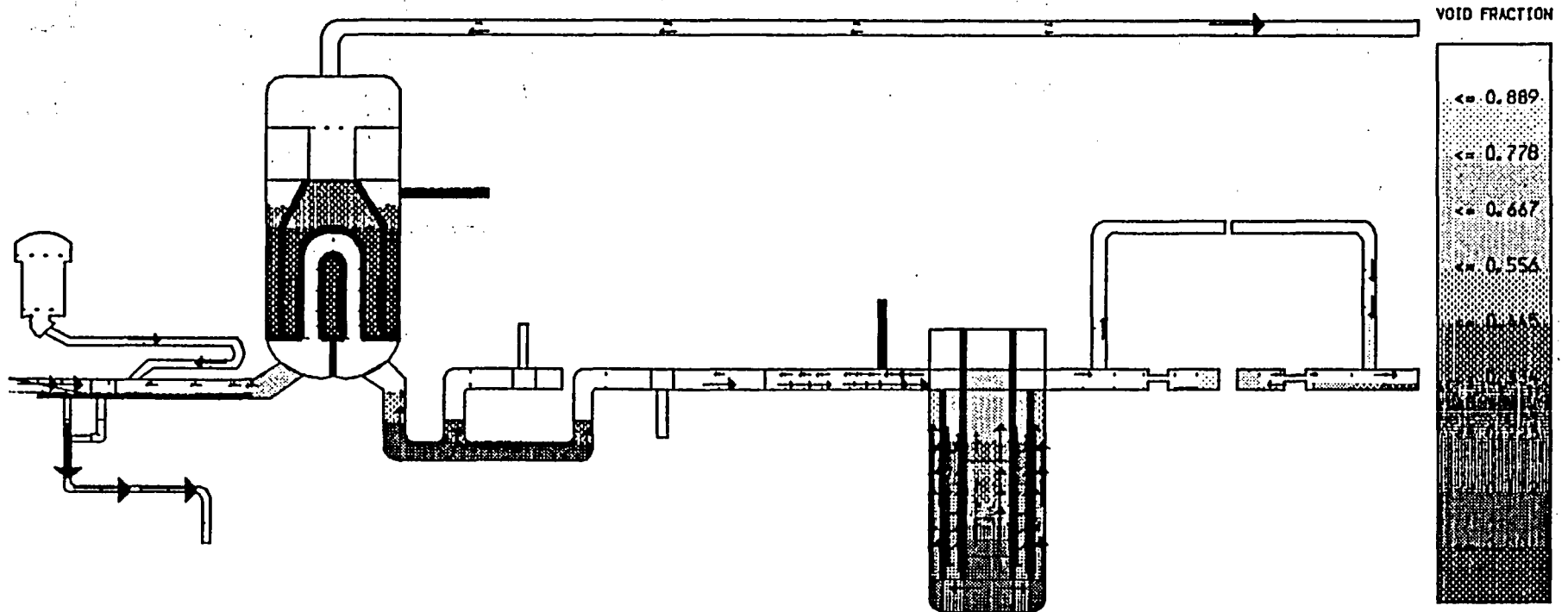TITLE OF FRAME.- TRAC PREDICTION OF LOFT SB-1 (BASE + EPRI CORRELN + INPUT MODS)

T: 2403.1

VLIQ ——▶

(5.00)

VVAP ——▶

(5.00)

VOID FRACTION

<= 0.889

<= 0.778

<= 0.667

<= 0.554

S.M.A.R.T. SYSTEM MIMIC FOR ANALYSIS OF REACTOR TRANSIENTS

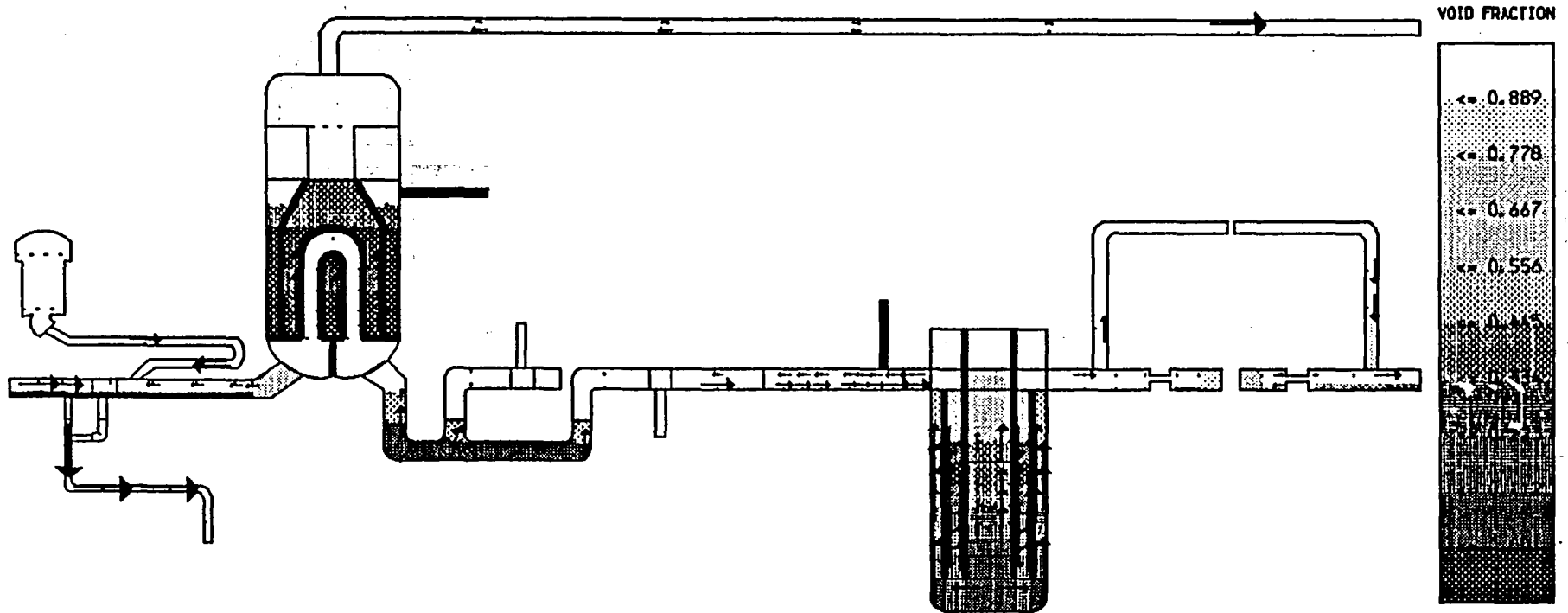TITLE OF FRAME:- TRAC PREDICTION OF LOFT SB-1 (BASE + EPRI CORRELN + INPUT MODS)

T: 2614.5

VLIQ ⟶

(5.00)

VVAP ⟶

(5.00)

VOID FRACTION

<= 0.889

<= 0.778

<= 0.667

<= 0.556

TITLE OF FRAME:- TRAC PREDICTION OF LOFT SB-1 (BASE + EPRI CORRELN + INPUT MODS)

T: 2825.6

VLIQ ⟶

(5.00)

VVAP ⟶

(5.00)

VOID FRACTION

<= 0.889

<= 0.778

<= 0.667

<= 0.556

AEEW - R 2254

S.M.A.R.T. SYSTEM MIMIC FOR ANALYSIS OF REACTOR TRANSIENTS

TITLE OF FRAME:- TRAC PREDICTION OF LOFT SB-1 (BASE + EPRI CORRELN + INPUT MODS)

T: 3006.8
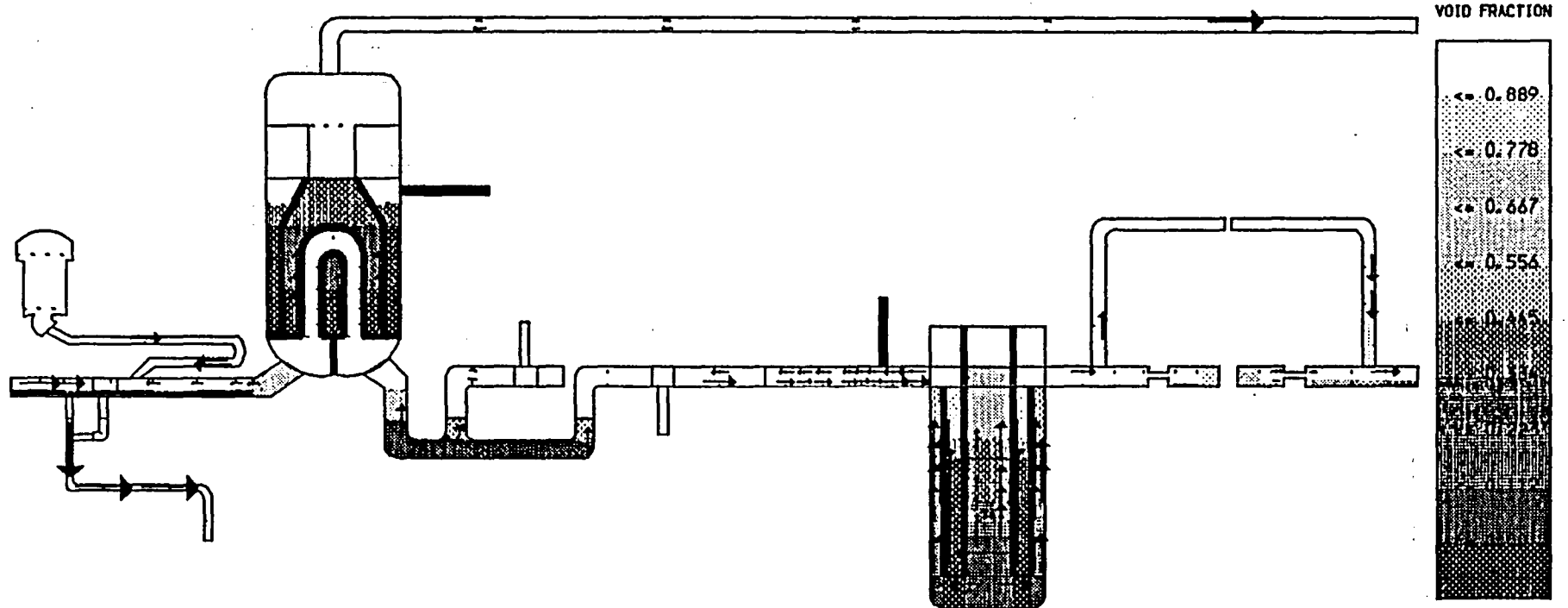VLIQ ⟶
(5.00)
VVAP ⟶
(5.00)

VOID FRACTION

<= 0.889
<= 0.778
<= 0.667
<= 0.556
<= 0.

S.M.A.R.T. SYSTEM MIMIC FOR ANALYSIS OF REACTOR TRANSIENTS

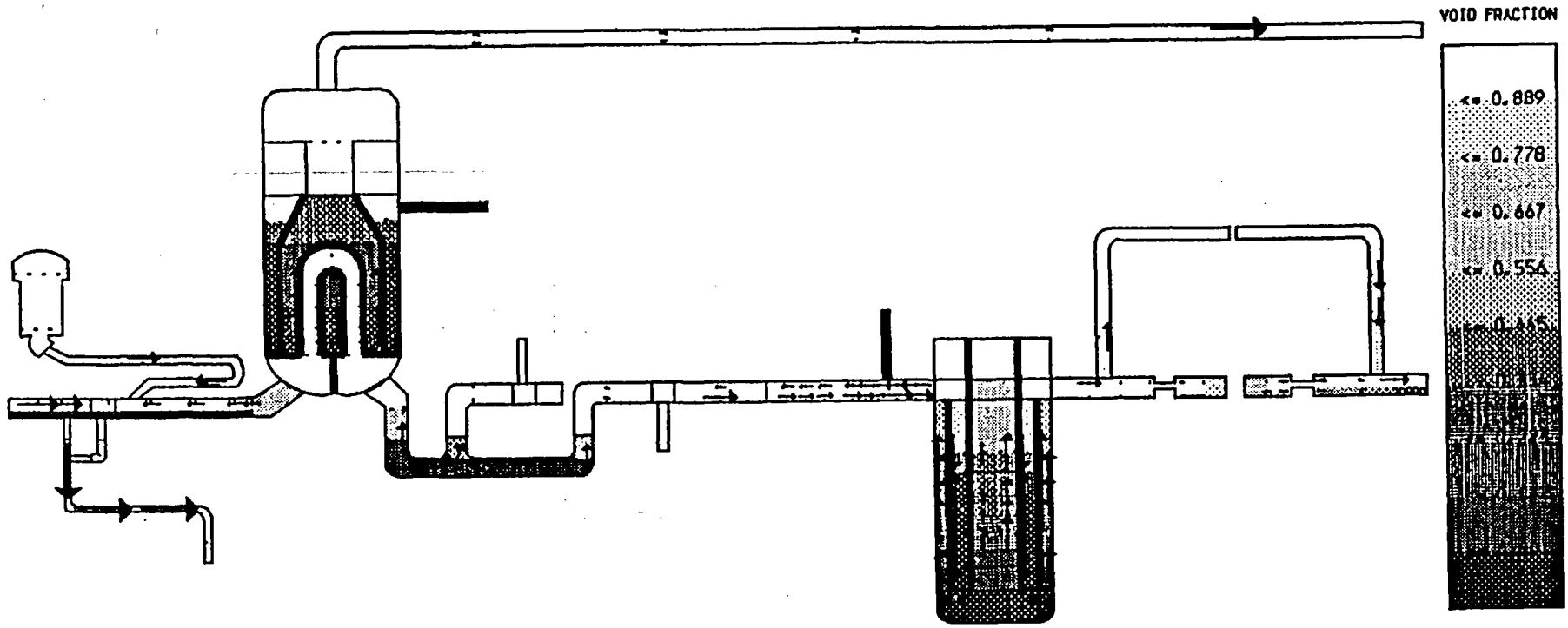TITLE OF FRAME:- TRAC PREDICTION OF LOFT SB-1 (BASE + EPRI CORRELN + INPUT MODS)

AEEW - R 2254

T: 3217.7

VLIQ ⟶
(5.00)

VVAP ⟶
(5.00)

VOID FRACTION

<= 0.889

<= 0.778

<= 0.667

<= 0.556

S.M.A.R.T. SYSTEM MIMIC FOR ANALYSIS OF REACTOR TRANSIENTS

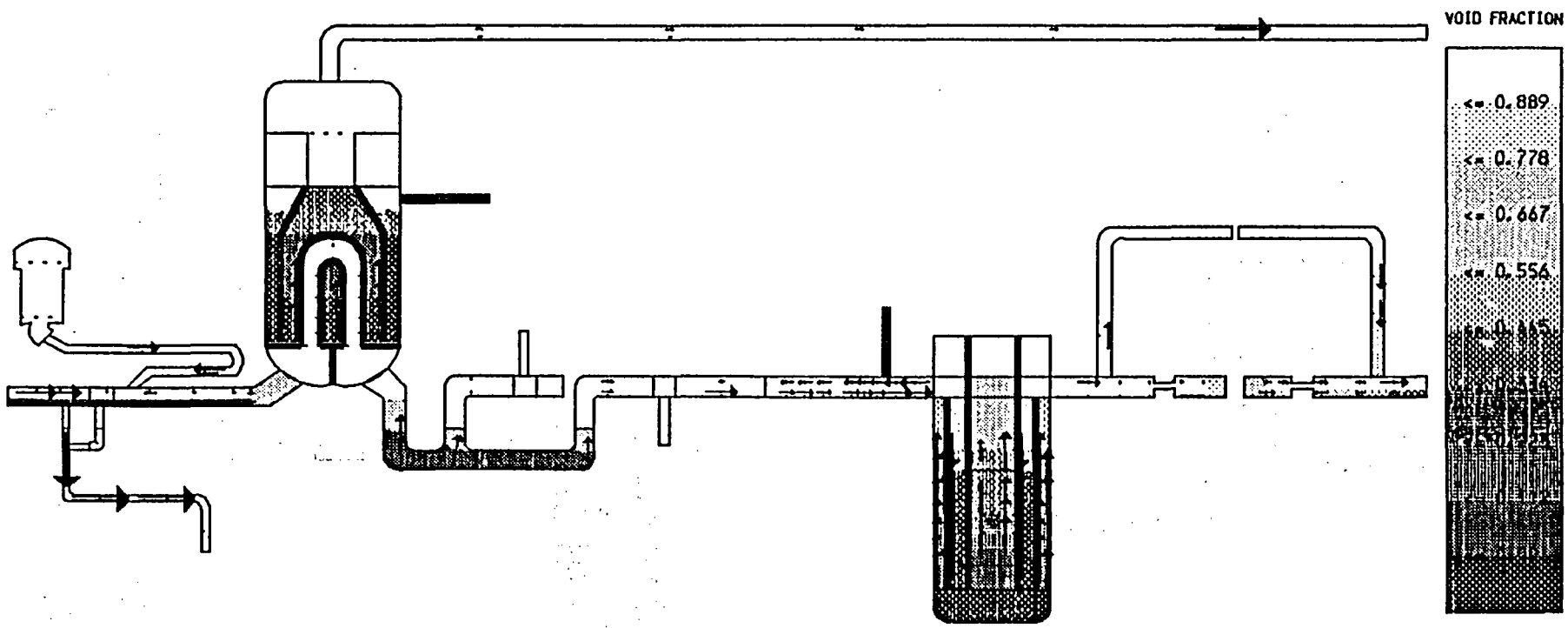TITLE OF FRAME:- TRAC PREDICTION OF LOFT SB-1 (BASE + EPRI CORRELN + INPUT MODS)

T: 3428.6

VLIQ ⟶

(5.00)
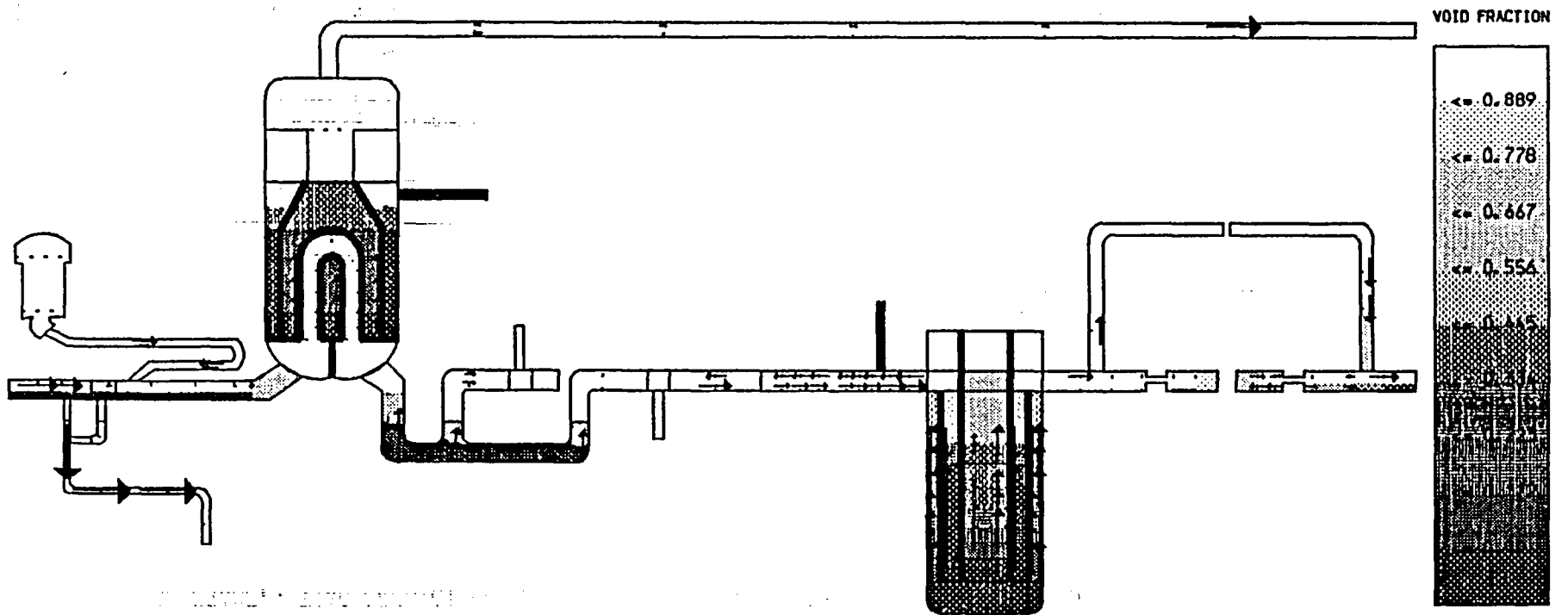
VVAP ⟶

(5.00)

VOID FRACTION

<= 0.889

<= 0.778

<= 0.667

<= 0.556

S. M. A. R. T. SYSTEM MIMIC FOR ANALYSIS OF REACTOR TRANSIENTS

TITLE OF FRAME:- TRAC PREDICTION OF LOFT SB-1 (BASE + EPRI CORRELN + INPUT MODS)

T: 3600.7

VLIQ ⟶
(5.00)

VVAP ⟶
(5.00)

VOID FRACTION

<= 0.889

<= 0.778

<= 0.667

<= 0.556

S.M.A.R.T. SYSTEM MIMIC FOR ANALYSIS OF REACTOR TRANSIENTS

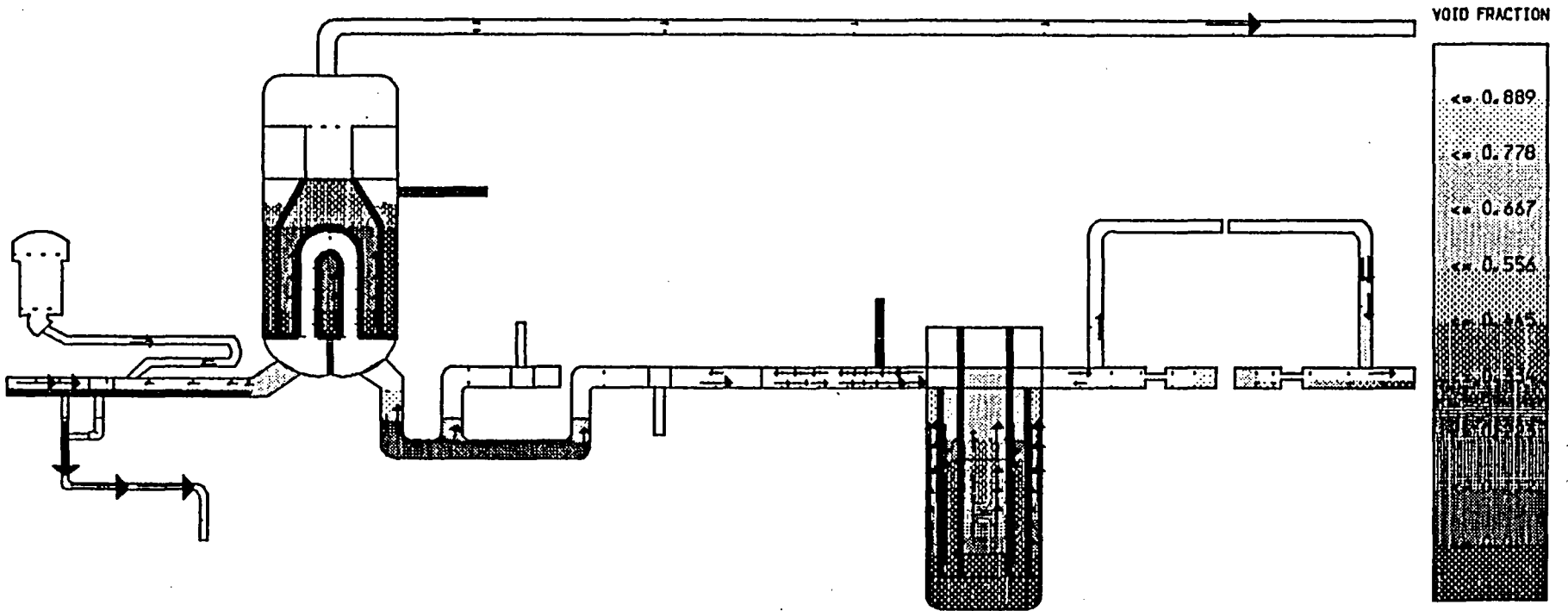TITLE OF FRAME,- TRAC PREDICTION OF LOFT SB-1 (BASE + EPRI CORRELN + INPUT MODS)

T: 3811.5

VLIO ⟶
(5.00)

VVAP ⟶
(5.00)

VOID FRACTION

<= 0.889

<= 0.778

<= 0.667

<= 0.556

S.M.A.R.T. SYSTEM MIMIC FOR ANALYSIS OF REACTOR TRANSIENTS

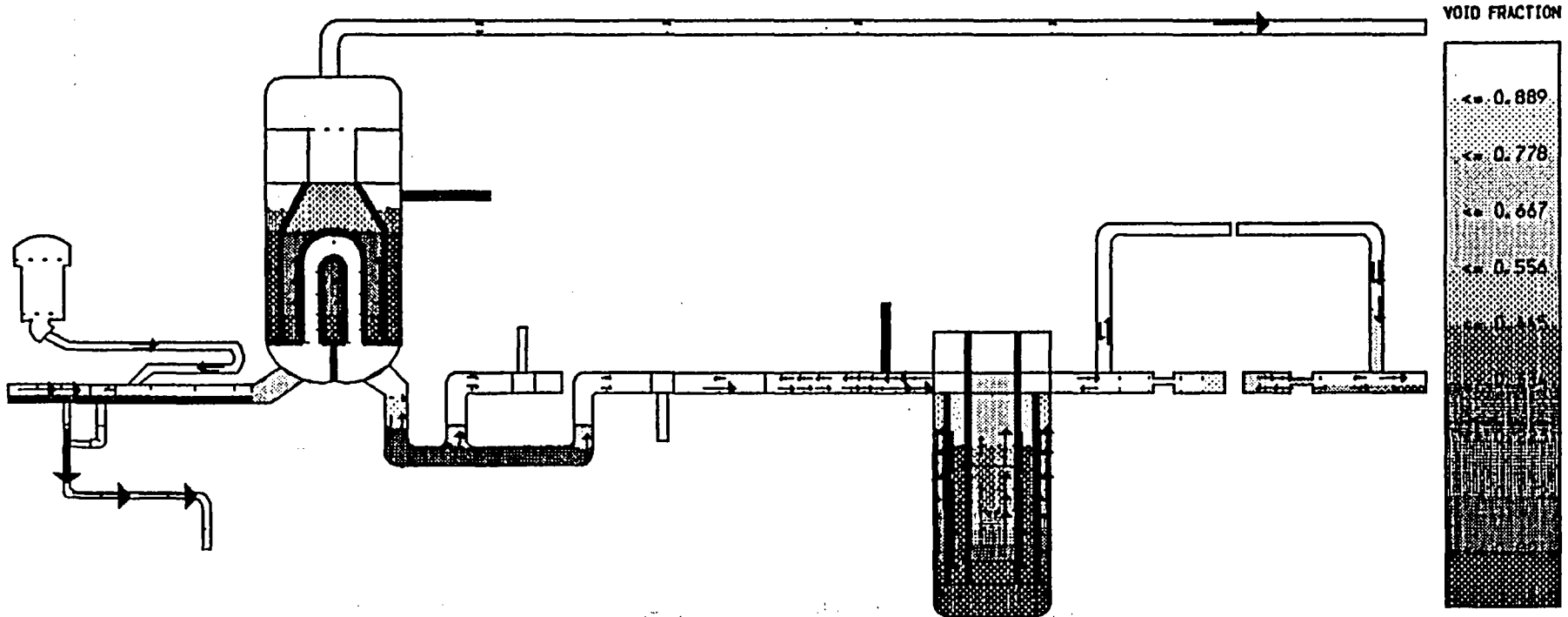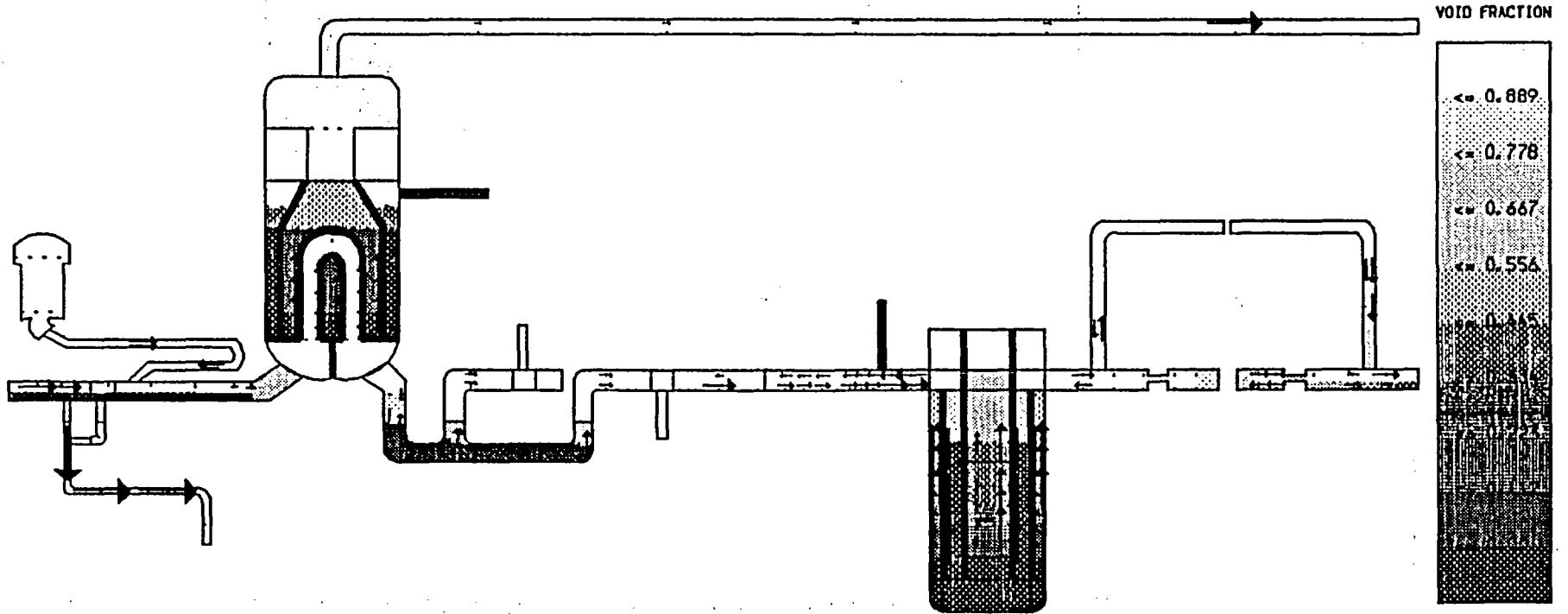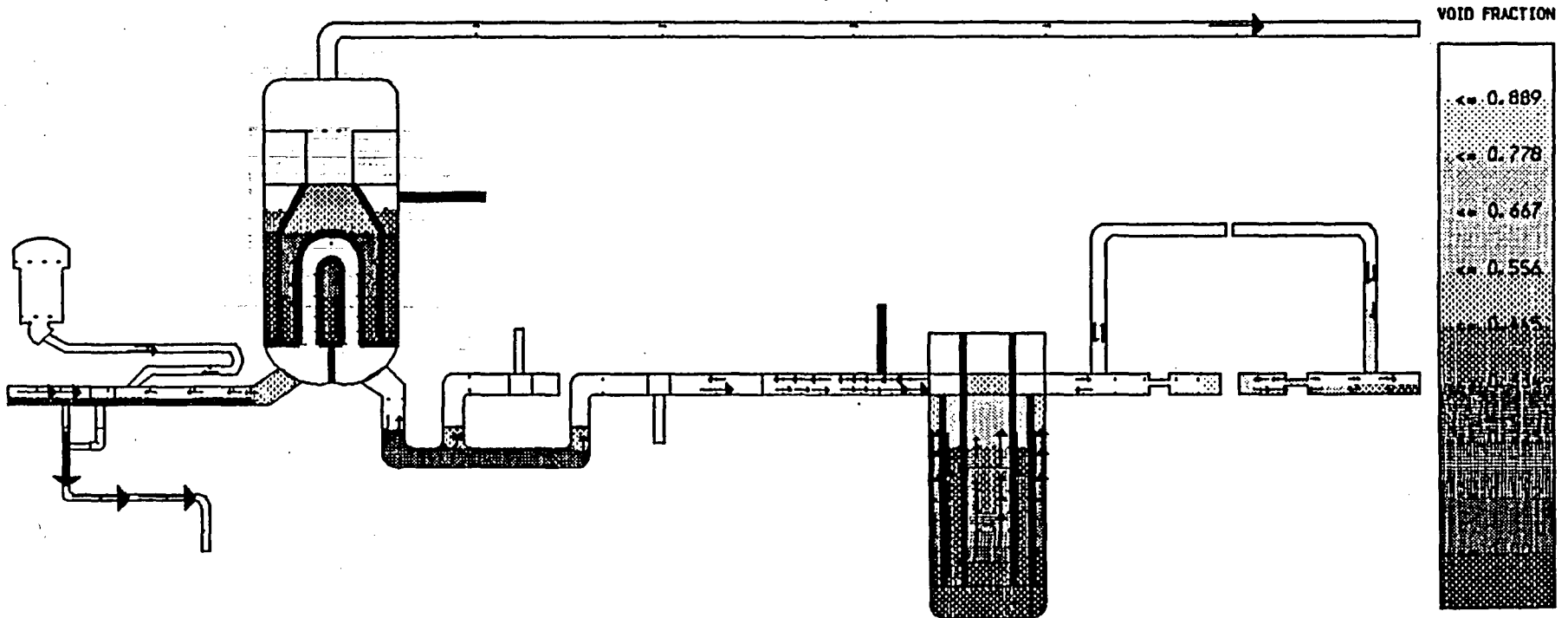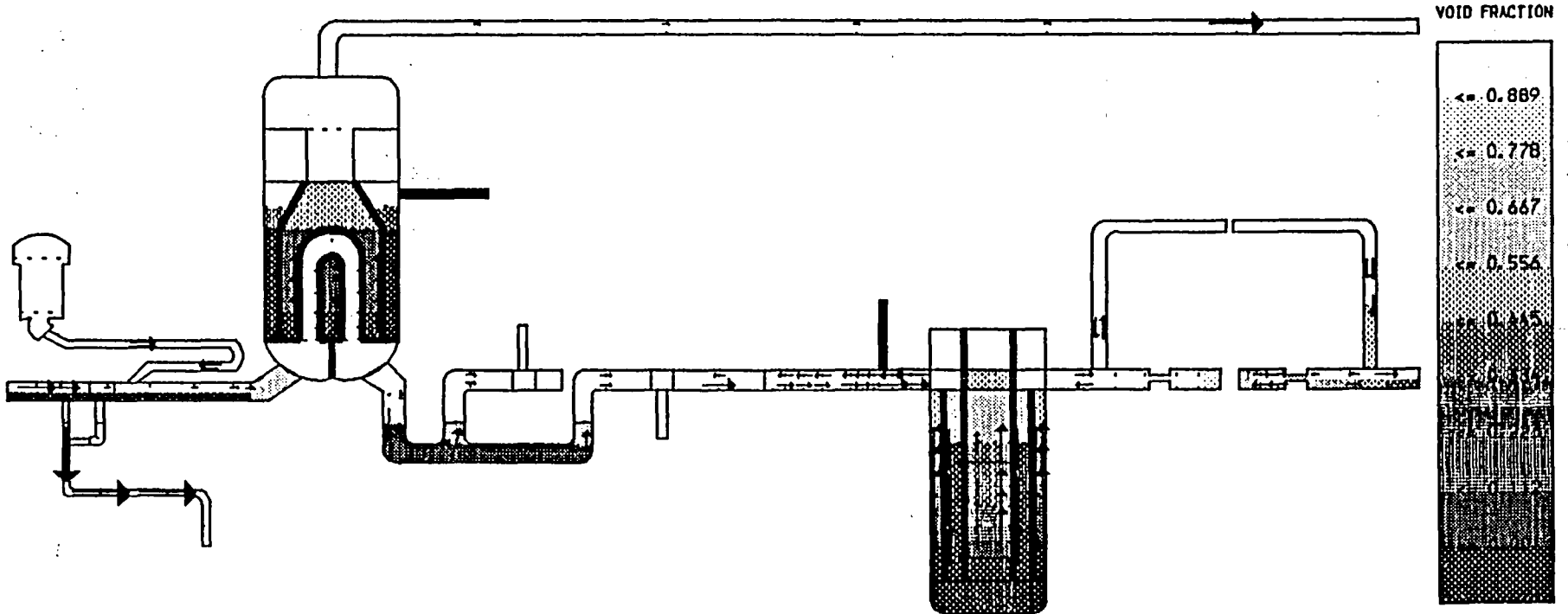TITLE OF FRAME:- TRAC PREDICTION OF LOFT SB-1 (BASE + EPRI CORRELN + INPUT MODS)

Ti 3932.0

VLIQ ⟶

(5.00)

VVAP ⟶

(5.00)

VOID FRACTION

<= 0.889

<= 0.778

<= 0.667

<= 0.556

PWR HEAT TRANSFER AND HYDRAULICS WORKING GROUP

Mr J Fell	AEEW	166/A32
Dr M J Bird	AEEW	338/B41
Mr P Dore	AEEW	114/B40
Mr I Brittain	AEEW	201/A32
Mr K G Pearson	AEEW	333/B41
Dr D B Utton	NNC	c/o Reports Section, Library, Booths Hall, Chelford Road, Knutsford, Cheshire WA16 9QZ
Mr K Routledge	NNC	c/o Reports Section, Library, Booths Hall, Chelford Road, Knutsford, Cheshire
Mr D Coucill	BNF	Springfields Works, Salwick, Preston, Lancs
Mr P C Hall	CEGB	Barnett Way, Barnwood, Gloucestershire
Dr P R Farmer	CEGB	HSD, Courtenay House, 18 Warwick Lane, London EC4P 3EB
Mr M W E Coney	CEGB	CERL Kelvin Avenue, Leatherhead, Surrey
Dr L C Daniels	UKAEA	Bldg 392, AERE Harwell
Dr T J Haste	UKAEA	Springfields NPDL, Salwick, Preston, Lancs
Mr D W McLaughlin	UKAEA	CLF 125, SRD Culcheth, Warrington
Mr B Chojnowski	CEGB	Marchwood Engineering Labs, Marchwood, Southampton
Dr M El-Shanawany	CEGB	HSD, Nuclear Safety Branch, Courtenay House, 18 Warwick Lane, London EC4P 3EB

ADDITIONAL

AEE WINFRITH, DORCHESTER, DORSET, DT2 8DH

Mr M H Butterfield	309/B41	
Dr I H Gibson	236/A32	
Dr G R Kimber	221/A32	
Dr P Coddington	270/A32	
Mr R Potter	209/A32	
Mr R Herbert	172/A32	
Dr A J Wickett	214/A32	
Mr A Neill	267/A32	(3 copies)
Miss E Allen	266/A32	(3 copies)
Dr C Richards	260/A32	(5 copies)
Dr D A Williams	210/A32	
Dr A L Nichols	102/A50	
Dr S R Kinnersly	203/A32	
Dr J N Lillington	217/A32	

UKAEA, SAFETY AND RELIABILITY DIRECTORATE, WIGSHAW LANE, CULCHETH, WARRINGTON

Mr R N H McMillan	CLF 112
Dr A A Debenham	CLC 002
Mr P Clough	

UKAEA, RISLEY NPDE, WARRINGTON, WA3 6AT

Reports Library
Mr A Parry	E417

UKAEA, AERE HARWELL, DIDCOT, OXON, OX11 ORA

Dr D Hicks	G35, Bldg 77
Mr M R Everett	Bldg 329
Dr G F Hewitt	TH 392.7
Mr P Black	TH 392.4

UKAEA, RISLEY, NPDL, WARRINGTON, WA3 6AT

Dr W E Gardner	3/103

UKAEA SPRINGFIELDS NPDL, SALWICK, PRESTON, PR3 ORR

Mr R D Stacey	Bldg 321
Mr A J Manley	

UKAEA, WINDSCALE NL, SELLAFIELD, SEASCALE, CUMBRIA

Mr A Garlick

BNFL, SPRINGFIELDS WORKS, SALWICK, PRESTON, PR3 OXJ

Mr D A Howl	Bldg 382
Mr J P Cooch	Bldg 382

NNC, BOOTH'S HALL, CHELFORD ROAD, KNUTSFORD, CHESHIRE

Library	Reports Section - 4 copies
Mr K Routledge	
Dr K R Barry	
Mr R J Tinsley	

NNC Risley, Warrington Road, Risley, Warrington

Dr D Briney

CEGB, COMPUTING BUREAU, 85 PARK STREET, LONDON SE1

Mr L Wilson

CEGB, HEALTH AND SAFETY DEPARTMENT, NUCLEAR SAFETY BRANCH, 18 WARWICK LANE LONDON, EC4 4EB

Mr J R Harrison

LOFT PROGRAMME REVIEW GROUP

TECHNICAL RESEARCH CENTER OF FINLAND (VTT), NUCLEAR ENGINEERING LABORATORY, POB 169, SF-00181 HELSINKI 18, FINLAND

Mr Heikke Holmstrom

EIDGENÖSSISCHES INSTITUT FÜR REAKTORFORSCHUNG, CH-8303 WÜRENLINGEN, SWITZERLAND

Mr O M Mercier

ÖSTERREICHISCHES FORSCHUNGSZENTRUM, SEIBERSDORF GESELLSCHAFT MBH, C/O EG&G IDAHO INC, PO BOX 1625, IDAHO FALLS, ID 83415, USA

Dipl Phys S Michael Modro

UNIDAD ELECTRICA SA, C/ FRANCISCO GERVAS 3, E-28020 MADRID, SPAIN

Mr Jose Puga

OFFICE OF NUCLEAR REACTOR REGULATION, US NUCLEAR REGULATORY COMMISSION, WASHINGTON DC 20555, USA

Dr Brian Sheron

JAPAN ATOMIC ENERGY RESEARCH INSTITUTE, TOKAI-MURA, NAKA-GUN, IBARAKI-KEN 219-11, JAPAN

Dr Kanji Tasaka

US DEPARTMENT OF ENERGY, OFFICE OF NUCLEAR POWER SYSTEMS, MS B-107, WASHINGTON DC 20555, USA

Mr D F Giessing

GDCD, CENTRAL ELECTRICITY GENERATING BOARD, BARNETT WAY, BARNWOOD, GLOUCESTER, GL4 7RS, UK

Mr P D Jenkins

EPRI, PO BOX 10412, PALO ALTO, CA 94304, USA

Mr M Merilo

ENTE NAZIONALE ENERGIE ALTERNATIVE, CRE CASACCIA, SP ANGUILLARESE KM 1 + 300, CP NR 2400, 1-00100 ROME, ITALY

Dr Giorgio Palazzi

STUDSVIK ENERGITEKNIK AB, S-61182 NYKOPING, SWEDEN

Mr O Sandervaag

US NUCLEAR REGULATORY COMMISSION, WASHINGTON DC 20555, USA

Dr Robert Van Houten

EG&G, IDAHO INC, PO BOX 1625, IDAHO FALLS, ID 83415, USA

Dr D Croucher

OECD NUCLEAR ENERGY AGENCY, 38 BOULEVARD SUCHET, F-75016 PARIS, FRANCE

Mr Ralph Caruso

LIBRARIES:

Dounreay   2
Harwell   2
Risley   4
Springfields   2
Windscale   2
Winfrith   4

U.S. NUCLEAR REGULATORY COMMISSION

BIBLIOGRAPHIC DATA SHEET

(See instructions on the reverse)

1. REPORT NUMBER
(Assigned by NRC. Add Vol., Supp., Rev.,
and Addendum Numbers, if any.)

NUREG/IA-0011
AEEW-R 2254

2. TITLE AND SUBTITLE

TRAC-PF1/MOD1 Post-Test Calculations of the OECD LOFT
Experiment LP-SB-1

3. DATE REPORT PUBLISHED

MONTH	YEAR
April	1990

4. FIN OR GRANT NUMBER

A6827

5. AUTHOR(S)

E. J. Allen

6. TYPE OF REPORT

Technical

7. PERIOD COVERED *(Inclusive Dates)*

8. PERFORMING ORGANIZATION – NAME AND ADDRESS *(If NRC, provide Division, Office or Region, U.S. Nuclear Regulatory Commission, and mailing address; if contractor, provide name and mailing address.)*

United Kingdom Atomic Energy Authority
Atomic Energy Establishment, Winfrith
Dorchester, Dorset DT2 BDH
United Kingdom

9. SPONSORING ORGANIZATION – NAME AND ADDRESS *(If NRC, type "Same as above"; if contractor, provide NRC Division, Office or Region, U.S. Nuclear Regulatory Commission, and mailing address.)*

Office of Nuclear Regulatory Research
U. S. Nuclear Regulatory Commission
Washington, DC 20555

10. SUPPLEMENTARY NOTES

11. ABSTRACT *(200 words or less)*

Analysis of the small, hot leg break, OECD LOFT Experiment LP-SB-1. using the
"best-estimate" computer code TRAC-PF1/MOD1 is presented.

Descriptions of the LOFT facility and the LP-SB-1 experiment are given and development
of the TRAC-PF1/MOD1 input model is detailed. The calculations performed in achieving
the steady state conditions, from which the experiment was initiated, and the
specification of experimental boundary conditions are outlined.

12. KEY WORDS/DESCRIPTORS *(List words or phrases that will assist researchers in locating the report.)*

TRAC-PF1, LOFT, ICAP Program

13. AVAILABILITY STATEMENT

Unlimited

14. SECURITY CLASSIFICATION

(This Page)

Unclassified

(This Report)

Unclassified

15. NUMBER OF PAGES

16. PRICE
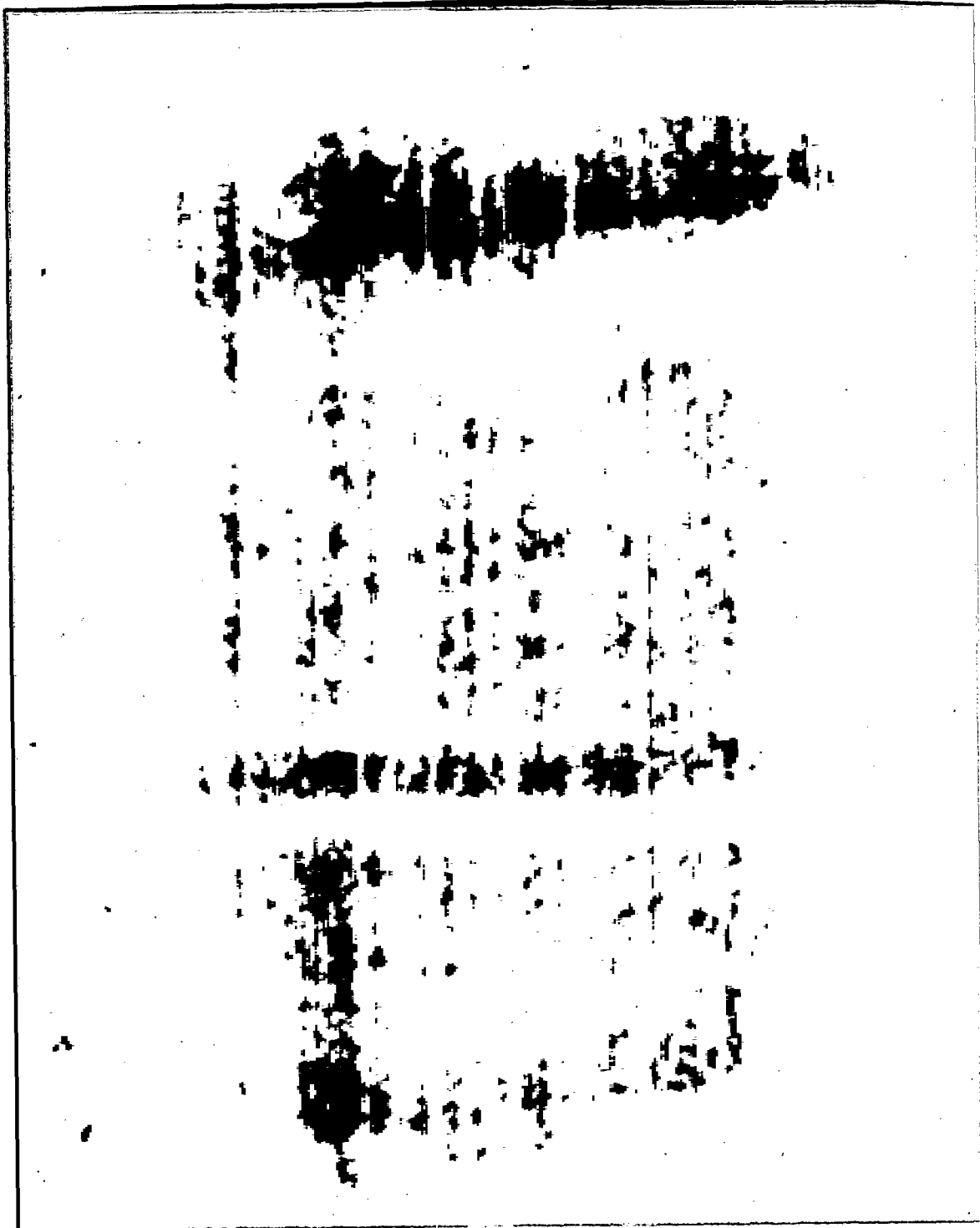
UNITED STATES
NUCLEAR REGULATORY COMMISSION
WASHINGTON, D.C. 20555

———

OFFICIAL BUSINESS
PENALTY FOR PRIVATE USE, $300